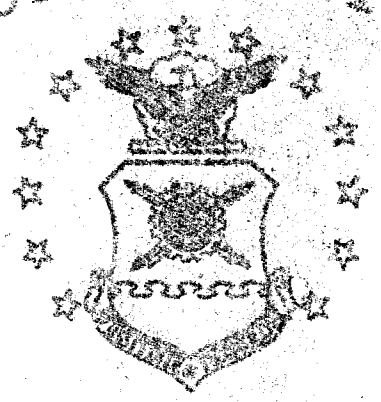

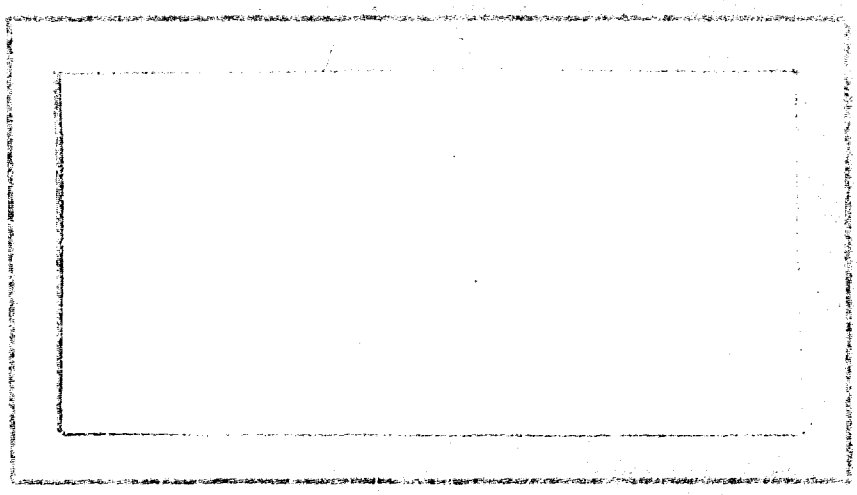

SCHOOL OF ENGINEERING

IMPROVED DUTCH ROLL STABILITY AUGMENTATION SYSTEM FOR A MODIFIED C-135B AIRCRAFT

THESIS

Lynn L. Gamble
Captain USAF

William L. Smith
Captain USAF

GGC/EE/77-8

IMPROVED DUTCH ROLL STABILITY AUGMENTATION SYSTEM FOR A MODIFIED C-135B AIRCRAFT

THESIS

Presented to the Faculty of the School of Engineering

the Air Force Institute of Technology

Air University

in Partial Fulfillment of the

Requirements for the Degree of

Master of Science

by

Lynn L. Gamble, B.S.E.E. Captain USAF

and

William L. Smith, B.S.E.E. Captain USAF

Graduate Guidance and Control

June 1979

Preface

This report presents the results of our investigation into the problem of poor lateral-directional flying qualities of a modified C-135B aircraft. A lateral-directional stability augmentation system is designed, and an analog simulation of the system is made. From an analysis of the design and simulation, we have attempted to predict the performance which can be expected from this system. The problems encountered, their effects, and the success of the system are discussed.

We wish to express our thanks to the many people who have helped to make this report possible. In particular, we wish to thank Mr. John M. Griffin, our Thesis Sponsor, for providing the topic and the much needed technical assistance.

Our thanks is also extended to Major John C. Schoop, our Faculty Thesis Advisor, for his critical evaluation of our first draft. We especially thank him for his continued encouragement at the times when there seemed to be no end in sight.

A special thanks goes to Mr. James Crider, of the Analog Simulation Branch, ASD, for his dedicated services during the analog simulation. Without his techical competence and extreme patience with us, none of this would have been possible.

Last, but not least, we wish to thank our wives, Mary and Linda, who have been as understanding as humanly possible during the extremely long period of preparing the report.

Lynn L. Camble

William L. Smith

Contents

Contents

List of Figures

List of Tables

List of Symbols

a_y – Acceleration in Y-direction (Lateral)

K – Ratio of Measured Roll Angle to Required Roll Angle

K_A – Accelerometer Static Loop Sensitivity

K_P – Primary Flap Switch Gain

K_S – Secondary Flap Switch Gain

K_{SLS} – Static Loop Sensitivity

L – Rolling Moment

l_x – Distance from Aircraft c.g. to Point of Measurement of Acceleration

M – Pitching Moment

MC-135 – Modified C-135B

N – Yawing Moment

P – Roll Angular Velocity

P_{osc}/P_{av} – Ratio of Oscillatory Component of Roll Rate to Average Component of Roll Rate

Q – Pitch Angular Velocity

R – Yaw Angular Velocity

SAS – Stability Augmentation System

T_D – Dutch Roll Period

TPR – Transient Peak Ratio

U – Velocity in X-direction

U_o – Reference Velocity in X-direction

V – Velocity in Y-direction

v – Disturbed Velocity in Y-direction

W – Velocity in Z-direction

X, Y, Z – Aerodynamic Force Components

YD – Yaw Damper System

β – Sideslip Angle

δ_a – Aileron Deflection

δ_r – Rudder Deflection

ϕ – Roll Angle

$\dot{\phi}$ – Roll Rate

ϕ_{comm} – Command Roll Angle

ϕ_{req} – Required Roll Angle

ψ – Yaw Angle

$\dot{\psi}$ – Yaw Rate

ψ_β – Phase Angle of Dutch Roll Component of Sideslip

θ – Pitch Angle

ω_n – Undamped Natural Frequency

ζ – Damping Ratio

$\phi\beta$ – Phase Angle Between Roll Rate and Sideslip Angle

$\Delta\beta_{max}$ – Maximum Change of Sideslip in Two Seconds or One Half Dutch Roll Period

Abstract

A stability augmentation system was designed for a C-[illegible] aircraft which is modified by the installation of a large external [illegible]. Aerodynamic data for the modified C-[illegible] were simulated from wind tunnel testing of the aircraft model.

The SAS consists of the basic Boeing series yaw damper augmented with lateral acceleration feedback. Analysis and design were done using root locus techniques.

The aircraft was then simulated on the analog computer to verify the design and make final system adjustments. Three flight conditions were simulated — two cruise conditions and power approach. In all the cases, the lateral-directional flying qualities were markedly improved when the SAS was used. The biggest advantage of this particular SAS, namely, the acceleration feedback, is that both the damping ratio and the frequency of the Dutch roll were significantly increased without degrading flying qualities in some other area.

As required, the SAS is simple and inexpensive, and requires a minimum of subsystem redesign. In addition to the requirement that the standard series yaw damper be installed, the SAS consists of only one accelerometer and one additional flap switch.

[redacted]

[redacted]

[redacted]

I. Introduction

Background

Research and development, conducted by the U.S. Air Force, has, in past years, required a wide variety of aircraft. Since it is not practical to design and build a new aircraft for each new test, it has become common practice to modify existing aircraft. In recent years, the C-135B has been a popular aircraft to modify and use as a "test bed" for flight testing the many subsystems undergoing R&D. Many such modifications are in the form of external structural changes such as the addition of nose cones, antenna pylons, and a variety of other types of fairings. Quite often the modification results in the flying qualities being so degraded that the aircraft cannot be flown safely. Such is the case of particular interest in this thesis.

Air Force mission requirements call for a C-135B aircraft to be modified with a large fairing installed on the top of the fuselage. Wind tunnel tests of the aircraft model have shown that the modification significantly reduces the basic stability of the aircraft. In particular, the tests have revealed an extensive reduction in static directional stability for all flight conditions.

It has been demonstrated in the wind tunnel that the modification has little or no effect on the longitudinal flight characteristics, which are already acceptable. However, the lateral-directional performance is far below the required flying qualities. As a result of

three wind tunnel tests. It has become necessary to design a stability augmentation system (SAS) which will improve the performance to an acceptable level as specified under MIL-F-8785B (Ref 5).

At present, the C-135B is equipped with a parallel yaw damper. However, it has been decided that a full-time series yaw damper should be required so that the pilots can have full rudder pedal authority during power approach. Preliminary investigations (Ref 6) have indicated that using the present series yaw damper (obtainable kit from from the Boeing Company) is not, by itself, adequate to improve the flying qualities to the required level.

The objective of this thesis is, therefore, to design a stability augmentation system that when implemented will adequately improve the lateral-directional flying qualities of the modified C-135 aircraft (hereafter designated the KC-135). For simplicity and ease of installation, the design starts with the presently available series yaw damper. If at all possible, the SAS will be limited to a rudder controller as opposed to rudder control supplemented with aileron control. An important design criterion is that the required flying qualities be met with a minimum of subsystem redesign, expense, and complexity.

The stability derivatives for three different flight configurations of the KC-135 were obtained from the Airframe Subsystems Division, Deputy of Engineering, ASD. The method by which these stability derivatives were obtained is discussed in ASD-TR-69-97 (Ref 9).

Definition of Lateral-Directional Motion

Lateral-directional motion of an aircraft is characterized by three modes as seen from the characteristic equation of any of the

transfer functions that describe a lateral position, rate, or acceleration resulting from a control surface deflection. The three modes are identified as, (1) spiral mode, (2) rolling convergence, and (3) coupled lateral-directional oscillation (Dutch roll).

Spiral Mode. Spiral motion actually occurs as either divergent or convergent. If convergent, the motion is seen as a flat curve in the horizontal plane, in which the aircraft slowly approaches the reference heading following a disturbance. On the other hand, if the mode is divergent, the flight of the aircraft is seen as a banked turn of ever-decreasing radius, i.e., a tightening spiral.

Rolling Convergence. Rolling convergence is almost entirely a one-degree-of-freedom converging motion about the aircraft X-axis. This mode is used to describe the rolling ability of an aircraft.

Lateral-Directional Oscillation (Dutch Roll). The Dutch roll mode falls between the extreme conditions for the spiral mode and rolling convergence. When disturbed in roll or yaw, an aircraft response is a combination roll and yaw-sideslip oscillation. The resulting frequencies and damping ratios of each oscillation are identical, however the roll oscillation slightly leads the yaw oscillation.

Plan of Attack

A conventional feedback control systems approach was followed throughout this thesis using the root locus technique as the primary tool for design. All the root locus plots needed for the design were made using Fisher's root locus computer program (Ref 5). A computer program for solving the lateral-directional equations of motion (Ref 7)

was used to solve for all the modified airframe dynamic characteristics and transfer functions in each of the three flight configurations. Knowing the necessary airframe transfer functions and characteristics, it was then possible to analyze the aircraft as equipped with the basic series yaw damper.

The airframe with yaw damper was thoroughly analyzed for each flight condition using root locus. Differences in performance of each flight condition were carefully noted so as to establish positive guidelines for the design. First design efforts involved trying to find a rather simple cascade compensator to modify the yaw damper. Following this, a multiple feedback approach was investigated.

The system is characterized primarily by two sets of second order roots neither of which are dominant. This makes analysis by conventional feedback control techniques extremely difficult. For this reason, all results are verified by analog computer simulation. Time histories of the analog computer output showing the aircraft response to both rudder and aileron inputs are recorded for the basic MC-135, MC-135 with basic series yaw damper, and MC-135 with the final SAS design in each of the three flight configurations.

Sign Conventions

The sign conventions for forces and moments, as used throughout this thesis, are shown in Fig. 1. More particularly, the sign conventions for lateral motion are shown in Fig. 2.

Rudder. Rudder deflection to the left is defined as positive. This causes a positive β, positive v, negative N, and negative R.

Ailerons. Deflection of right aileron up and left aileron down

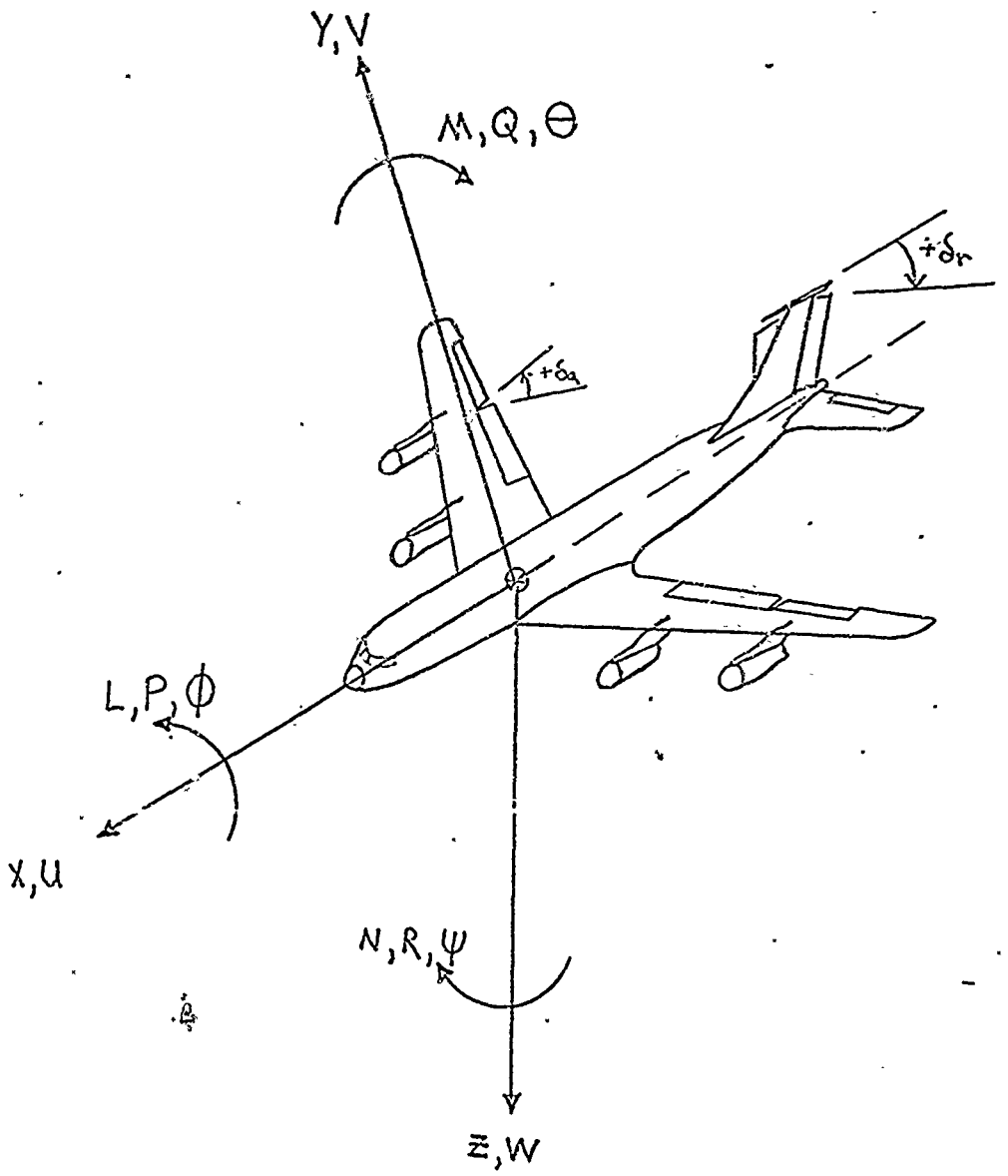

P - Roll Angular Velocity

Q - Pitch Angular Velocity

R - Yaw Angular Velocity

X, Y, Z - Aerodynamic Force Components

U, V, W - Velocity Components

L - Rolling Moment

M - Pitching Moment

N - Yawing Moment

Φ - Roll Angle

Θ - Pitch Angle

Ψ - Yaw Angle

Figure 1. Sign Conventions

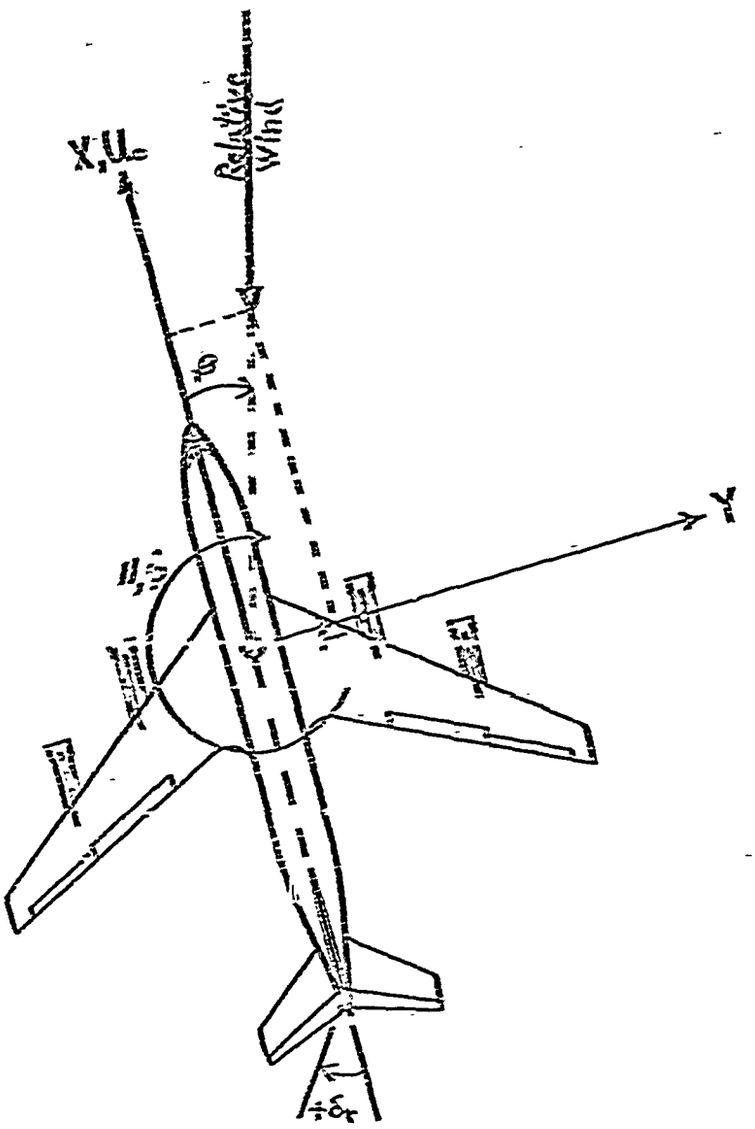

β - Sideslip Angle

v - Disturbed Velocity in Y-direction Due to Positive β

Figure 2. Lateral Sign Conventions

is defined as positive. This causes a positive L, positive β, and positive P. Note, that this definition of positive aileron is not standard.

Stability Axis System. When the aircraft axes are so oriented that, during the steady flight condition, the X-axis is always parallel to the relative wind, the axes are referred to as stability axes. When the aircraft is disturbed from the steady flight condition, the axes rotate with the airframe and do not change direction with respect to the aircraft.

Simplifying Assumptions

The following is a list of major assumptions that are made throughout this thesis. All of these assumptions are considered as valid, especially at subsonic velocities, and should therefore cause little degradation to the actual system analysis.

-Longitudinal motion is neglected, thus making it possible to analyze the system in three degrees of freedom rather than the more complex six degrees of freedom.

-Disturbances from the steady flight condition are small and confined to the XY and YZ planes.

-The aircraft is considered as a rigid body with its mass and c.g. remaining constant.

-During the steady unaccelerated flight condition, the aircraft is flying with wings level and at constant altitude with all components of velocity equal to zero except U_o.

Division of Responsibility

Although both partners are thoroughly familiar with all portions of this thesis, there is a definite division of responsibility as dictated by AFIT Department of Electrical Engineering policy.

Captain Gamble is primarily responsible for the control systems analysis including the development of the necessary control transfer functions and block diagrams. As a result, he wrote Chapter II and assembled the appendices.

Captain Smith is primarily responsible for the analog computer simulation including interpretation of the requirements in MIL-F-8785A. As a result, he wrote Chapters III and IV.

As necessary, both partners contributed to the aspects of design and the analysis and interpretation of the analog computer time histories. Also, both writers collaborated on the introduction, and conclusions and recommendations, Chapters I and V, respectively. All drawings, figures, and graphs were prepared jointly.

II. System Design

The objective of this thesis is to design the necessary stability augmentation system (SAS) which will provide the control needed for successful performance of the MC-135. The performance criteria to be met was extracted from MIL-F-8785A, "Flying Qualities of Piloted Airplanes" (Ref 9). Since a SAS will be installed in an actual modified C-135B to be used in a future Air Force R&D flight test, it is necessary to design a SAS that will perform within the limitations of MIL-F-8785A. The particular specifications (requirements) that served as the design criteria were furnished by ASD's Deputy of Engineering, Airframe Subsystems Division. It was decided that the damping ratio, ζ, the undamped natural frequency, ω_η, and the product, $\zeta\omega_\eta$, of the system's Dutch roll would serve as the primary design criteria. Tests against the specifications would be done in the final analog computer simulation analysis.

Conventional feedback control systems design techniques were used in the investigation and actual design. Root locus techniques were used in designing a system which would adequately improve the ζ and ω_η of the Dutch roll. Frequency response plots were used to determine the required filtering for the system.

The standard C-135B is equipped with a parallel yaw damper, however, it is felt necessary that in order for the pilot to have full rudder pedal control, a series yaw damper would be used. Such a damper is readily available in kit form from the Boeing Aircraft Company. Therefore, the design undertaken in this thesis essentially starts not

with the basic unmodified MC-135 but rather with the MC-135 equipped with the standard series yaw damper.

The performance characteristics of the basic system, i.e., the MC-135 equipped with the standard series yaw damper, were thoroughly studied to determine the extent to which the yaw damper could be used and what modification could be made that would result in satisfactory performance. The objectives were not only to meet certain preselected criteria but also to keep the cost and complexity of the design to a minimum. Therefore, a wide variety of common passive cascade compensators were tried in addition to sensing and feeding back other lateral-directional parameters. Every effort was made to preclude using more sophisticated multi-loop systems or systems containing elaborate active network filters and compensators.

Equations of Motion

To fully describe the motion of an aircraft requires a set of six differential equations - one for each of the six degrees of freedom of movement. By assuming that no coupling exists between motion in the lateral-directional plane and motion in the longitudinal plane, the original six differential equations can be decoupled into two sets of three equations each. One set describes motion of the aircraft only in the longitudinal plane or plane of symmetry while the other describes motion only in the lateral and directional planes or motion out of the plane of symmetry. Thus the problem can be reduced to one of three degrees of freedom which describes either longitudinal or lateral-directional motion depending on which is of interest.

Since the MC-135 differs primarily from the standard C-135B in

that its flying characteristics exhibit an unusually large oscillation yaw-sideslip-rolling motion when perturbed, the set of lateral-direction equations of motion was normally chosen for the analysis. Further approximations can be made which ultimately reduce the three degrees of freedom problem to a one degree of freedom problem. However, such an approximation was considered not valid for this study since the Dutch roll, being so large, produced substantial amounts of yaw, sideslip, and roll.

A thorough development of the lateral-directional equations of motion in the form as used for this study is given in Ref 2. The final three equations, the Y-force, L-moment, and N-moment are listed below.

$$\frac{\Sigma F_y}{\dot{v} + U_0 r - g\phi\sin\theta_0 - g\phi\cos\theta_0 = Y_r r + Y_v v + Y_p p + Y_{\dot{v}}\dot{v} + Y_{\delta_a}\delta_a + Y_{\delta_r}\delta_r} \qquad (2\text{-}1)$$

$$\frac{\Sigma L}{\dot{p} - \frac{I_{xz}}{I_{xx}}\dot{r} = L_r r + L_v v + L_p p + L_{\dot{v}}\dot{v} + L_{\delta_a}\delta_a + L_{\delta_r}\delta_r} \qquad (2\text{-}2)$$

$$\frac{\Sigma N}{\dot{r} - \frac{I_{xz}}{I_{zz}}\dot{p} = N_r r + N_v v + N_p p + N_{\dot{v}}\dot{v} + N_{\delta_a}\delta_a + N_{\delta_r}\delta_r} \qquad (2\text{-}3)$$

As explained in the reference, these are the three lateral-directional equations which are linearized for small perturbations about a steady reference flight condition of straight and level, unaccelerated flight.

Since perturbations about the reference flight condition of straight and level flight are considered to be small,

$$p = \dot{\phi} \qquad (2\text{-}4)$$

$$r = \dot{\psi} \qquad (2-5)$$

From Figure 2 it can be seen that the sideslip angle, β, is related to the sideslip velocity, v, as

$$\tan\beta = \frac{v}{U_0}$$

Since v has been assumed to be small,

$$\beta = \frac{v}{U_0} \qquad (2-6)$$

Substituting (2-4), (2-5), and (2-6) into (2-1), (2-2), and (2-3), taking the Laplace transform, and putting the result in matrix form yields

$$\begin{bmatrix} s(1 - Y_{\dot{\beta}}) - Y_\beta & -\frac{1}{U_0}(sY_p + g\cos\theta_0) & s(1 - \frac{Y_r}{U_0}) - \frac{g}{U_0}\sin\theta_0 \\ -sL_{\dot{\beta}} - L_\beta & s^2 - sL_p & -s^2\frac{I_{xz}}{I_{xx}} - sL_r \\ -sN_{\dot{\beta}} - N_\beta & -s^2\frac{I_{xz}}{I_{zz}} - sN_p & s^2 - sN_r \end{bmatrix} \begin{bmatrix} \beta(s) \\ \phi(s) \\ \psi(s) \end{bmatrix} = \begin{bmatrix} \frac{Y_\delta}{U_0}\delta(s) \\ L_\delta\,\delta(s) \\ N_\delta\,\delta(s) \end{bmatrix} \qquad (2-7)$$

The transfer functions are found from (2-7) by repeated applications of Cramer's rule.

For this thesis, all necessary transfer functions were determined by using the IBM 7094 digital computer. A complete calculation of all the transfer functions as well as instructions for using the lateral-directional computer program are included in SEG-TR-66-52 (Ref 7). The outputs of the program for each of the three flight conditions are

[illegible]

Included as Appendix D.

Flight Conditions

In an effort to adequately cover the performance envelope of the aircraft, three different flight configurations were considered. Selection of the three flight configurations was based primarily on the performance envelope of the existing C-135A. Data which describe each of the flight conditions is listed in Table I, below.

Table I

KC-135 Flight Conditions

Flight Condition	Altitude H (ft)	Mach No. M	Gross Weight W (lbs)	Velocity V (ft/sec)
Cruise 1	40000	.75	[illegible]	725
Cruise 2	25000	.65	250000	660
Power Approach	Sea Level	—	[illegible]	275

All the necessary stability derivatives were determined from wind tunnel testing of the KC-135 model with adjustments made for actual flying conditions. Such a procedure is quite complex and beyond the intent of this thesis. Reference is made to ASD-TR-63-97 for a more detailed analysis. The final set of stability derivatives and other necessary parameters that were used throughout this study are listed in Table II. All stability derivatives are referenced to degrees rather than radians and θ_o has the units of degrees.

The Basic System

The denominator of the aircraft transfer function (characteristic equation) can, in general, be written as

$$s(s + \frac{1}{\tau_s})(s + \frac{1}{\tau_r})(s^2 + 2\zeta_d \omega_{n_d} s + \omega_{n_d}^2) \qquad (2-8)$$

Table [illegible]

[illegible] Stability Derivatives

Parameter	Cruise 1	Cruise 2	Power Approach
Y_β	[illegible]	[illegible]	[illegible]
$Y_{\dot\beta}$	0	0	0
Y_p	[illegible]	[illegible]	[illegible]
Y_r	[illegible]	[illegible]	[illegible]
Y_{δ_a}	0	0	0
Y_{δ_r}	[illegible]	[illegible]	[illegible]
L_β	[illegible]	[illegible]	[illegible]
$L_{\dot\beta}$	0	0	0
L_p	-.4695	[illegible]	[illegible]
L_r	[illegible]	[illegible]	[illegible]
L_{δ_a}	[illegible]	[illegible]	1.423
L_{δ_r}	[illegible]	[illegible]	[illegible]
N_β	[illegible]	.7745	.2545
$N_{\dot\beta}$	[illegible]	0	[illegible]
N_p	[illegible]	[illegible]	[illegible]
N_r	[illegible]	-.1506	[illegible]
N_{δ_a}	[illegible]	.0600	.0403
N_{δ_r}	-.4365	-.2273	[illegible]
I_{xx}	[illegible]	[illegible]	[illegible]
I_{zz}	[illegible]	[illegible]	[illegible]
I_{xz}	[illegible]	[illegible]	[illegible]
θ_0	0	0	-3.0

where τ_s – spiral mode time constant

τ_r – rolling mode time constant

ζ_d – damping ratio of the Dutch roll

ω_{n_d} – undamped natural frequency of the Dutch roll

The term "s" denotes heading insensitivity. In other words, if the aircraft heading is changed there is no tendency for it to return to the original heading but rather it will assume the new heading. The particular numerical values of the roots of the characteristic equation for each of the three flight conditions of the NC-135 are determined by computing any one of the aircraft transfer functions using Eq (2-7). Retaining only the denominators, the following results are obtained.

Cruise 1:

$$s(s + .00935)(s + .62)(s^2 + .012s + .794) \qquad (2\text{-}9)$$

Cruise 2:

$$s(s + .0114)(s + .385)(s^2 + .009s + 1.05) \qquad (2\text{-}10)$$

Power Approach:

$$s(s + .024)(s + 1.14)(s^2 + .052s + .55) \qquad (2\text{-}11)$$

Analysis of these equations reveals that the spiral mode, with time constant, τ_s, is of nominal magnitude but now is stable. Normally this mode is slightly unstable. The time constant, τ_r, of the rolling mode is also seen to be nominal. However, determining ζ_d and ω_{n_d} from the second order roots reveals a characteristic Dutch roll that is far from the limit allowed under the specified criteria. In fact, Cruise 2 is slightly unstable producing an ever increasing Dutch roll. The damping

ratio for Cruise 1 and Power Approach is .0106 and .035, respectively. The minimum allowable ζ_d, as specified in MIL-F-8785A, is .19.

Because of the very poor damping characteristics of the Dutch roll, it was immediately decided not to begin the analysis and subsquent SAS design based on the performance of the basic aircraft but rather to begin with the aircraft as equipped with the standard series yaw damper. A block diagram of the general system is shown in Fig. 3. Substituting in all the transfer functions, reducing the servo amplifier loop, and repositioning the rate filter, the block diagram reduces to that shown in Fig. 4. To facilitate a root locus study, the block diagram of Fig. 4 is further reduced to that shown in Fig. 5. Note that the pilot's input has been relocated. This is not intended for the actual system but is done here only to simplify the analysis.

The airframe transfer function is found by first calculating the numerator of $\frac{\dot{\psi}}{\delta_r}$ from (2-7) and substituting in the appropriate constants from Table II, depending on the flight condition of interest. This calculation yields

Cruise 1:

$$\left.\frac{\dot{\psi}}{\delta_r}\right|_{num} = -.524\, s(s + .68)(s - .09 \pm j.35) \qquad (2\text{-}12)$$

Cruise 2:

$$\left.\frac{\dot{\psi}}{\delta_r}\right|_{num} = -.838\, s(s + .875)(s - .0716 \pm j.387) \qquad (2\text{-}13)$$

Power Approach:

$$\left.\frac{\dot{\psi}}{\delta_r}\right|_{num} = -.335\, s(s + 1.13)(s - .044 \pm j.396) \qquad (2\text{-}14)$$

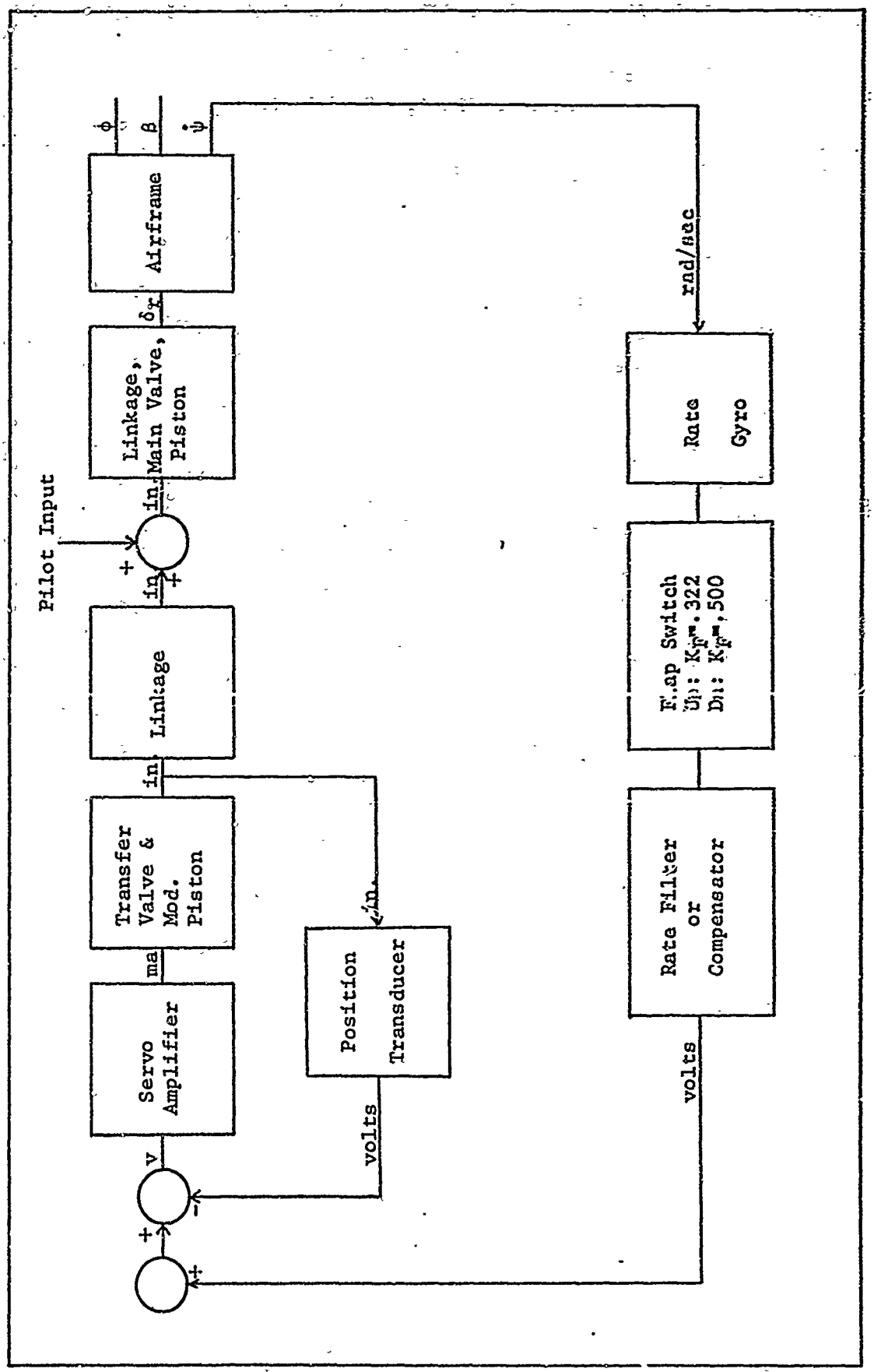

Figure 3. Basic Yaw Damper System

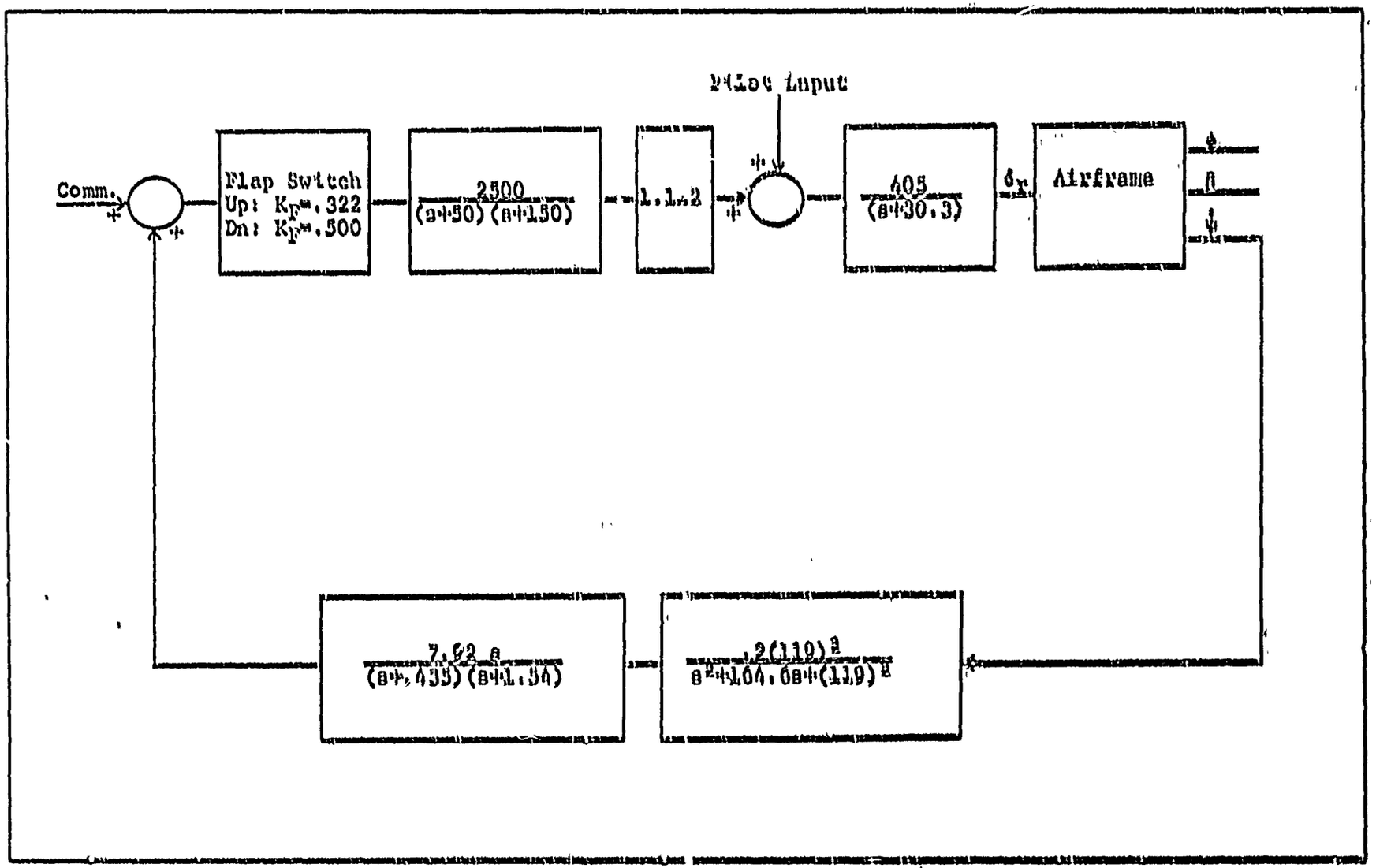

Figure 4. Yaw Damper System for MC-135

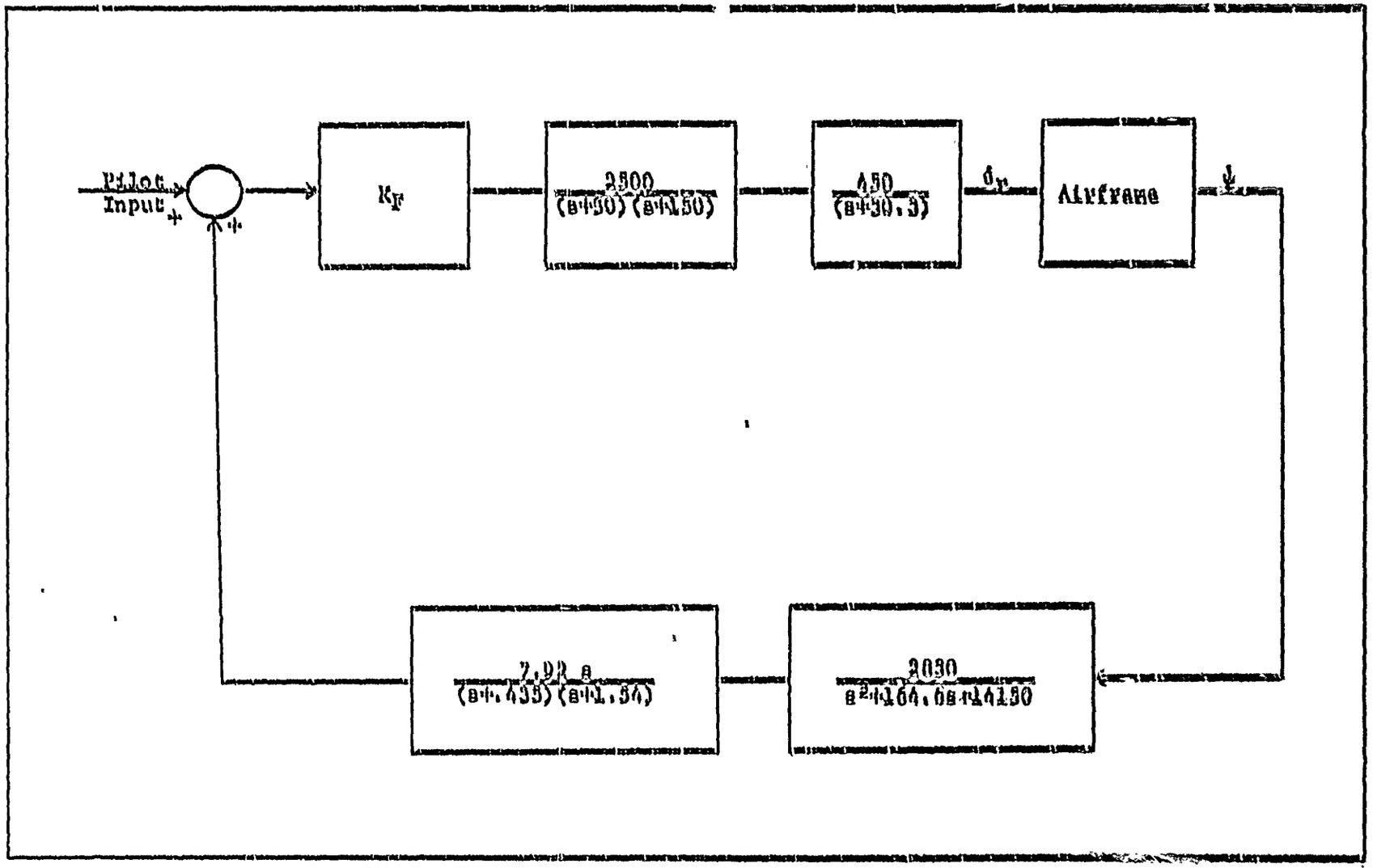

Figure 5. Yaw Damper System for Root Locus Analysis

Finally the complete airframe transfer functions for each of the three flight conditions are formed by combining (2-12) and (2-9), (2-13) and (2-13), and (2-14) and (2-11) for Cruise 1, Cruise 2, and Power Approach, respectively. The final airframe transfer functions are given as equations (2-15), (2-16), and (2-17).

Cruise 1:

$$\frac{\dot{\psi}}{\delta_r} = \frac{-.524\, s(s + .68)(s - .09 \pm j.35)}{s(s + .00935)(s + .62)(s^2 + .0189s + .793)} \qquad (2\text{-}15)$$

Cruise 2:

$$\frac{\dot{\psi}}{\delta_r} = \frac{-.838\, s(s + .875)(s - .0716 \pm j.387)}{s(s + .0114)(s + .886)(s^2 - .009s + 1.05)} \qquad (2\text{-}16)$$

Power Approach:

$$\frac{\dot{\psi}}{\delta_r} = \frac{-.335\, s(s + 1.13)(s - .044 \pm j.396)}{s(s + .024)(s + 1.14)(s^2 + .052s + .55)} \qquad (2\text{-}17)$$

Root Locus Analysis

To get an overall idea as to the effectiveness of the standard series yaw damper, a root locus was plotted for each of the three flight conditions. The procedure is illustrated for only Cruise 1. Root locus plots for Cruise 2 and Power Approach are determined by simply changing the transfer function of the airframe. All other blocks remain the same.

Equation (2-15), the transfer function which represents the yaw rate to rudder input for the airframe in Cruise 1, is substituted into the block diagram of Fig.5. The open-loop transfer function for the yaw damper system for Cruise 1 is then determined as given in equation (2-18).

$$GH = \frac{K\, s(s+.69)(s-.09\pm j.35)}{(s+.009)(s+.435)(s+.62)(s+1.54)(s+30.3)(s+50)(s+150)(s+.009\pm j.89)(s+82.3\pm j85.9)} \qquad (2\text{-}18)\,(1)$$

where $K = -132 \times 10^8\, K_F$

K_F = flap switch gain

The root locus plot of the basic yaw damper system for Cruise 1 is shown in Fig. 6. The root locus plots of the same system but for Cruise 2 and Power Approach are shown in Fig. 7 and 8. It should be noted that, for simplicity, only those branches of the root locus that contain the most dominant closed-loop roots are plotted. However, all of the poles and zeros were used to compute the root locus. For an illustration, the output of the root locus program, which was used to plot the root locus in Fig. 6, is given as Appendix E.

To better organize the analysis and design of an effective SAS, it was decided to concentrate the efforts on just one of the flight conditions. Once a satisfactory system was designed, adjustments could then be made as necessary for the other two flight conditions. Since a large part of the overall performance envelope is covered by the cruise conditions, it was felt the system design should be based on one of these conditions. Root locus analysis of the basic system for Cruise 1 and 2 (Figs. 6 and 7) showed that the aircraft performance with the damper ON was likely to be less desireable in Cruise 1 than Cruise 2. Therefore, it was then decided to develop a SAS that would sufficently improve the performance in Cruise 1. Cruise 2 should then follow with at least as good a performance.

(1) For clarity, second order terms are written in factored form, $s + \zeta\omega_\eta \pm j\omega_\eta\sqrt{1-\zeta^2}$, rather than as $s^2 + 2\zeta\omega_\eta s + \omega_\eta^2$.

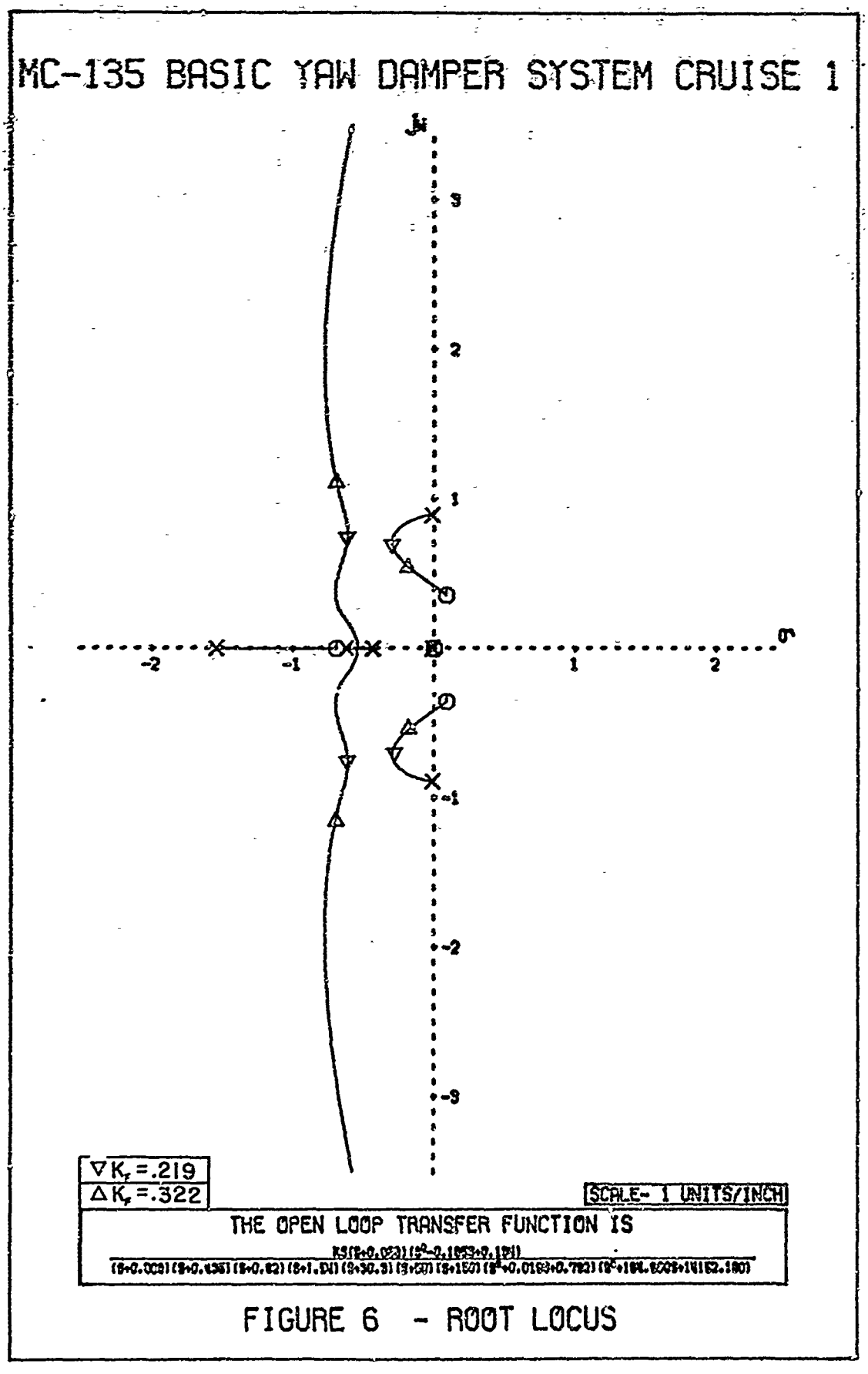

FIGURE 6 - ROOT LOCUS

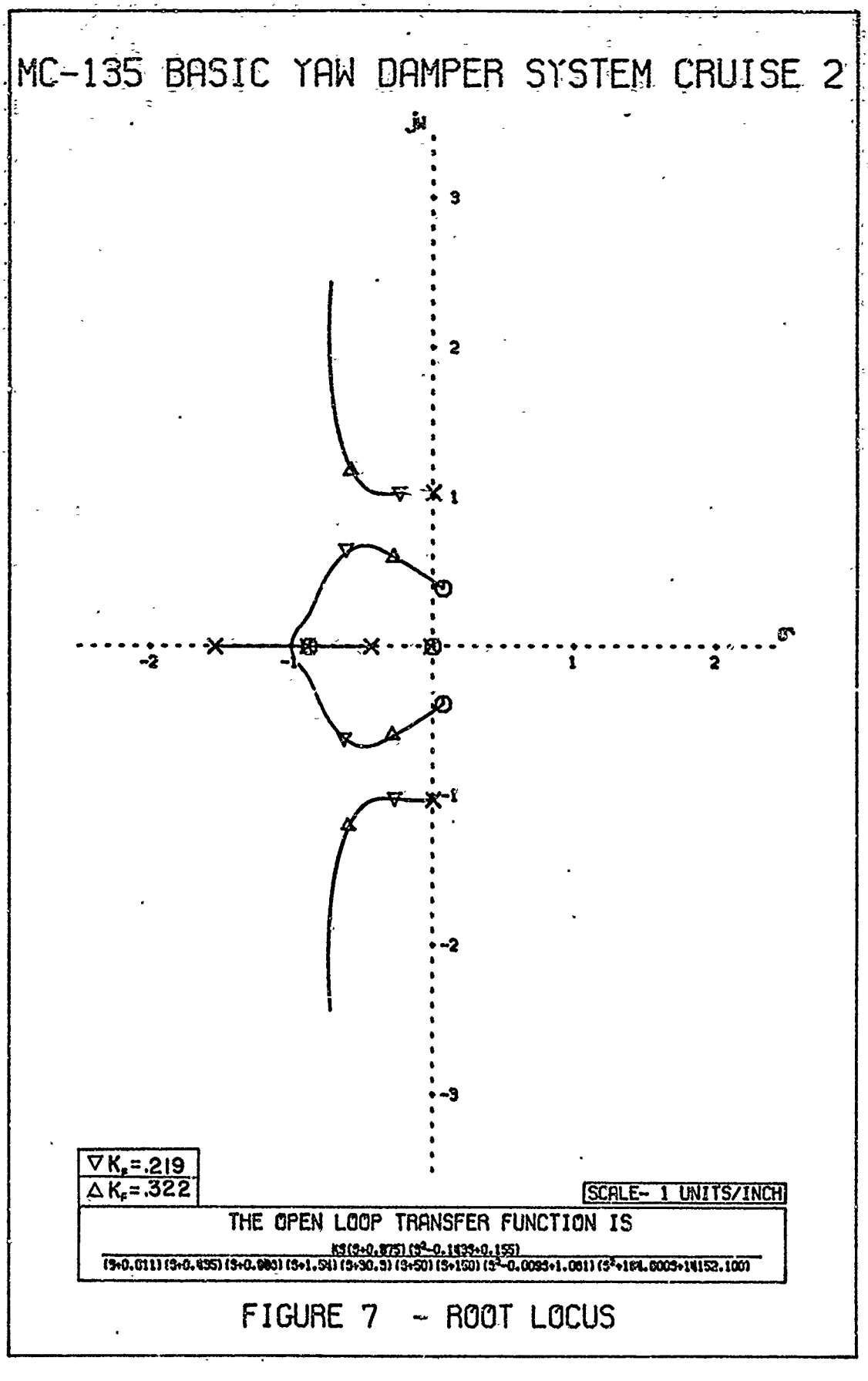

FIGURE 7 - ROOT LOCUS

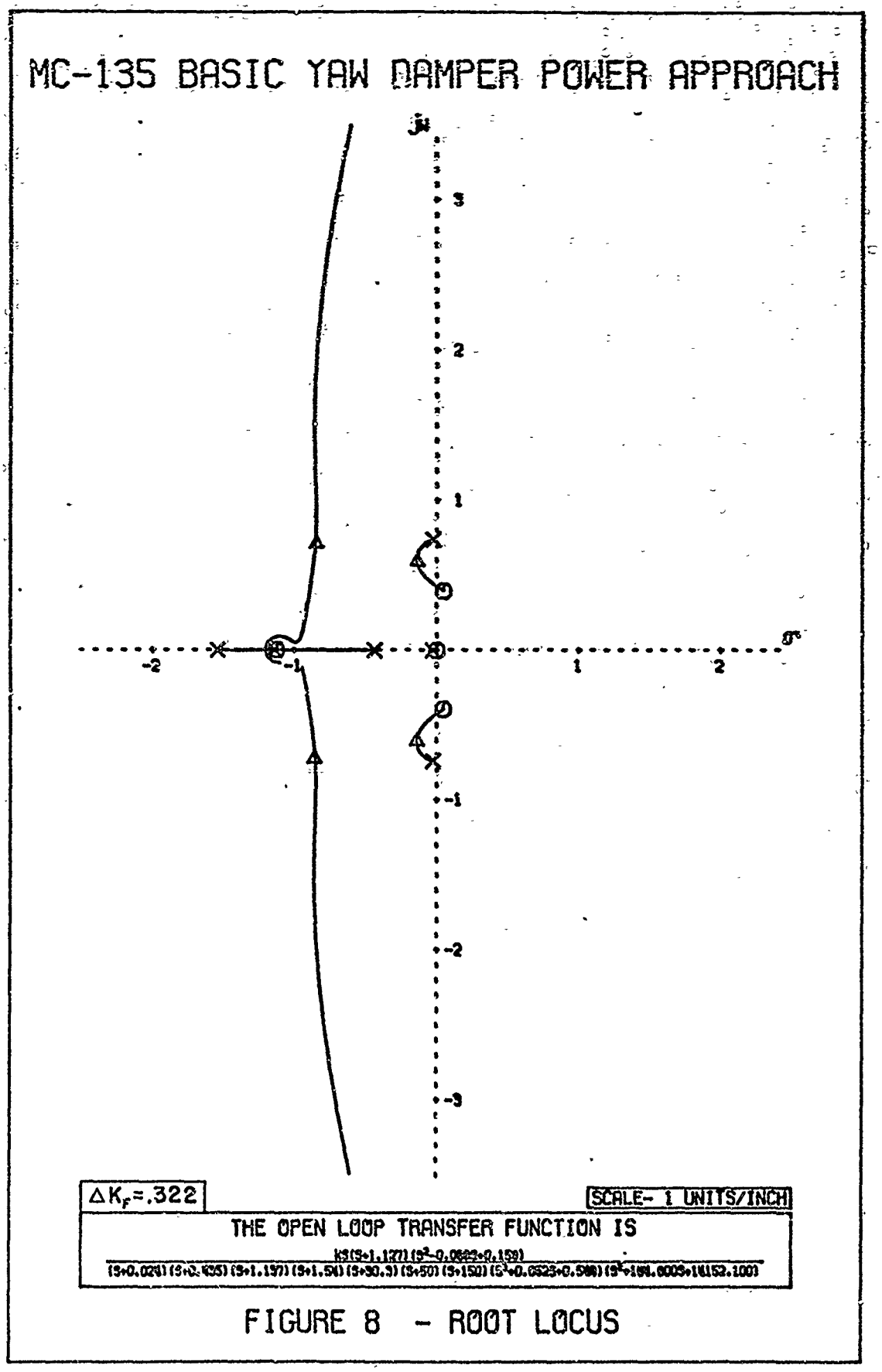

FIGURE 8 - ROOT LOCUS

Investigation of Power Approach was reserved until last. Since the transition from cruise to Power Approach is not gradual but rather is well defined as beginning when flaps are lowered, it was felt that, if necessary, additional compensators and gain adjustments could be added at the time the power approach mode was entered.

Naturally, one would first try to improve the system performance by a simple gain adjustment. From Fig. 6, the root locus of the basic airframe and damper, it is seen that when the loop gain is set at the normal value, i.e., $K_F = .322$, the system becomes predominantly one of fourth order (two complex pairs of roots). Immediately, this poses a major problem with system analysis since the theory that has been developed for this kind of work applies basically to systems which exhibit oscillatory characteristics that are predominantly second order. Therefore, the analysis becomes one of a series of rather judicious assumptions.

Assume for now that the complex roots, located along the branches which go from the poles at $(s + .009 \pm j.89)$ to zeros at $(s - .09 \pm j.354)$, are dominant. Then, at the normal gain setting ($K_F = .322$) it is seen from the root locus plot (Fig. 6) that the performance could be improved if the gain was decreased to the value that positioned the closed loop roots at the largest negative real value possible. As discussed earlier, the main criterion for the root locus analysis is to achieve the required $\zeta\omega_\eta$ which is, in fact, the negative real part, σ, of a complex pair of roots. For this case, the maximum $\zeta\omega_\eta$ is obtained if K_F is set at .219.

However, it is immediately seen that even though it is the maximum $\zeta\omega_\eta = .29$, it does not satisfy the criterion of $\zeta\omega_\eta \geq .35$. Remember

that, due to the fourth order effect, the system performance cannot be based entirely on just this complex pair. However, later analog computer simulation did show that the root in question does have the primary effect on output response of the system and that the specified value for $\zeta_n \geq .35$ could not be reached.

In order to develope a SAS to achieve the necessary value of ζ_n some sort of compensation must be incorporated. The immediate objective was to reposition the branches of the root locus through the use of a cascade compensator. Eventually, several forms of cascade compensators were tried as discussed in Appendix C. As is shown, even the more sophisticated compensators had only a minor effect on reshaping the root locus, particularly the branches going from the poles at $(s + .009 \pm j.89)$ to the zeros at $(s - .09 \pm j.354)$. Since no simple or practical passive compensator could be found that produced any significant improvement, it was decided that the response would have to be improved by augmenting the yaw rate feedback with an additional feedback quantity. As is known, the Dutch roll is characterized as a combined motion of yaw, ψ, sideslip, β, and roll, ϕ. Since in the original yaw damper, ψ is suppressed by sensing and feeding back $\dot{\psi}$, as a rudder control, it was decided to augment the system by sensing and feeding back β to the rudder.(2) However, to do this requires that a complete sideslip sensor be installed on the aircraft. In the interests of simplicity, the idea of a sideslip sensor was abandoned in favor of a simpler method - that of sensing lateral acceleration, a_y, which requires only an accelerometer at the aircraft c.g. Referring to Fig. 2,

(2) Augmenting $\dot{\psi}$ feedback with $\dot{\phi}$ feedback was also tried, but proved unsuccessful as discussed in Appendix C.

it can be seen that $\beta = \frac{v}{U_0}$ and $a_y = \dot{v}$. Then, in effect, sensing a_y is analogous to sensing $\dot{\beta}$ which is quite desireable to minimize β itself.

It is important to point out at this time, that feeding back signals to the aileron was considered and found not to be practical. Adapting such a SAS to a C-1353 would require quite an extensive hardware modification.

Development of Acceleration Feedback System

Before proceeding with a root locus analysis of the yaw damper augmented with acceleration feedback (hereafter referred to as simply the SAS), the transfer function for lateral acceleration, a_y, must be incorporated into the block diagram of Fig. 3.

The required transfer function for lateral acceleration to rudder deflection is given as Eq (2-19).

$$\frac{a_{yt}}{\delta_r} = Y_{\beta\delta_r}\frac{\beta}{\delta_r} + Y_{r\delta_r}\frac{\dot{\psi}}{\delta_r} + Y_{p\delta_r}\frac{\dot{\phi}}{\delta_r} + Y_{\delta_r} + \ell_x\ddot{\psi} \qquad (2\text{-}19)$$

where a_{yt} - total lateral acceleration

ℓ_x - distance of the c.g. to the point of measurement (forward is positive)

A detailed development of Eq (2-19) is presented in Appendix A.

Substituting the appropriate transfer functions and constants from Appendix D and Table II for Cruise 1 with $\ell_x = 0$, Eq (2-19) becomes

$$\frac{a_{ycg}}{\delta_r} = \frac{16.68\,(s + .193)(s + .967)(s - .068)(s - .61)}{(s + .00935)(s + .62)(s + .00945 \pm j.89)} \qquad (2\text{-}20)$$

The block diagram of the system with acceleration feedback is shown in Fig. 9. In the actual system, the two feedbacks, $\dot{\psi}$ and a_y,

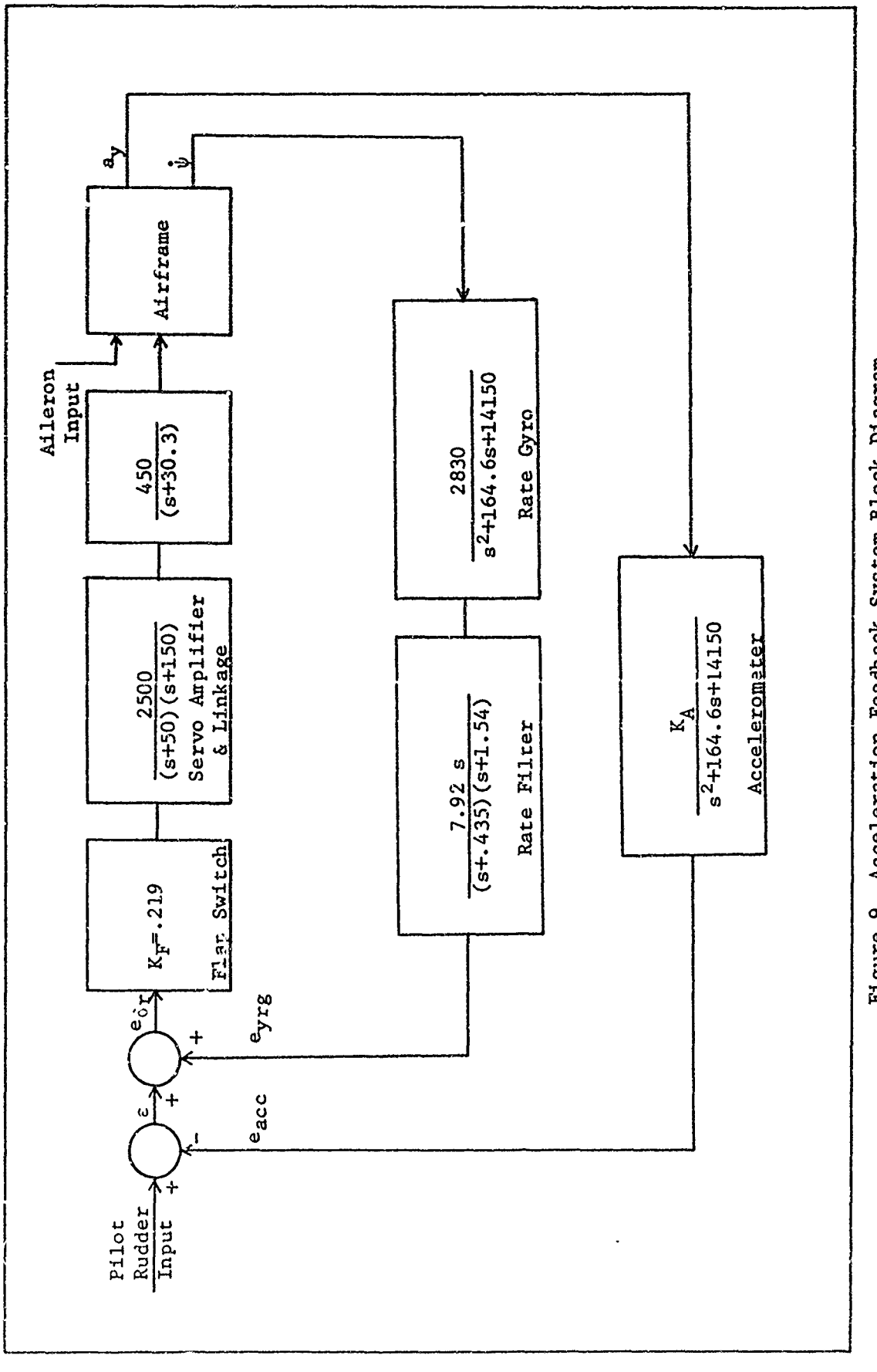

Figure 9. Acceleration Feedback System Block Diagram

would be blended first and their sum fed back. However, to simplify the analysis, the acceleration feedback loop is treated as a complete outer loop. It can be shown that the two systems are in fact equal.

To facilitate a root locus analysis, it is necessary to reduce the block diagram of Fig. 9 to one with a single input and single output. This requires a transfer function for $\frac{a_y}{\dot{\psi}}$. Since the yaw rate and lateral acceleration transfer functions have the same denominator, the ratio $\frac{a_y}{\dot{\psi}}$ is simply the ratio of the numerators. Thus

$$\frac{a_y}{\dot{\psi}} = \frac{-31.9\ (s + .343)(s + .945)(s - .076)(s - .62)}{(s + .6884)(s - .0923 \pm j.354)} \qquad (2\text{-}21)$$

Using (2-21) and combining the blocks of the inner loop, the system can be redrawn as shown in Fig. 10.

To find the closed-loop transfer function, $\frac{\dot{\psi}}{\epsilon}$, of the inner loop, the numerator is determined by forming the product of the numerator of the forward loop and the denominator of the feedback loop (denoted by N_1D_2). The denominator of $\frac{\dot{\psi}}{\epsilon}$ is determined by finding all the closed-loop roots of the inner loop on the root locus at a static-loop sensitivity, $K_{SLS} = -2900 \times 10^6$. After cancelling the open-loop roots of the rate gyro, the transfer function, $\frac{\dot{\psi}}{\epsilon}$, becomes

$$\frac{\dot{\psi}}{\epsilon} = \frac{-12.9\times10^4(s+.435)(s+.6884)(s+1.54)(s-.0923\pm j.354)}{(s+.009)(s+.605\pm j.768)(s+.74)(s+30.5)(s+49.9)(s+150)(s+.3\pm j.7)} \qquad (2\text{-}22)$$

Substituting (2-22) for the inner loop of Fig. 10, the system can be redrawn as shown in Fig. 11.

The open loop transfer function of the outer loop, GH_{OL}, can now be obtained from the block diagram of Fig. 11. The result is given as Eq (2-23).

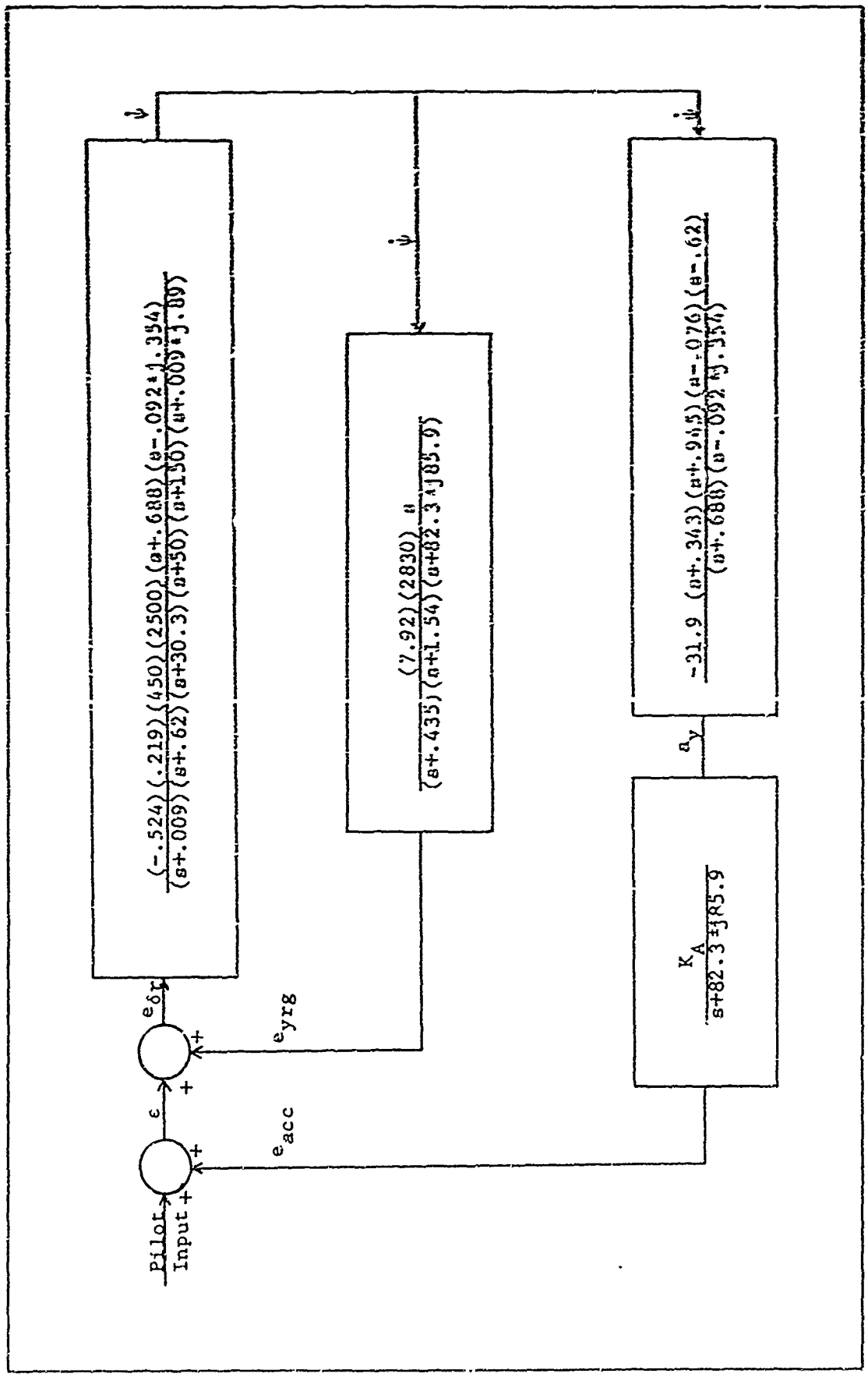

Figure 10. Simplified Block Diagram of Accelaration Feedback System

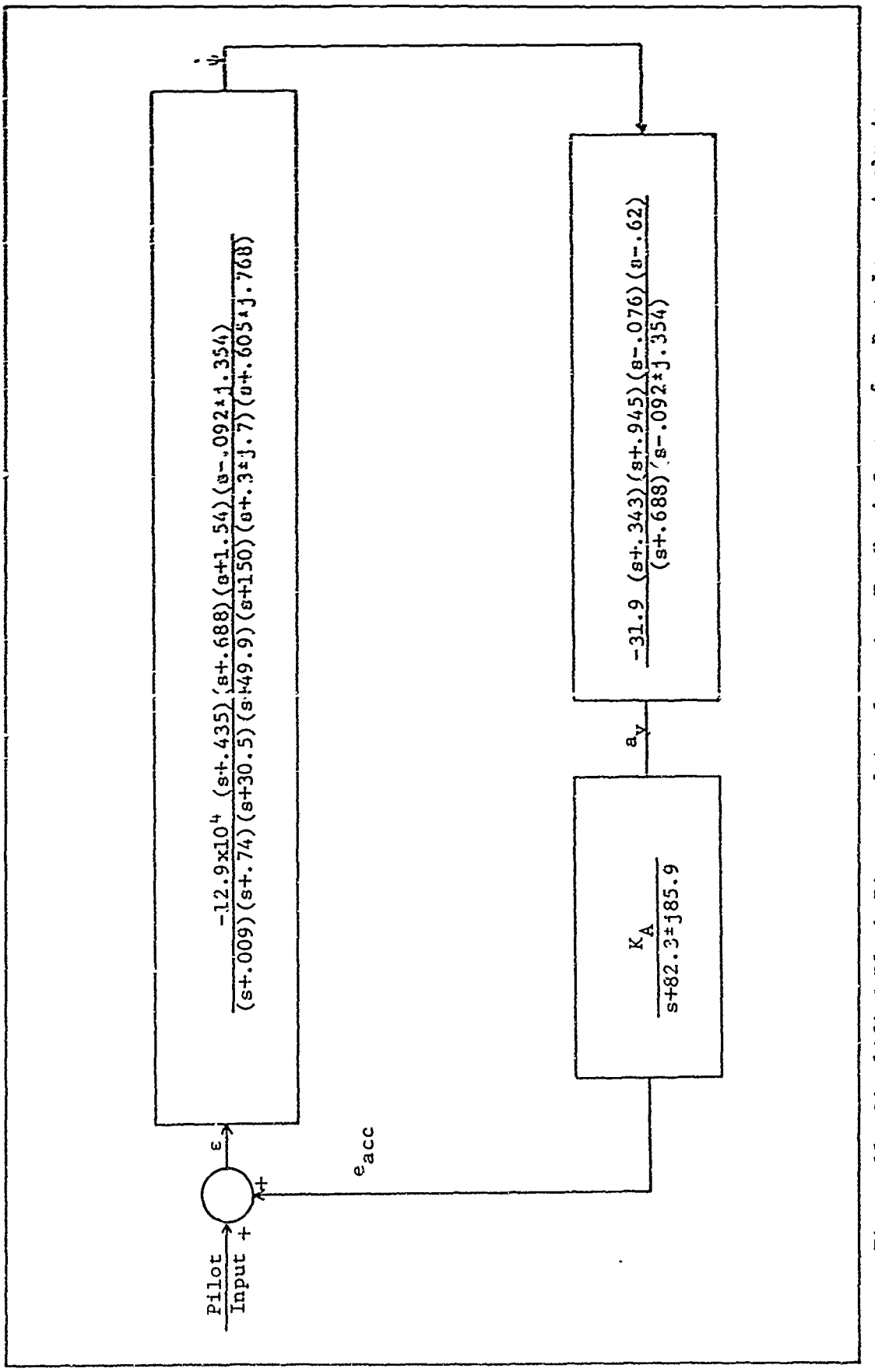

Figure 11. Simplified Block Diagram of Acceleration Feedback System for Root Locus Analysis

$$GH_{OL} = \frac{4.12\times10^{6}\, K_A(s+.435)(s+1.54)(s+.343)(s+.945)(s-.076)(s-.62)}{(s+.009)(s+.74)(s+30.5)(s+49.9)(s+150)(s+.3\pm j.7)(s+.605\pm j.768)(s+82.3\pm j85.9)} \quad (2\text{-}23)$$

Note, that in writing (2-23), the factors of $(s + .688)$ and $(s - .092 \pm j.354)$ were cancelled.

The addition of acceleration feedback creates a non-minimum phase angle transfer function which means that, for best results, the sign of the feedback must be reversed. To properly analyze this system requires a zero angle root locus rather than the conventional 180 degree root locus. Using Eq (2-23), the root locus for the outer loop can now be drawn as shown in Fig. 12.

The final question that now remains is where to select the location of the closed loop roots to achieve the desired oscillatory characteristics, namely $\zeta > .19$, $\omega_n > .65$, and $\zeta\omega_n > .35$. As illustrated in Fig. 12, the system is not predominantly second order but one of at least fourth order (two sets of complex roots) or even higher depending on how close the real roots are to their respective zeros. The analysis is further complicated by the fact that the specified quantities of ζ and ω_n really have meaning only with regard to a simple second order system. However, one advantage to the SAS is immediately evident. The location of both sets of closed loop roots can now be selected such that each pair has a $\zeta\omega_n > .35$ for a given value of K_{SLS}. Before with just yaw rate feedback, the $\zeta\omega_n$ of the troublesome root could never have a value greater than .29.

Since this system is not predominantly second order, the analysis was done by selecting a root location such that the average $\zeta\omega_n$ of both pairs of dominant roots were the largest possible. Proof that such a

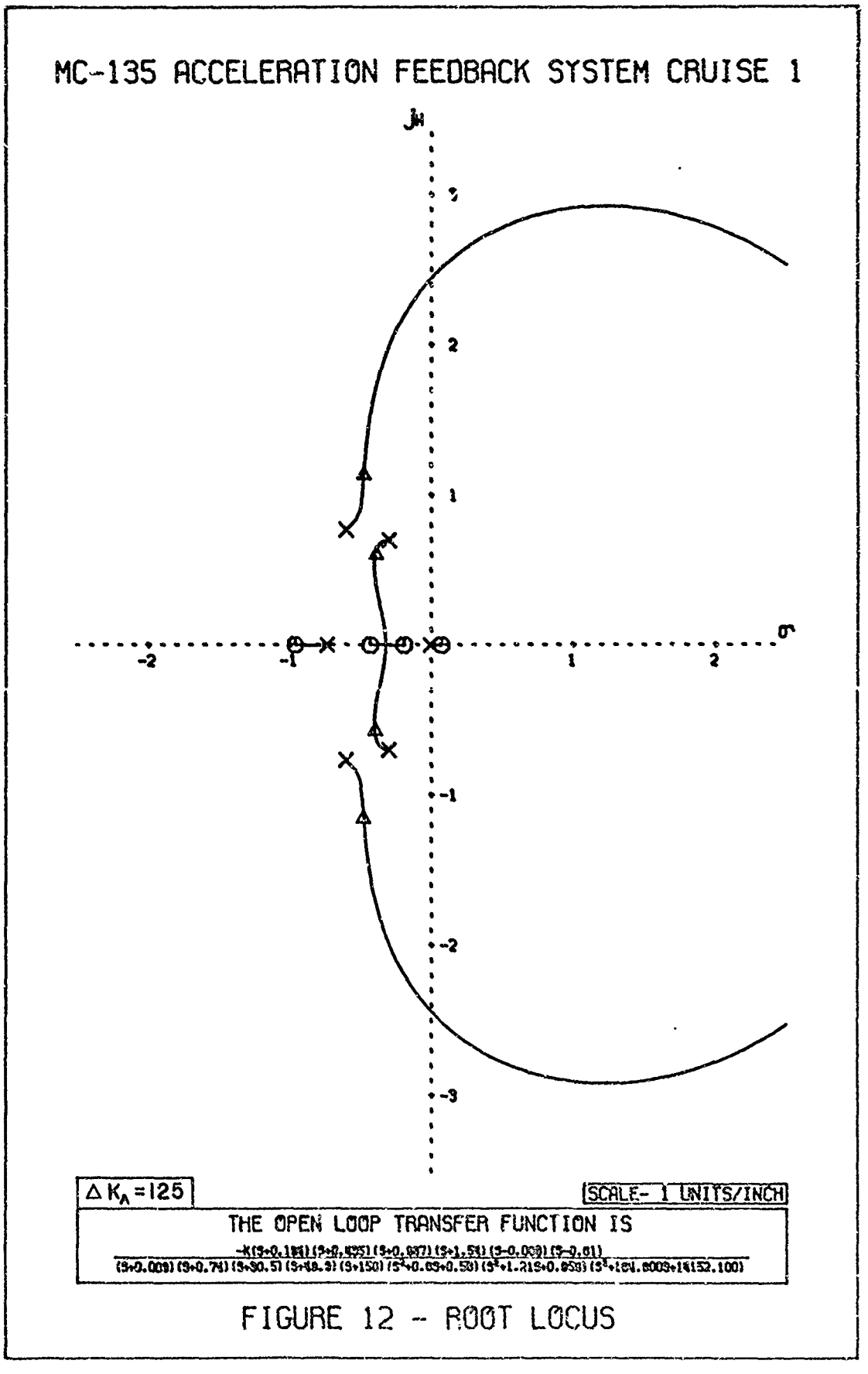

FIGURE 12 - ROOT LOCUS

procedure is valid can best be seen from analog computer results. These are discussed in detail in the next chapter.

Referring to the root locus of the SAS (Fig. 12) and comparing it to that of the basic yaw damper system (Fig. 6), it appears that by using acceleration feedback, the ω_n of one of the roots can be substantially increased while a relatively high ζ is maintained. (A rapidly decreasing ζ was the major problem with the original system.) It can further be seen from Fig. 12 that several root locations result in an average $\zeta\omega_n$ of approximately .45. However, to take full advantage of the resulting higher ω_n, a K_{SIS} that would result in a root being located at the highest ω_n was used while a $\zeta\omega_n$ of .45 was maintained. The K_{SIS} required for this location of roots is $K_{SIS} = 45 \times 10^7$. From Eq (2-23),

$$K_{SIS} = 41.2 \times 10^5 K_A$$

Then the required acceleration feedback constant is

$$K_A = \frac{45 \times 10^7}{41.2 \times 10^5} = 110$$

From this value of K_A, the actual gain or sensitivity, S_A, of the accelerometer is computed by taking the limit as $s \to 0$ of the accelerometer transfer function. The result is then

$$S_A = \lim_{s \to 0} \frac{110}{s^2 + 164.6s + 14152}$$

$$S_A = .008$$

Acceleration Feedback System for Cruise 2. As stated earlier, the objective was to design a complete SAS for Cruise 1, assuming that when

transferring to Cruise 2, the performance would improve slightly or at least would not deteriorate. With all gains held constant, Eq (2-16) and $\frac{a_{yc_B}}{\delta_r}$ from Table XV are substituted into the block diagram in Fig. 10. This now represents the complete SAS for Cruise 2. The open loop transfer function can now be found and the root locus plotted. The resulting root locus is shown in Fig. 13.

From Fig. 13, it can be seen that Cruise 2 differs from that of Cruise 1 primarily in that the closed loop root on the upper branch now has an ω_n = 1.55 as compared to an ω_n = 1.1 for Cruise 1. However, ζ for the same root has decreased from .40 to .30. The other pair of roots is unchanged. It can therefore be assumed that the net oscillatory response of the system in Cruise 2 will have a higher frequency but less damping with $\zeta\omega_n$ remaining approximately constant. Later analog verification shows the oscillatory response to indeed have a higher ω_n but with the ζ remaining approximately constant so that $\zeta\omega_n$ is actually improved. With such results, a gain adjustment when transitioning from Cruise 1 to Cruise 2 was not necessary.

Acceleration Feedback System for Power Approach. From the root locus of the basic yaw damper system for Power Approach (Fig. 8), it can be seen that the one pair of closed loop roots (inner-loop closed loop roots) is now very close to the imaginary axis. From this, it can be expected that the damping of the oscillatory response will be very low. The maximum $\zeta\omega_n$ that can be obtained from this pair of roots is .14 as opposed to .29 for Cruise 1 and .33 for Cruise 2. Further analysis shows that when using the same gains as used for Cruise 1 and 2, the $\zeta\omega_n$ of this root is only .12. The best $\zeta\omega_n$, i.e., a $\zeta\omega_n$ = .14, is obtained if K_r is adjusted from .219 to .322. In the actual system

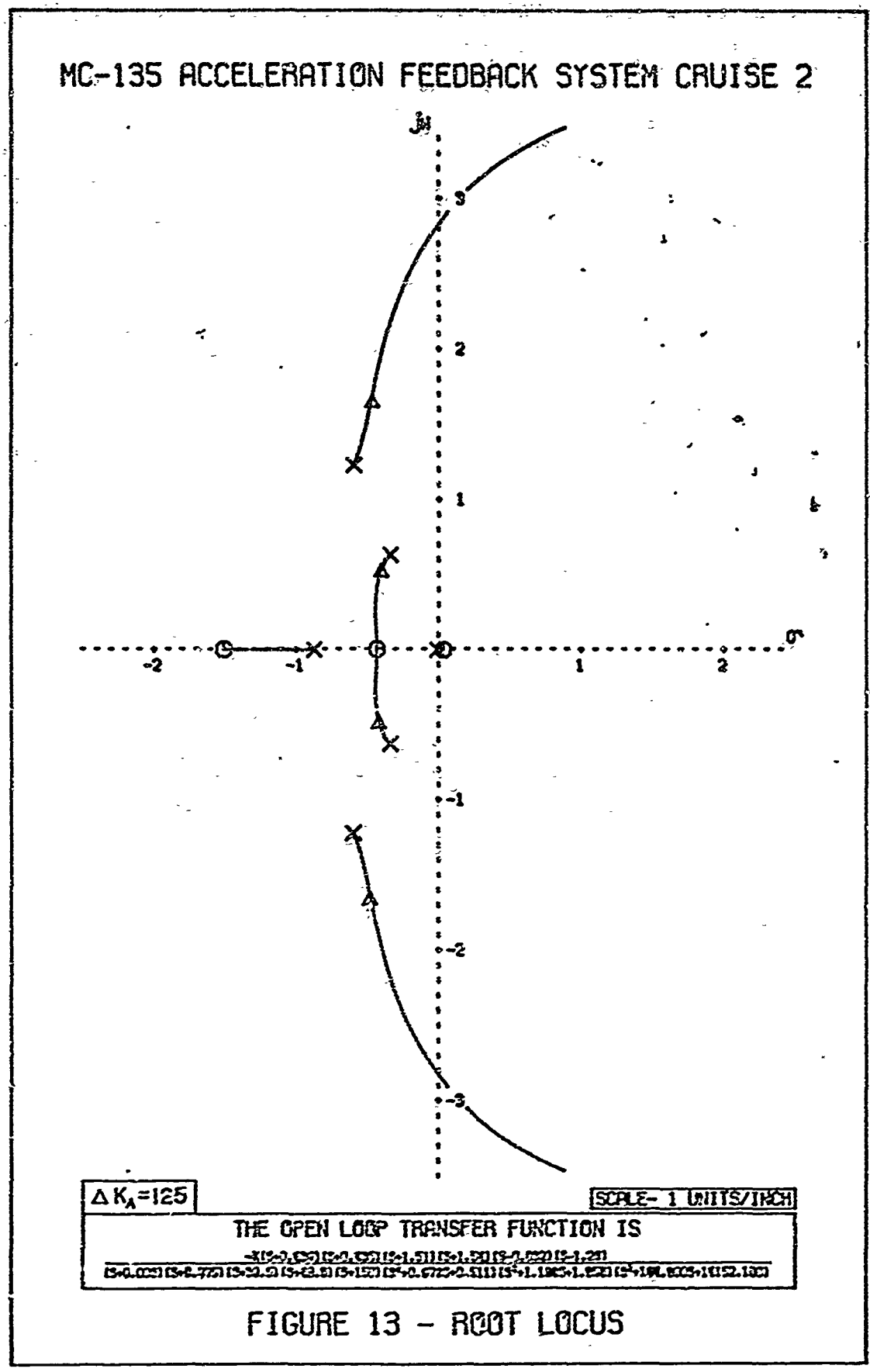

FIGURE 13 - ROOT LOCUS

this can be done quite easily by changing resistors in the flap switch which was originally setup to switch K_F from .322 to .500 when entering the power approach mode.

With the inner loop now adjusted, a block diagram of the complete system with acceleration feedback can be obtained by substituting (2-17) and $\frac{a_{ycg}}{\delta_r}$ for Power Approach from Table XV into the block diagram of Fig. 10. Again, the open loop transfer function is determined and the root locus plotted as shown in Fig. 14.

Note that the value of $K_A = 110$, as used in Cruise 1 and 2, results in the system having both pairs of second order roots at rather low ω_η. Even though the ζ for each pair is relatively high, experience from analyzing the cruise conditions has shown that the ω_η of the upper pair of roots has a great influence on the net oscillatory response of the system. It would therefore be expected that the lower ω_η obtained when $K_A = 110$ would result in a sluggish response in Power Approach. This was quite evident from the first analog computer runs for Power Approach.

In order to correct the undesirable response, the accelerometer constant, K_A, was merely increased to the point where the $\zeta\omega_\eta$ of each pair of roots reached the same value as for Cruise 1 and 2.

This criterion was used here primarily because these particular values of $\zeta\omega_\eta$ produced the most desirable response in the cruise conditions and it therefore seems logical to assume that the same would be true for Power Approach. The values of $\zeta\omega_\eta$ that are desired are .48 for the upper roots and .40 for the lower roots. Following this procedure, K_A was set at 538. Referring to the root locus (Fig. 14) it can be seen that, at this setting of gain, the ω_η of the upper root is now

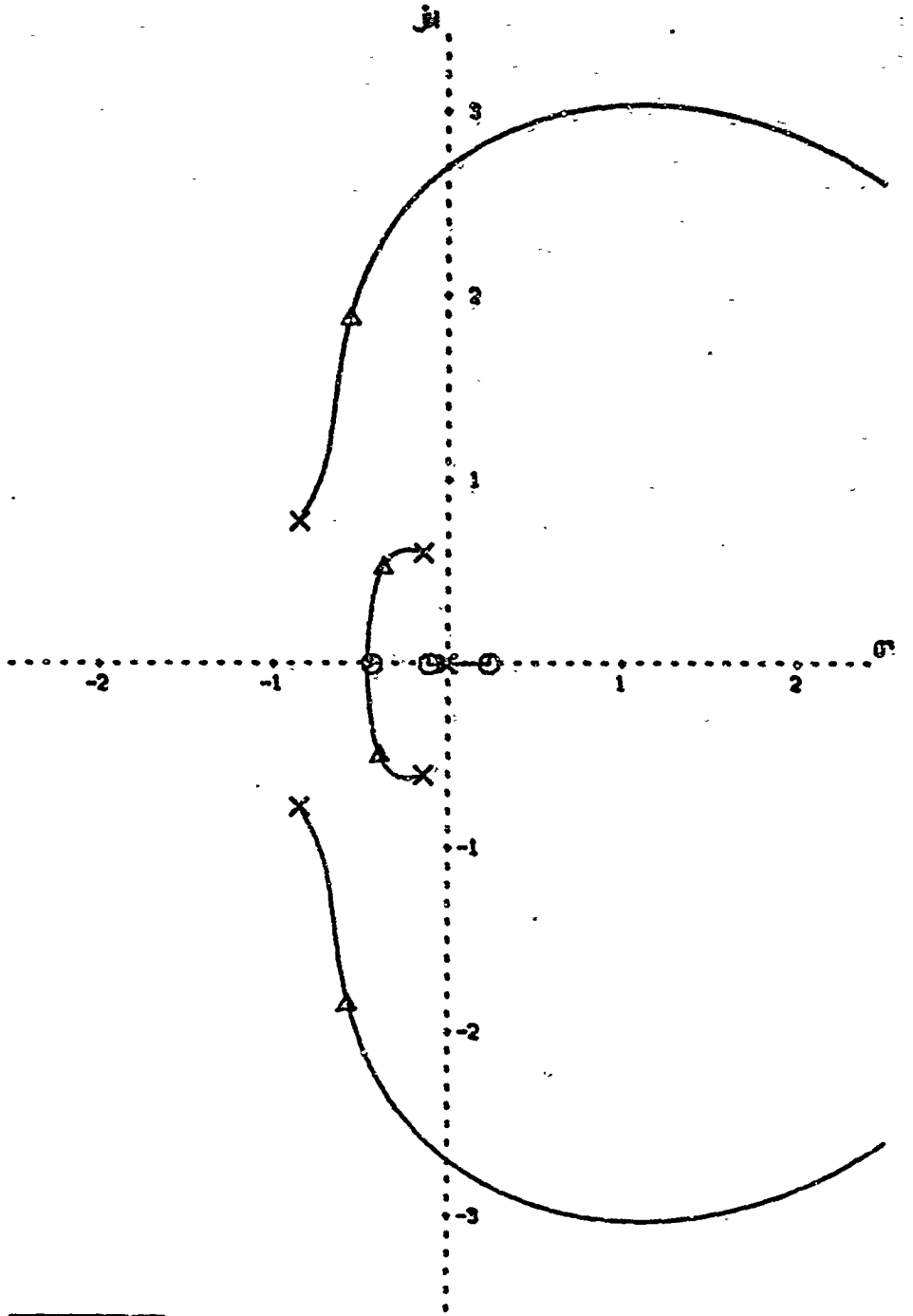

FIGURE 14 - ROOT LOCUS

2.1 radian per second while the $\zeta\omega_n$ of each root is the same as for Cruise 1 and 2. It can therefore be concluded, as is quite evident from the analog time histories, that the net frequency of the oscillatory response for Power Approach has been greatly increased.

Final System Adjustments

Final gain adjustments were made based on subsequent results from the analog simulation. It was determined that the optimum response for Cruise 1 is obtained for a $K_A = 125$ instead of the previously computed value of 110. The adjustment in K_A also improved the response for Cruise 2.

Similarly, final adjustments of K_A were made for Power Approach. It was determined that the optimum response is obtained for $K_A = 440$ as compared to the previously computed value of 538.

As evident from the design, in order to maintain satisfactory performance when transitioning from a cruise condition to Power Approach, an accelerometer gain change from $K_A = 125$ to 440 is required. Since a "variable gain" accelerometer is not practical, the same objective can be accomplished by using an accelerometer with $K_A = 440$ and simply attenuating its output when in cruise, such that the net effect would be a $K_A = 125$. This can most easily be done by adding a secondary "flap switch" located in the outer loop feedback loop. This second switch, designated K_S and equal to $\frac{125}{440} = .284$, can work in conjunction with the primary flap switch, K_F. During cruise, K_F is set at .219 while K_S is set at .284. When extending the flaps for Power Approach, K_F will be switched to .322 and K_S to 1.0. A block diagram of the final system is shown in Fig. 15.

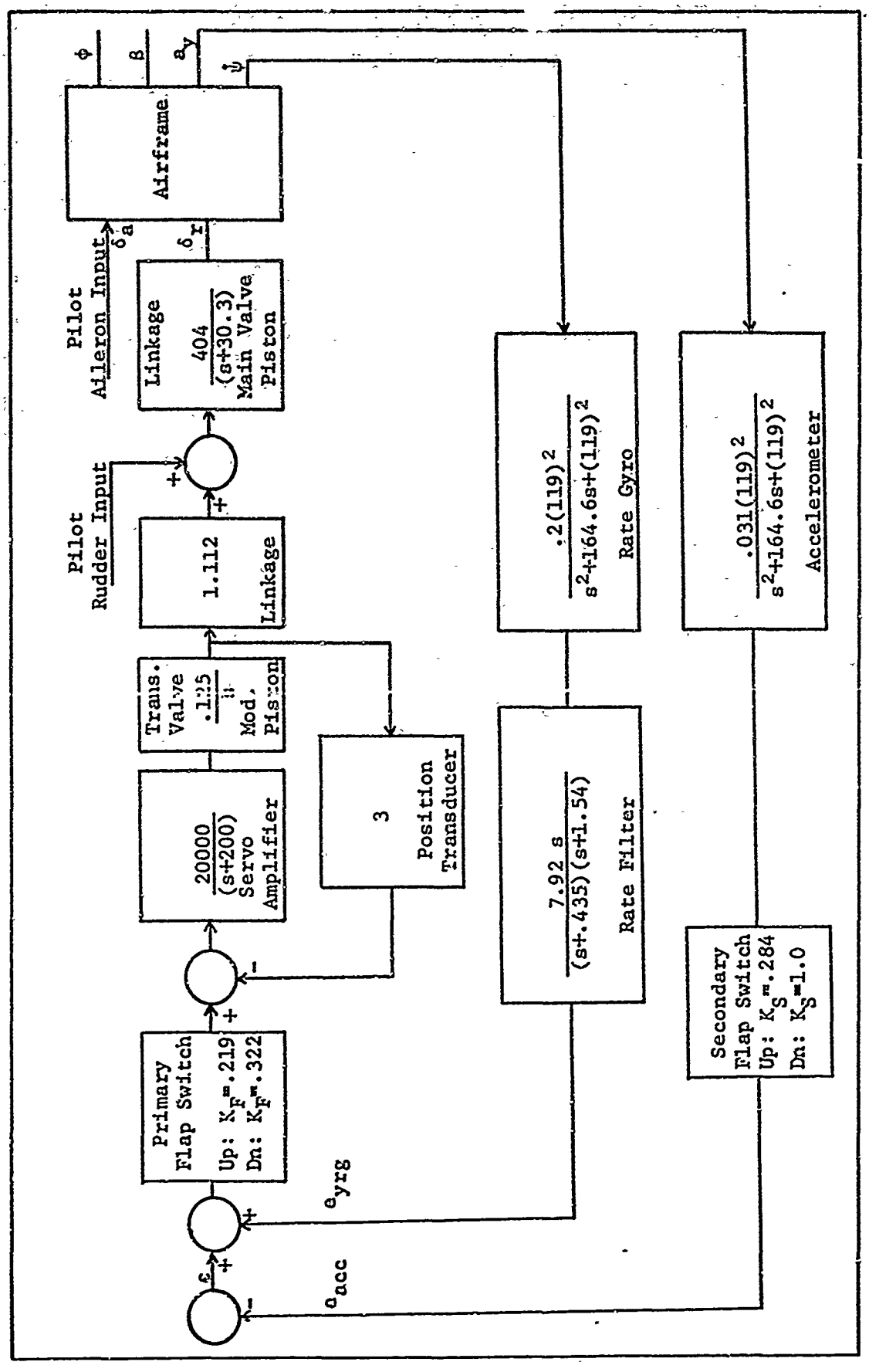

Figure 15. Complete System Block Diagram

III. Requirements

The SAS was designed, primarily, to improve the Dutch roll damping (ζ) and frequency (ω_η) to acceptable values. However, damping and frequency are not the only criteria that have to be investigated to determine good flying qualities. Therefore other requirements, in addition to ζ and ω_η, have to be considered. Performance requirements for the SAS plus airplane flying qualities were chosen from MIL-F-8785A, considered the latest in flying qualities criteria, and are listed in Table III.

Techniques of Measurements

The parameters required to check the first requirement are frequency (ω_η) and damping (ζ) as well as their combination ($\zeta\omega_\eta$). Since the simulated system contains two sets of complex roots, the techniques used to measure ζ and ω_η vary slightly from the techniques used for a simple second-order system.

Damping and Frequency. Figures 16 and 17 illustrate the method used to obtain ζ and ω_η. First, determine the transient peak ratio (TPR) from

$$TPR = \frac{\Delta X_2}{\Delta X_1} = \frac{\Delta X_3}{\Delta X_2} \tag{3-1}$$

Use this TPR value to read ζ from Fig. 17 (Ref 9). The damped period (T) is the time between two successive peaks or between every other crossing of the steady state value. With both the damped period and the damping ratio known, the undamped natural frequency can be deter-

Table III

Requirements

Req No	MIL-F-8785A Para	Requirement
1	3.3.1.1	Dutch roll damping $\geq$ .19 Dutch roll frequency $\geq$ .60 Damping x frequency $\geq$ .35 Note: The governing ζ requirement is that yielding the largest value
2	3.3.1.2	Roll mode time constant $\leq$ 1.4 sec
3	3.3.1.3	Spiral stability - time to double bank angle $\geq$ 20 sec
4	3.3.2.2	Roll rate (large inputs) - first minimum $\geq$ 25 per cent of first peak
5	3.3.2.2.1	Roll rate (small inputs) - P_{osc}/P_{av} must be within limits of Fig. 25
6	3.3.2.4	Sideslip (large inputs) - $\beta \leq$ 10K
7	3.3.2.4.1	Sideslip (small inputs) - $\Delta\beta_{max}$ must be within limits of Fig. 27

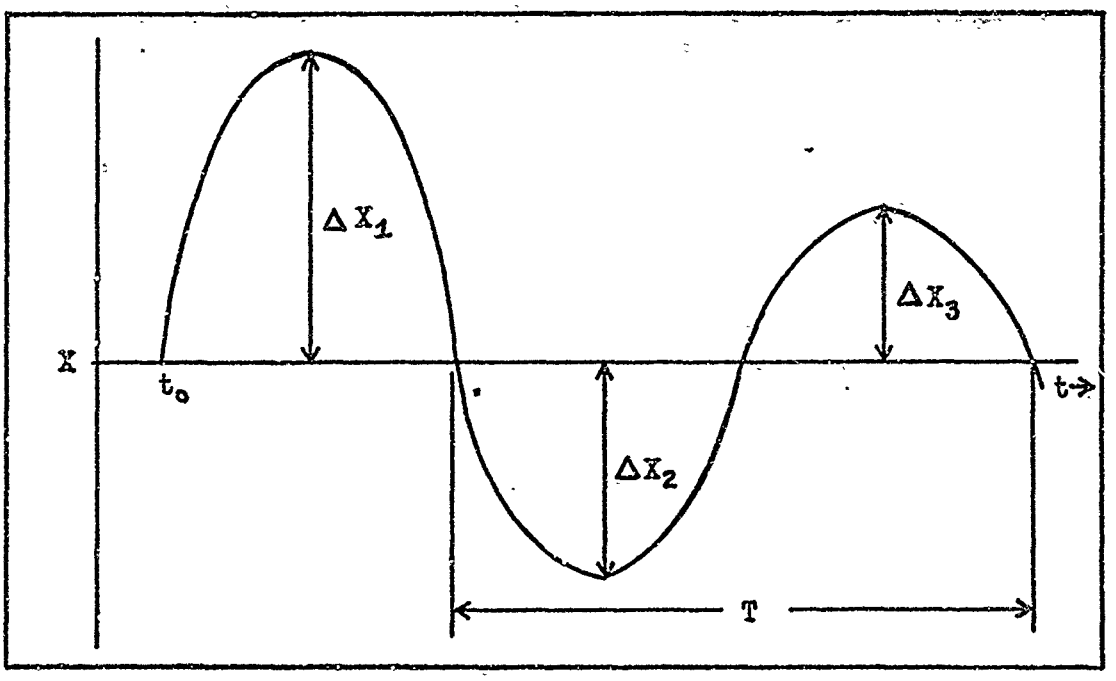

Figure 16. Determining Transient Peak Ratio (TPR)

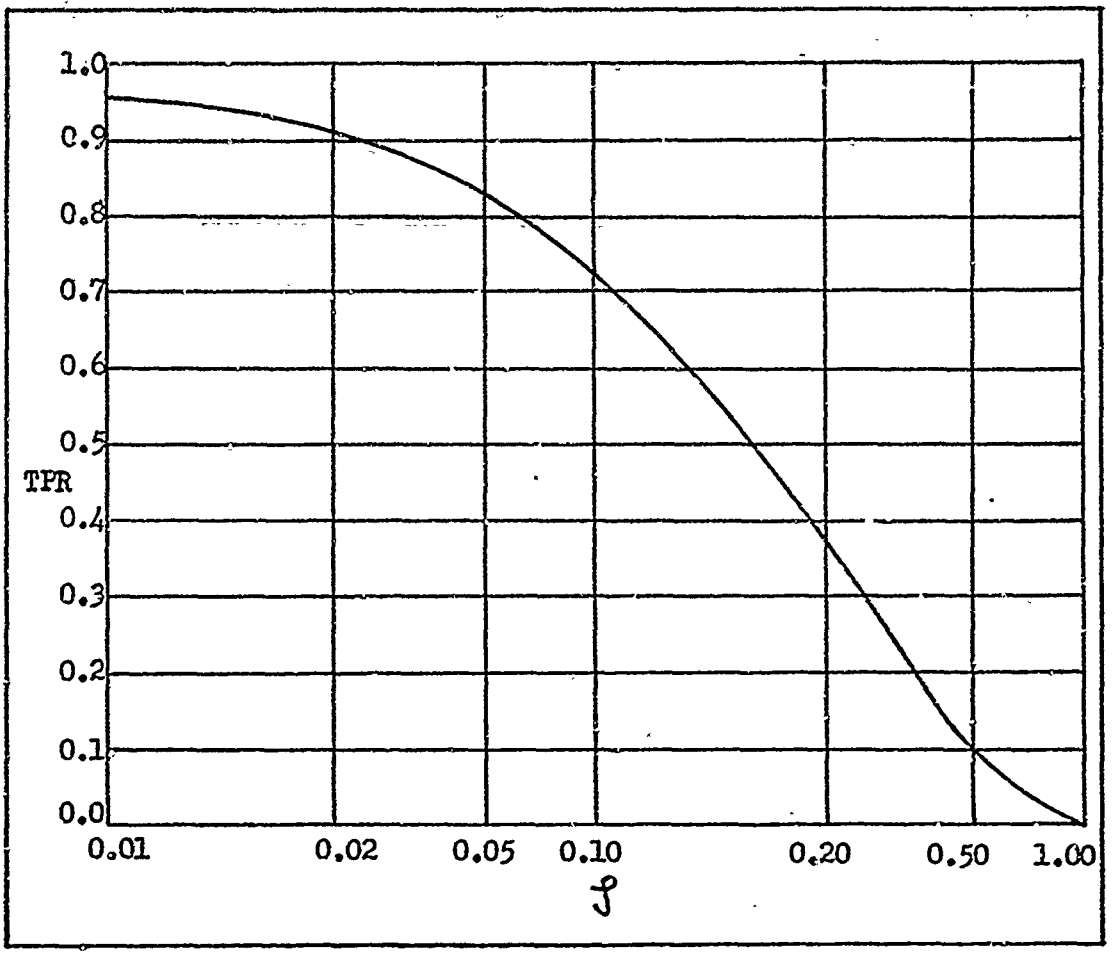

Figure 17. ζ Versus TPR

mined by Eq (3-2).

$$\omega_\eta = \frac{2\pi/T}{\sqrt{1-\zeta^2}} \tag{3-2}$$

A five degree rudder doublet input was used to insure that the steady state value of sideslip would equal zero since this method of measuring ζ and ω_η requires the steady state value be known. An impulse input could be used but has the disadvantage that the output trace has to be observed until the oscillations die out to get the steady state value. Because of the symmetry of a doublet input, the output trace does not have to be observed until the oscillations die out since the steady state value is known to be zero. The sideslip trace was chosen for the measurement, but other traces such as roll rate ($\dot{\phi}$) or bank angle (ϕ) could be used to obtain the same results.

In order to accurately measure the damping and frequency of the free oscillations, peaks or valleys occurring before the rudder input was completed (2 sec) were discounted. The first peak or valley occurring after two seconds is designated number one and the peaks and valleys are numbered sequentially from that point. As the rudder input would also disturb the frequency of the free oscillations, initial time (t_o) used to measure the damped period was chosen to coincide with the peak or valley designated number one.

For a simple second order system, the transient peak ratio, and therefore the damping ratio, would have the same value regardless of which two successive peaks were measured. For two sets of complex roots, the TPR varies with respect to which peaks are measured. This alone, as can be seen from Eq (3-2), would result in the frequency

varying with respect to where measured. Also the damped period itself is dependent on which peaks are measured.

Since damping and frequency varies with point of measurement, some consistent reference must be used to provide results suitable for comparison. It was decided to use the least favorable values in each run for this reference. A satisfactory SAS design should improve these least favorable values to acceptable values.

Roll Mode Time Constant. Figure 18 illustrates the method used to determine roll mode time constant. One time constant is defined as the time it takes the output to decay to 36.2 per cent of its original magnitude. The time when the output starts to decay from K is designated T_0 and the time when the output reaches 36.2 per cent of K is designated T_1. The actual value of K is irrelevant. The roll mode time constant is determined from Eq (3-3).

$$\tau_r = T_1 - T_0 \tag{3-3}$$

Spiral Stability. To measure this parameter, the simulation is rolled to a bank angle of twenty degrees and then the controls are released. The time it takes the bank angle to double (reach 40 degrees) is measured.

Roll Rate Oscillations (Large Inputs). Step aileron inputs, of varying magnitudes, are held fixed until the bank angle charges ninety degrees. Then, the roll rate ($\dot{\phi}$) at the first minimum is measured as a percentage of the first maximum.

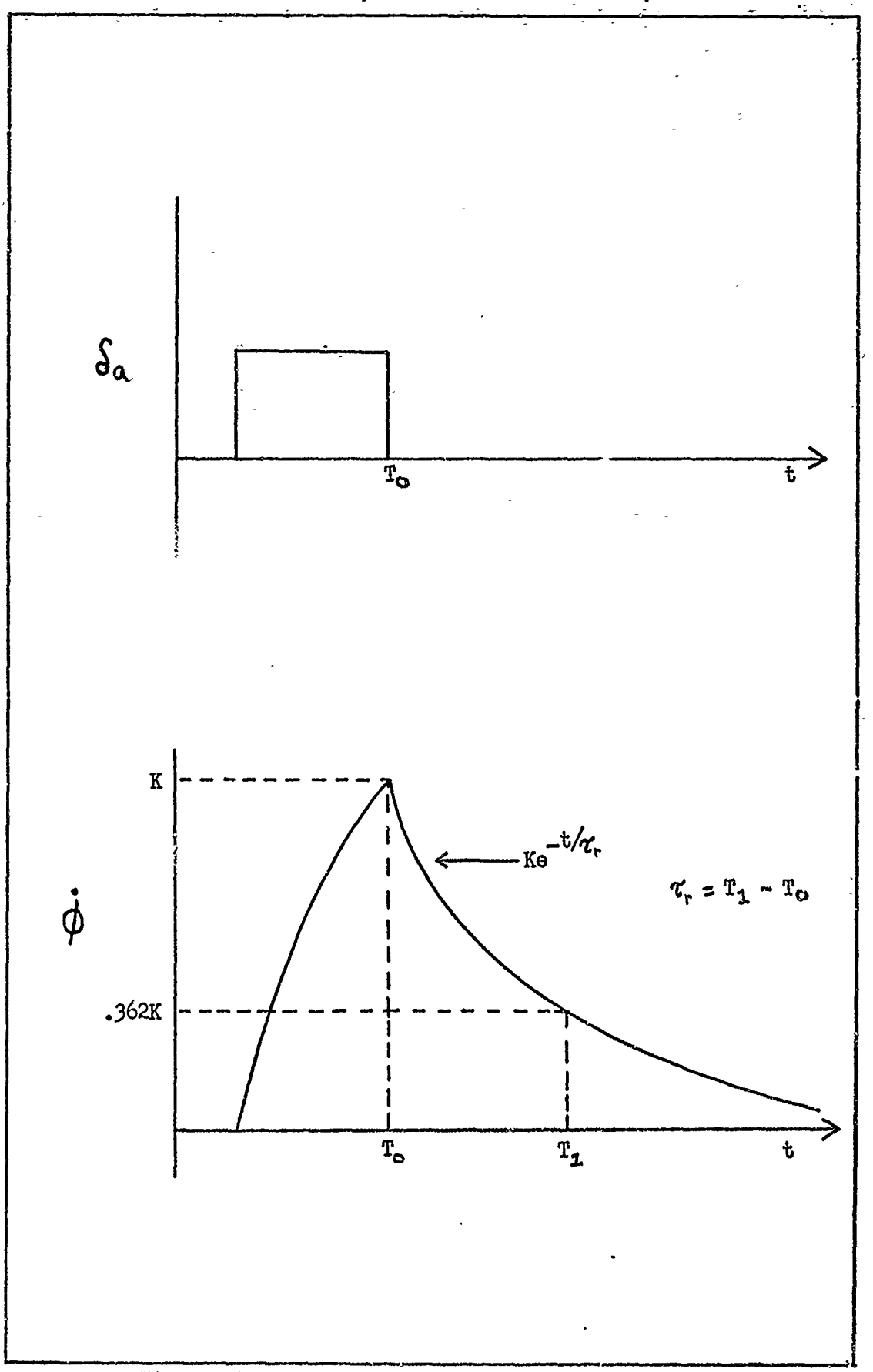

Figure 18. Determining Roll Mode Time Constant

Roll Rate Requirement (Small Inputs). Three parameters, (1) P_{osc}/P_{av}, (2) ψ_β, and (3) $\dot{P}/\beta$ must be measured for this requirement. P_{osc}/P_{av} is a measure of the ratio of the oscillatory component of roll rate to the average component of roll rate following a rudder-pedals-free step aileron input. Eq (3-4) and Fig. 19 show how P_{osc}/P_{av} is measured (Ref 9).

$$P_{osc}/P_{av} = \frac{P_1 - P_2}{P_1 + P_2} \qquad \text{if } \zeta > 0.2$$

$$P_{osc}/P_{av} = \frac{P_1 + P_3 - 2P_2}{P_1 + P_3 + 2P_2} \qquad \text{if } \zeta \leq 0.2 \qquad (3\text{-}4)$$

The parameter ψ_β is the phase angle of the Dutch roll component of sideslip. Eq (3-5) and Fig. 20 illustrate how to determine ψ_β.

$$\psi_\beta = [\frac{-360}{T_D} t_n + (n - 1)360] \text{degrees} \qquad (3\text{-}5)$$

where T_D = period of Dutch roll

t_n = time to the nth peak of sideslip trace

Several oscillations are needed to measure this parameter. It is necessary that the peak measured is not disturbed by the roll mode. Therefore peaks considered are ones that occur after one or two roll mode time constants.

Ramping of the sideslip trace is another effect which degrades accuracy if not taken into consideration. Ramping results in a movement of the portion of the peaks on the sideslip trace with respect

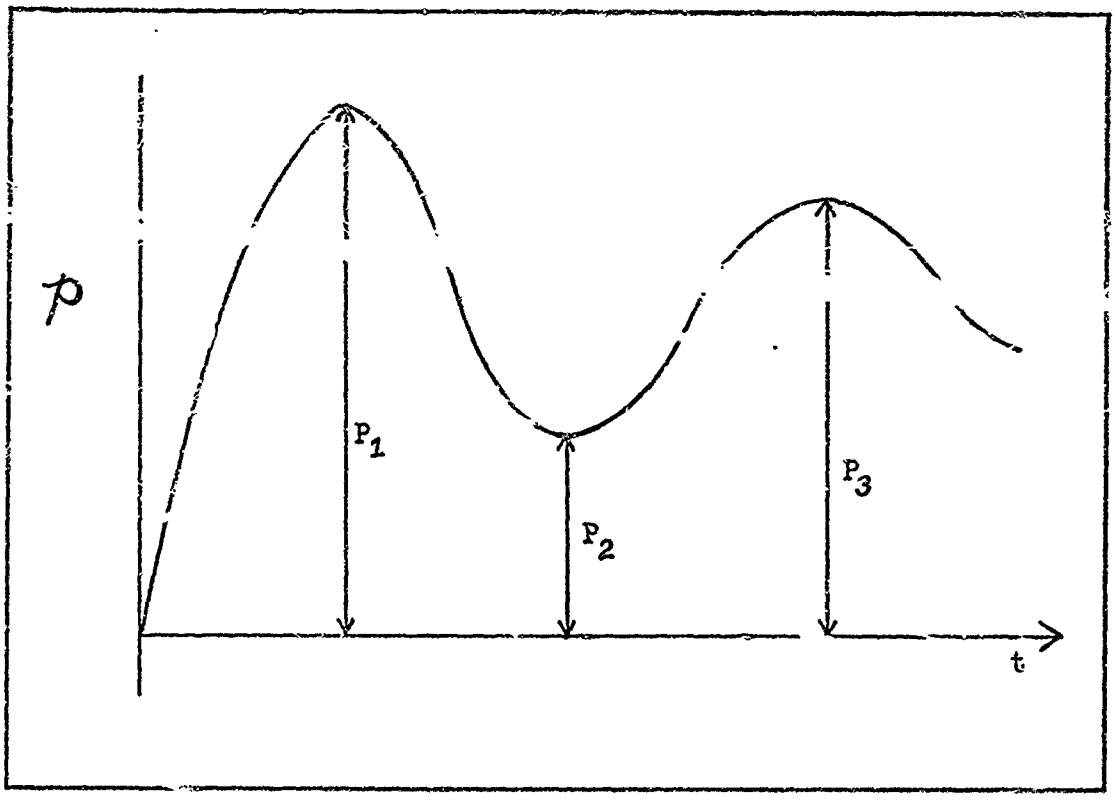

Figure 19. Determining P_{osc}/P_{av}

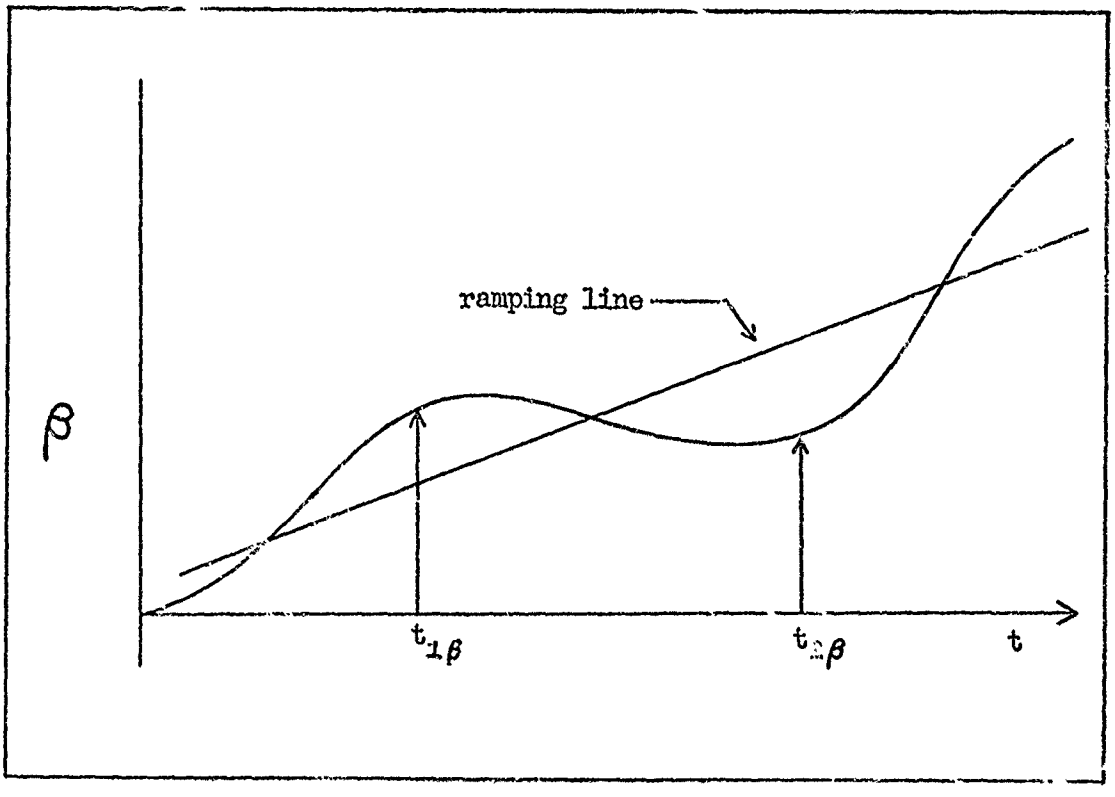

Figure 20. Determining ψ_β

to Dutch roll component peaks.

Dutch roll component peaks are designated by drawing a line through the ramping portion of the trace (see Fig. 20) and these peaks are located when the vertical distance between the ramping line and the sideslip trace is largest.

The parameter $\not{P}/\beta$ is the phase [illegible] rate and sideslip in the free Dutch roll oscillations. Eq (3-6) and Fig. 21 show how to measure this parameter.

$$\not{P}/\beta = \left[\frac{t_\beta - t_p}{T_D}360\right] \text{degrees} \qquad (3\text{-}6)$$

As before, the peaks chosen should be one or two roll mode time constants after the input to assure measurements of free Dutch roll oscillations.

The value of P_{osc}/P_{av} following a step aileron input must be within the limits of Fig. 22. This requirement exists up to an input of magnitude that causes a sixty degree bank angle change within $1.7T_D$ seconds.

Sideslip Excursions (Large Inputs). The amount of sideslip following a step aileron input must be less than 10K. The parameter K is the ratio of actual roll performance as measured from the roll trace to the required roll performance as specified in MIL-F-8785A. For this case, the required roll performance is thirty degrees in two seconds. Therefore, K equals the bank angle measurement at two seconds divided by thirty degrees. The sideslip is measured at the point where the bank angle has changed by ninety degrees. Essentially, K is a scale factor allowing corresponding larger amounts of sideslip for

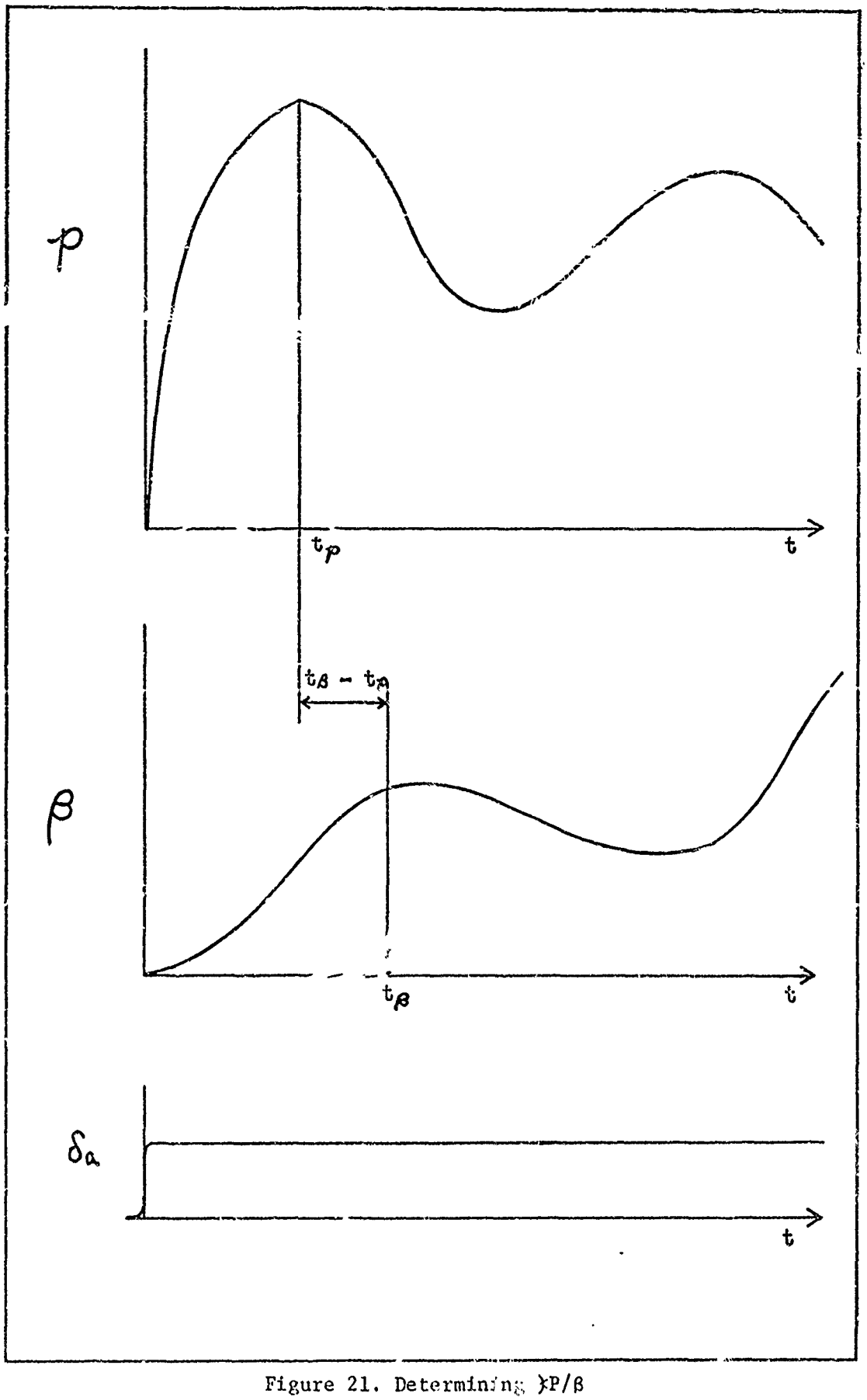

Figure 21. Determining $\partial P/\beta$

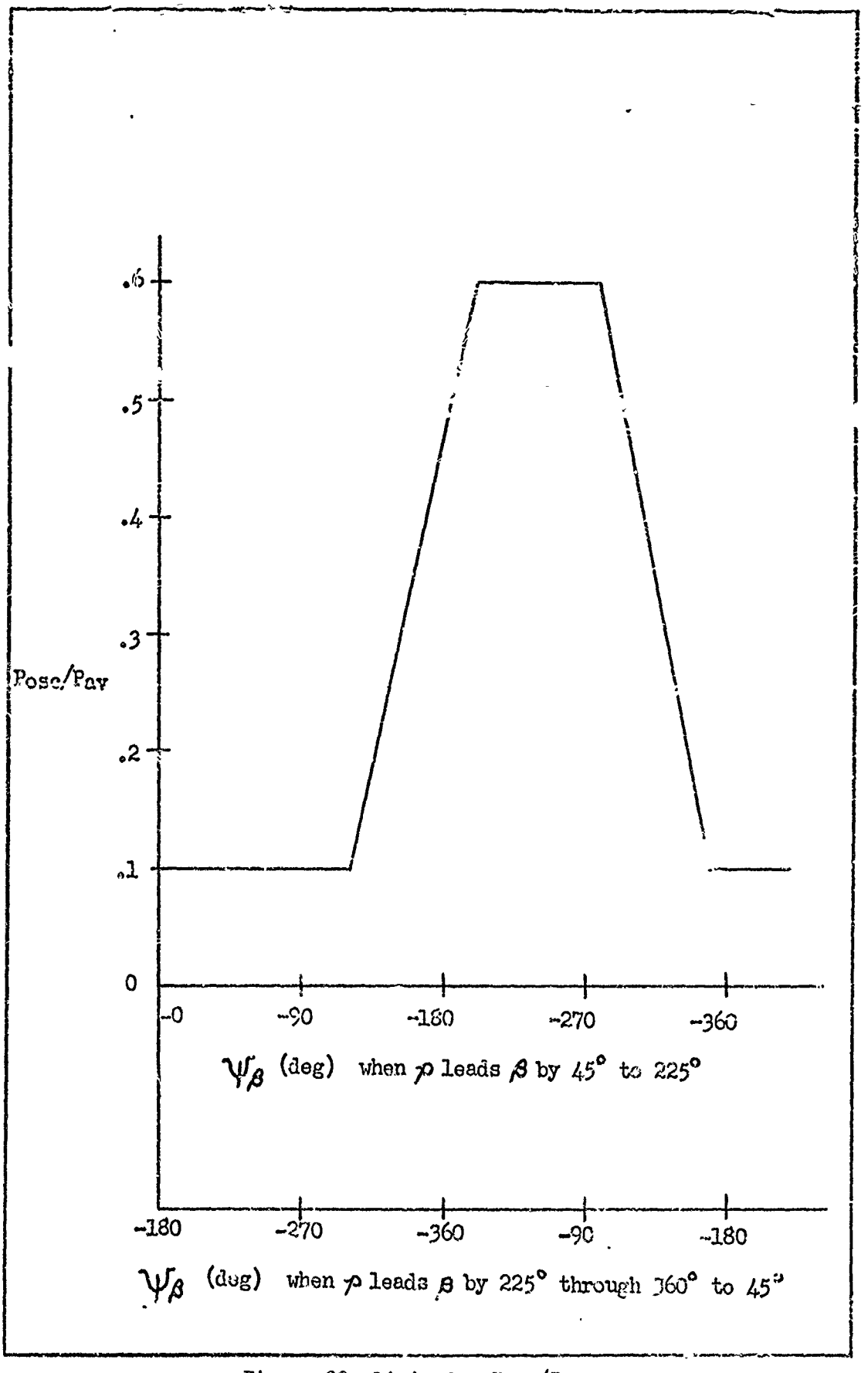

Figure 22. Limit for P_{osc}/P_{av}

larger inputs.

Sideslip Requirement (Small Inputs). The parameter $\Delta\beta_{max}$ is found by measuring the maximum change in sideslip occurring within two seconds or $(1/2)T_D$, whichever is greater, after a step aileron input. This parameter varies with respect to the magnitude of input.

The shape of the sideslip trace determines which two-second period of time is to be used for the measurement of $\Delta\beta_{max}$. Figure 23 shows this two-second period of time varying with respect to the shape of the sideslip trace. The limit for $\Delta\beta_{max}$ is shown in Fig. 24.

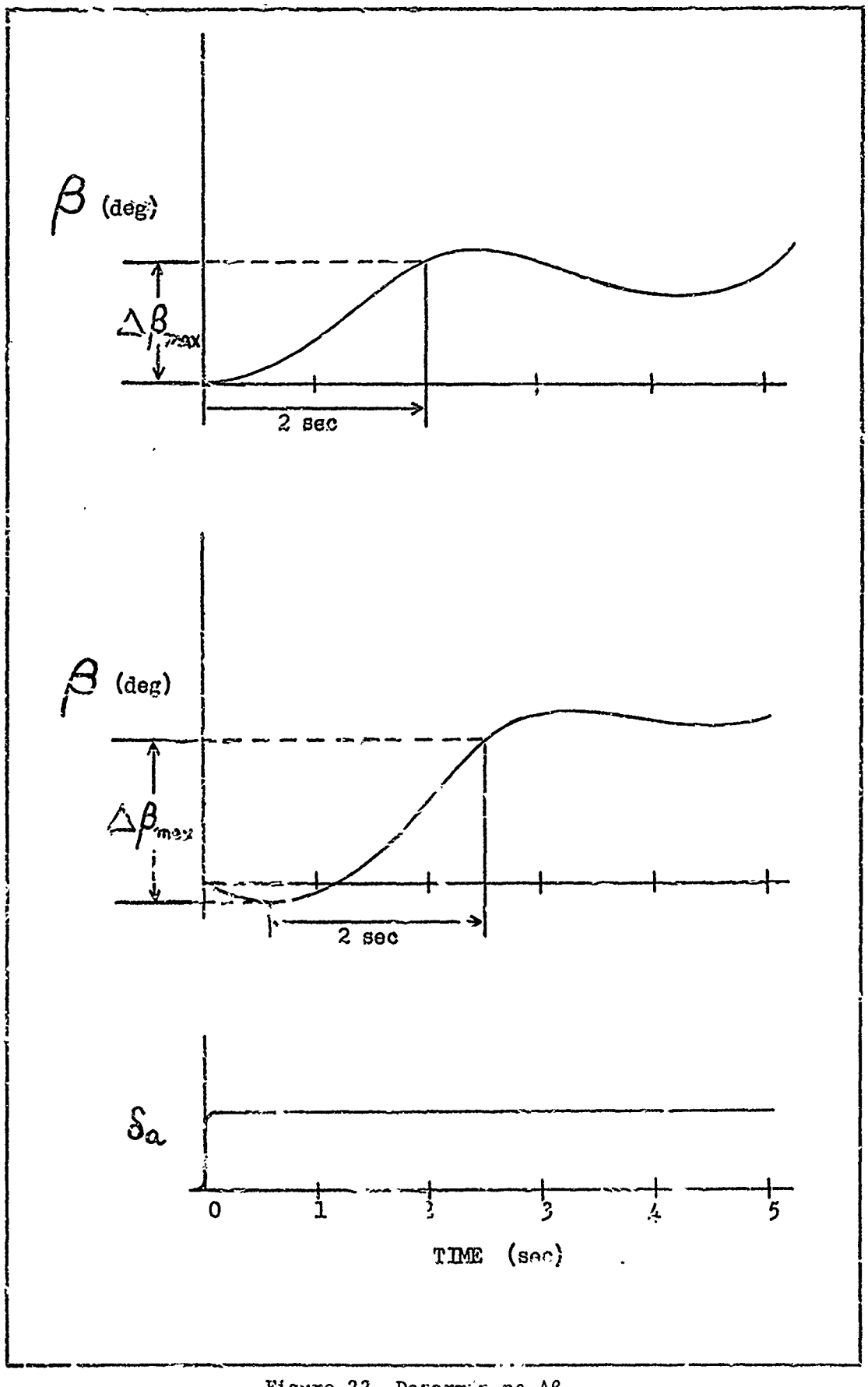

Figure 23. Determining $\Delta\beta_{max}$

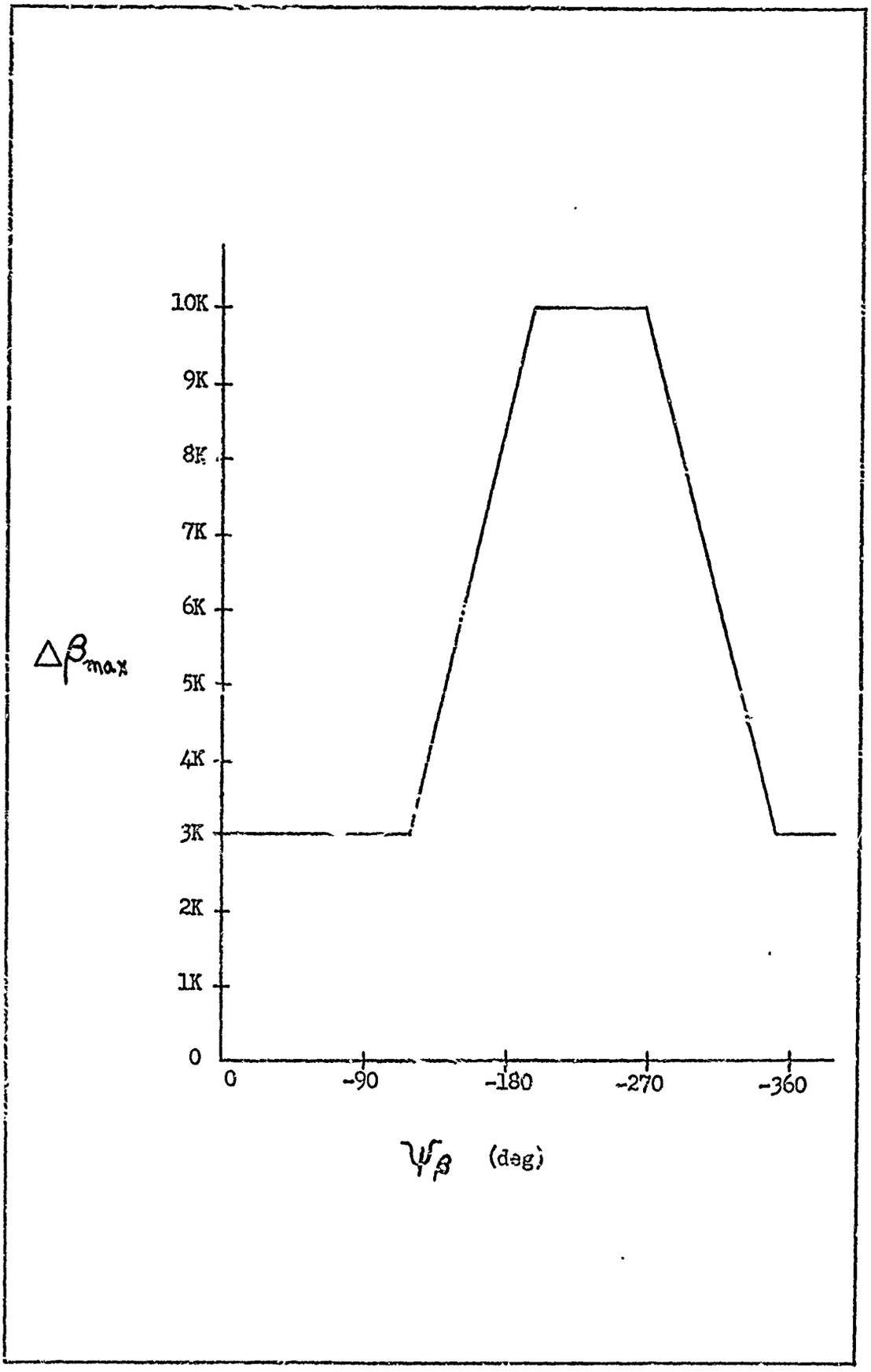

Figure 24. Limit for $\Delta\beta_{max}$

IV. Analog Results and Discussions

The final step was to demonstrate, through analog computer simulation, that the stability augmentation system (SAS) does indeed improve the lateral-directional flying qualities. The analog results were also used to specify the actual value of K_A to be used.

Previously, root locus analysis indicated an operating region, but since the system contains two sets of complex roots the analysis could not determine the best value for this parameter. The interaction of the two sets of complex roots is evident on the analog outputs and the optimum value (K_A) was chosen from these outputs. This procedure was followed in Cruise 1 and Power Approach. The Cruise 1 value was used in Cruise 2 with satisfactory results. The three flight conditions are listed in Chapter II, Table I.

Equations of Motion

The equations of motion used for the analog simulation are given in Chapter II (Eqs 2-1, -2, and -3). Table II shows the different stability derivatives for the three flight conditions. ASD's TR-69-97 (Ref 6) explains how these values were determined.

The analog wiring diagram is shown in Fig. 25. This wiring diagram represents the circuitry of the stability augmentation system (SAS) which includes the MC-135 with both feedback loops (yaw rate and Y-acceleration) connected. Throughout this chapter, the term "yaw damper" will denote the MC-135 with yaw rate feedback. A one degree step aileron input was applied to the MC-135 simulation to compare with the output from Griffin's digital program (Ref 7). The analog solution

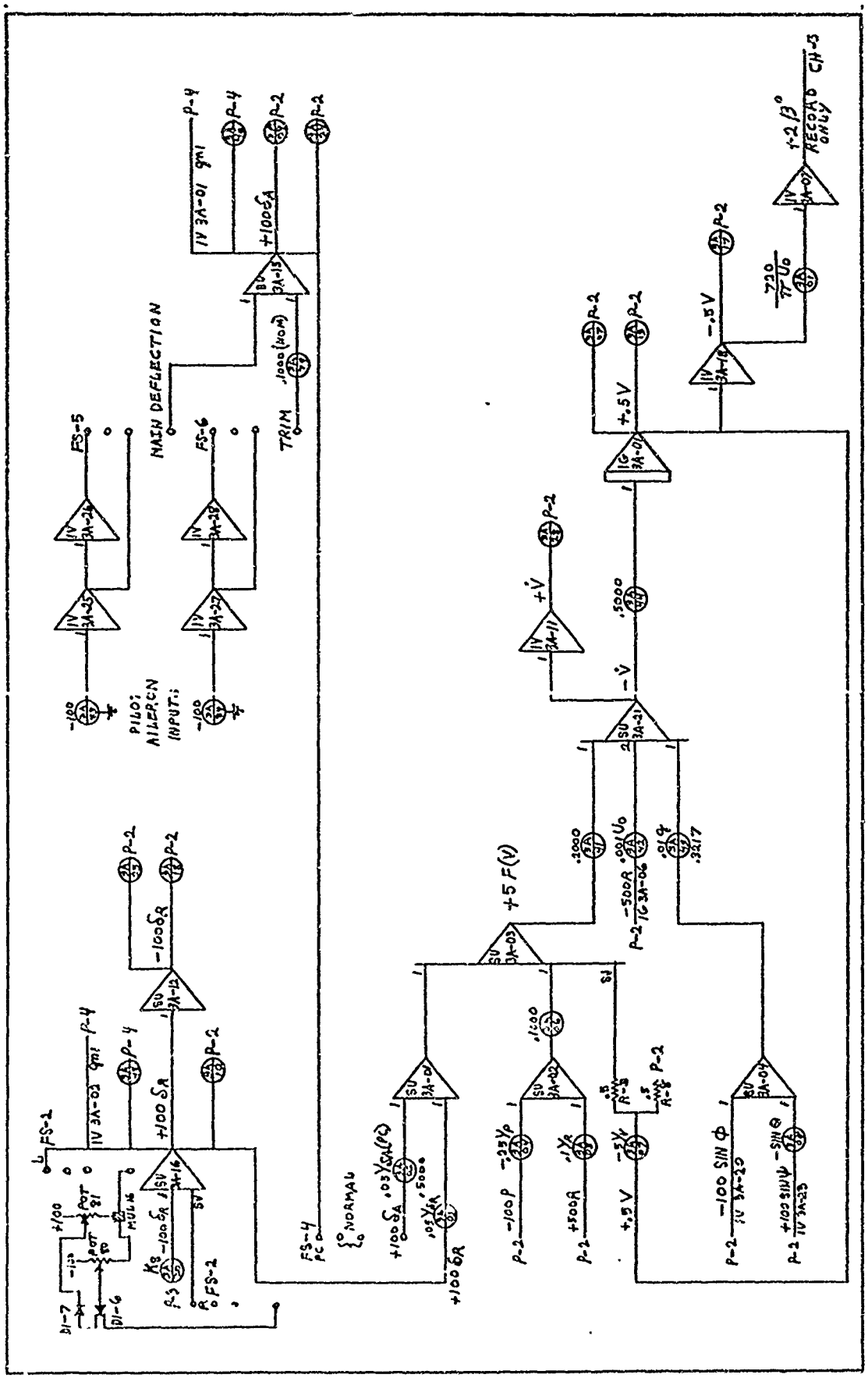

Figure 25. Analog Wiring Diagram (page 1 of 4)

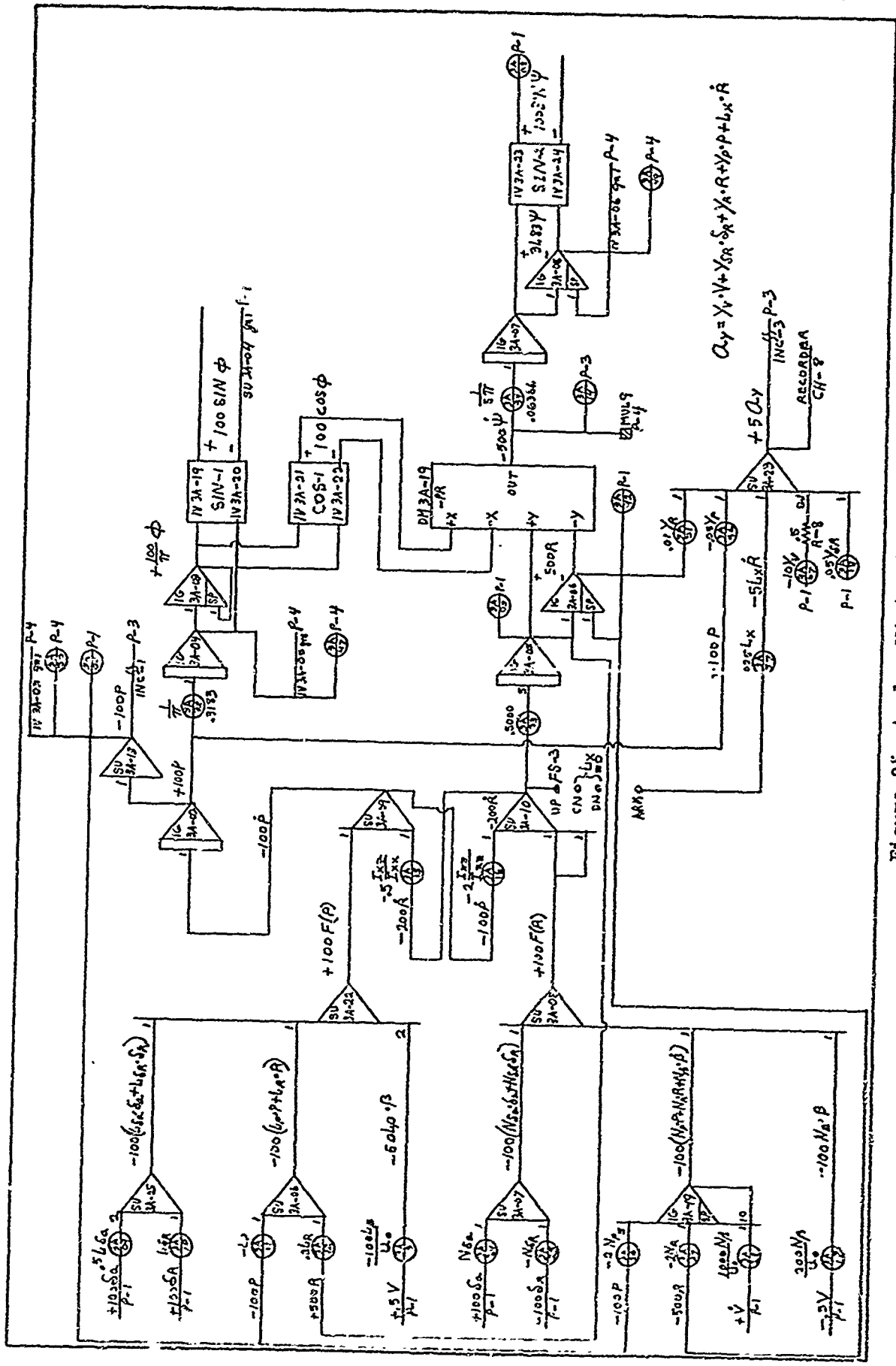

Figure 25. Analog Wiring Diagram (page 2 of 4)

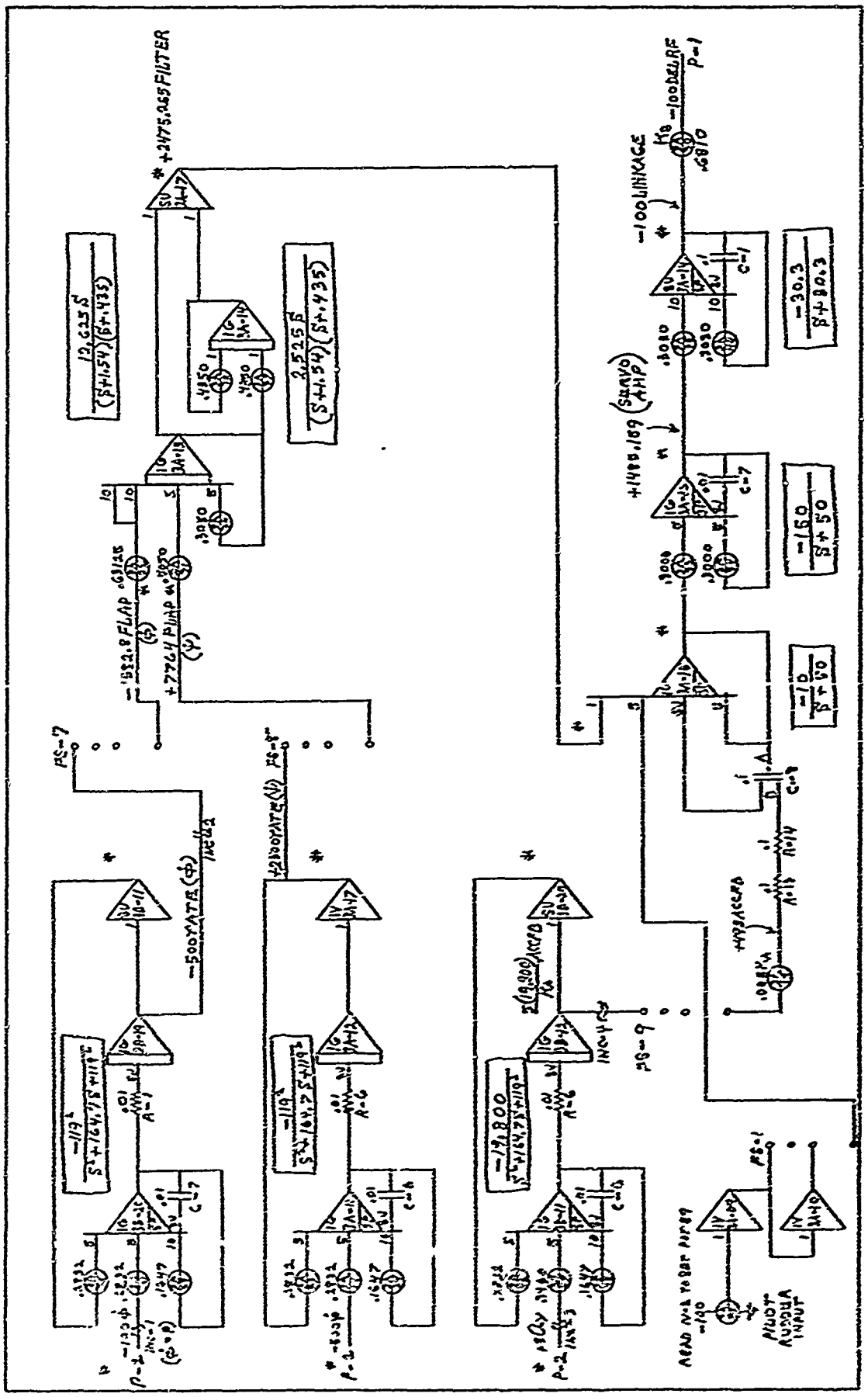

Figure 25. Analog Wiring Diagram (page 3 of 4)

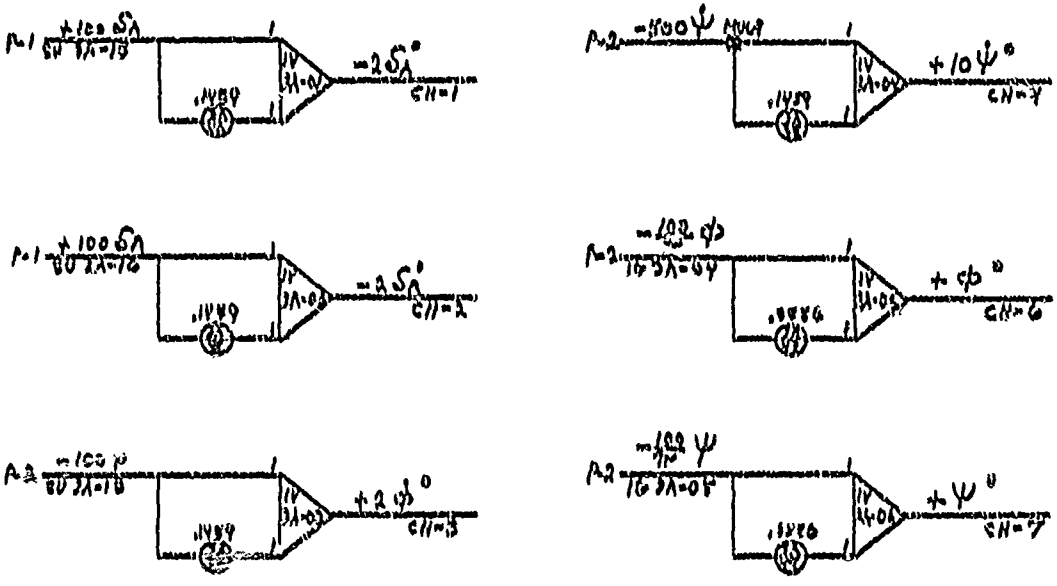

Figure 23. Analog Wiring Diagram (page 4 of 4)

compared favorably to the digital results, confirming that the analog simulation was working properly.

Flight Conditions

Cruise 1. Using ζ and ω_n as the parameters of primary importance, the optimum value of K_A was determined. Figure 26 illustrates how the values of ζ and ω_n change with varying K_A. The K_A values investigated were 60, 95, 125, and 155. Both the ζ and ω_n increase as K_A is increased, therefore $\zeta\omega_n$ increases with K_A. Even larger $\zeta\omega_n$ would result from larger K_A values. However, these larger values also result in a disadvantage. This disadvantage is the increased time for the sideslip trace to reach steady state. The time to reach steady state is large at the lower values of K_A because of the low damping and frequency. As the K_A value is increased, the time to steady state decreases while ζ and ω_n increases. As K_A is further increased, the time to steady state starts to increase again as a result of the ripple that appears at these higher values of K_A. This ripple is noticeable in the K_A = 155 output trace. A high $\zeta\omega_n$ is desirable but a long time to steady state is not. Therefore, a compromise between the value that has the shortest time to steady state (K_A = 95) and the value that has the largest $\zeta\omega_n$ (K_A = 155) was used to pick the optimum value of 125.

From the rudder trace, it can be seen how larger K_A values result in more rudder movement. It is this rudder movement that damps the oscillations in the sideslip trace.

The information taken from Fig. 26 is listed in Table IV. From this table, the compromise between time to steady state and large $\zeta\omega_n$ is apparent. The K_A value chosen (125) has a lower $\zeta\omega_n$ than a K_A value

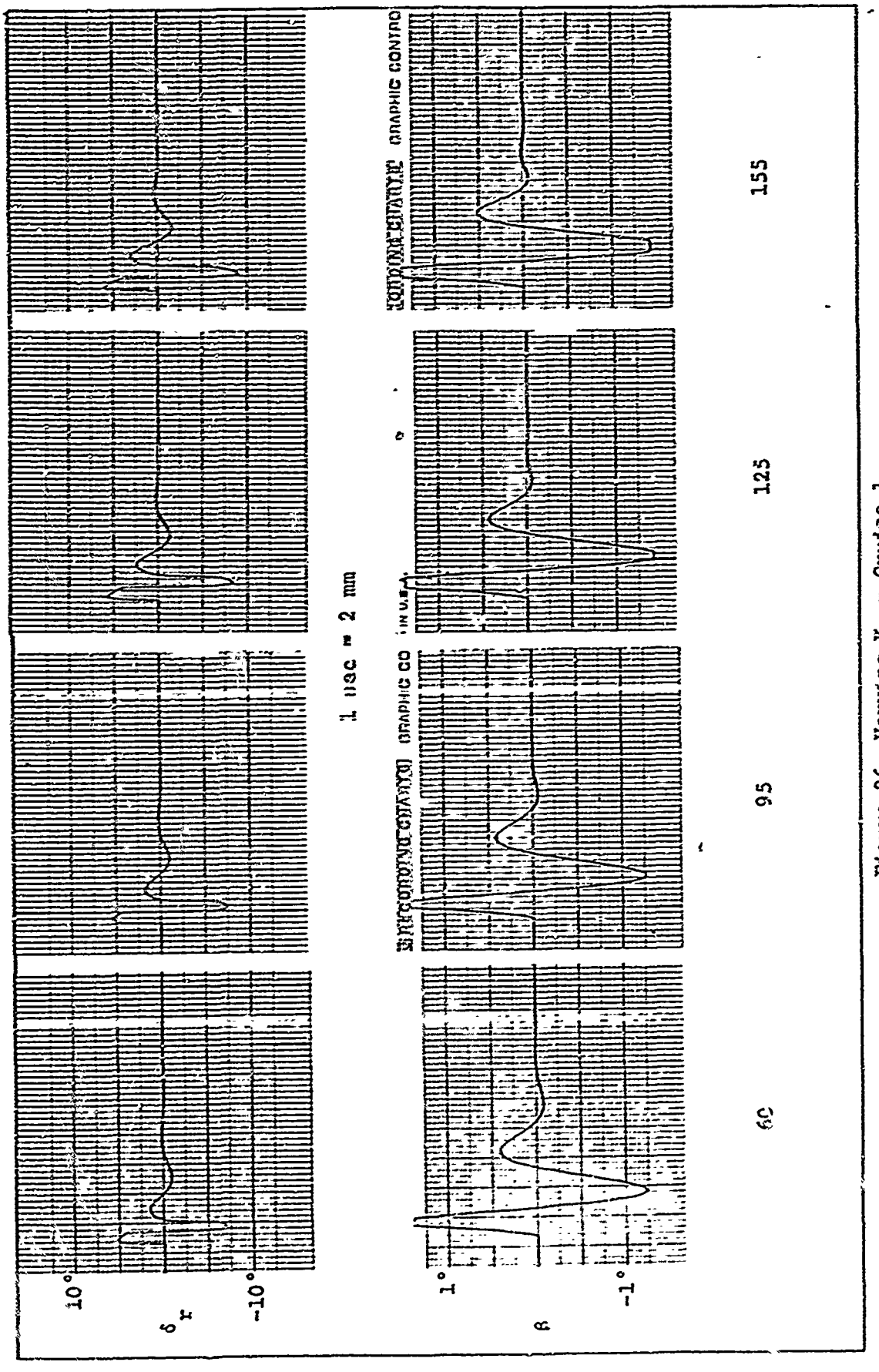

Figure 26. Varying K_A - Cruise 1

of 155. However, a K_A of 125 only takes 13.0 seconds to reach steady state as compared to the 15.5 seconds that a K_A of 155 takes to reach steady state.

Table IV

K_A Versus ζ, ω_η, $\zeta\omega_\eta$ and Time to Steady State - Cruise 1

K_A	ζ	ω_η	$\zeta\omega_\eta$	Time to S.S. (sec)
60	.425	.912	.387	16.25
95	.500	1.021	.510	12.50
125	.540	1.100	.595	13.00
155	.580	1.360	.787	15.50

A rudder doublet input, to measure ζ and ω_η, is shown in Fig. 27. From the β and ψ traces of the MC-135, it is apparent that ζ is far too small as the oscillations appear nearly constant. The frequency does meet the requirements; however $\zeta\omega_\eta$, as well as ζ, is below specifications. The output from the yaw damper shows a substantial increase in ζ but ω_η is decreased. Both ζ and ω_η are above minimum requirements, however their product ($\zeta\omega_\eta$) is below the accepted minimum.

The rudder traces show both the yaw damper and the SAS cause rudder movement in the attempt to damp out the oscillations. The rudder movement with SAS on is fifty per cent larger than with just the yaw damper, but the frequency of this rudder movement looks approximately the same for either yaw damper or SAS.

The SAS does not provide any significant increase in ζ, but it does increase ω_η such that $\zeta\omega_\eta$ is now acceptable. The parameters measured from Fig. 27 are shown in Table V.

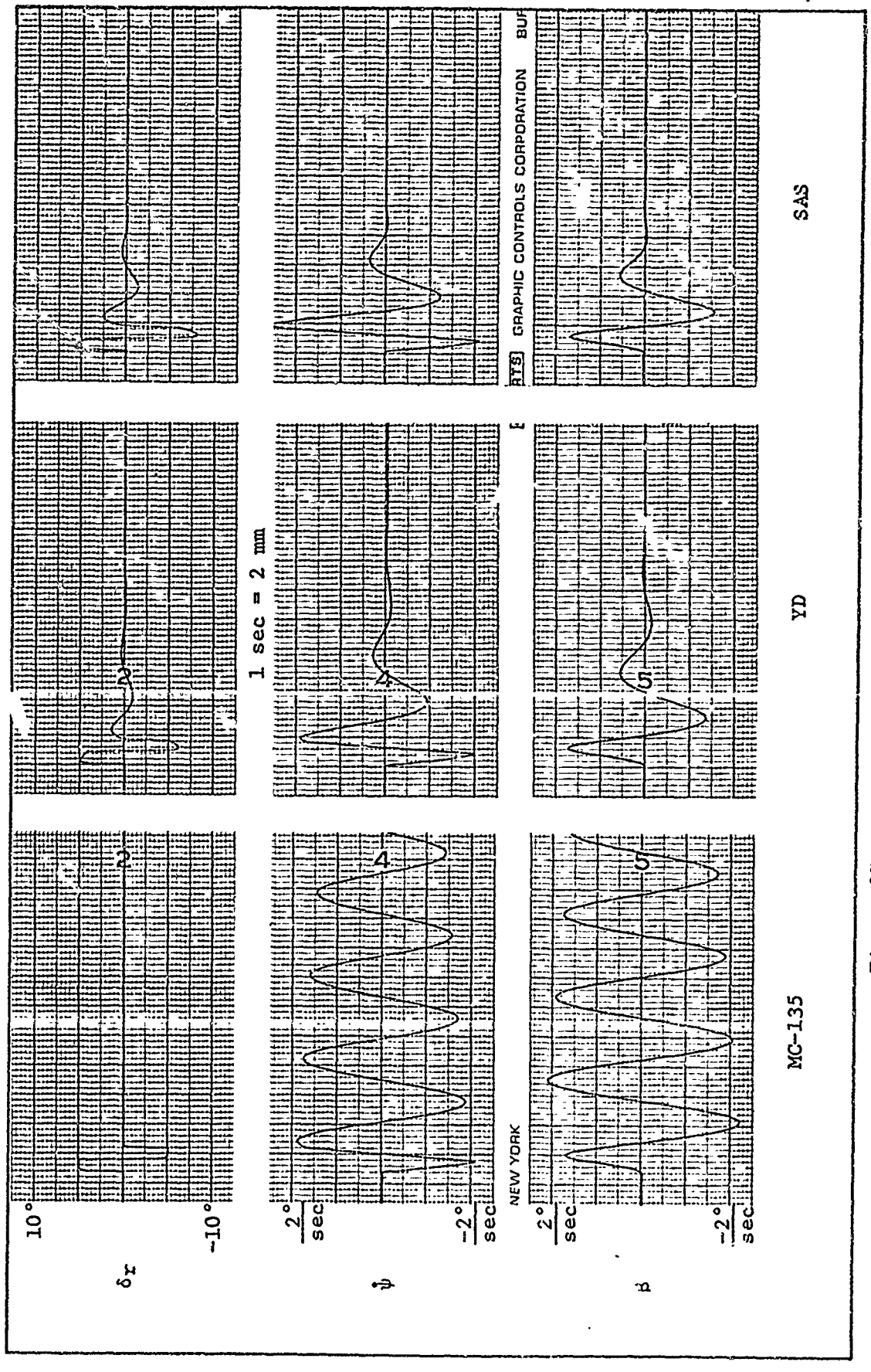

Figure 27. Comparison of ζ And ω_η - Cruise 1

Table V

ζ, ω_η, and $\zeta\omega_\eta$ Versus MC-135, YD, SAS - Cruise 1

Configuration	ζ	ω_η	$\zeta\omega_\eta$
MC-135	.02	.898	.0179
YD	.34	.810	.2764
SAS	.35	1.190	.4165

With ζ, ω_η, and $\zeta\omega_\eta$ satisfactory, the following figures were used to investigate the other requirements:

Figure	Requirements	
28	roll mode time constant	(2)
29	spiral stability	(3)
30 and 31	large aileron inputs	(4 and 6)
32, 33 and 34	small aileron inputs	(5 and 7)

Figure 28 compares the roll mode time constant. An aileron step of some small duration (1 or 2 sec) was used as the input. The length and magnitude of this input is insignificant since it is only used to get the roll rate to some initial value from which it starts to decay when the input is discontinued. The amount of undershoot becomes increasingly smaller from MC-135 to yaw damper to SAS. However, the roll mode time constant does not vary enough to measure any change from the analog output. The measured value is 1.1 seconds which meets the requirement of less than 1.4 seconds.

Figure 29 shows the test for spiral stability. In all three configurations, the bank angle converges back to zero rather than diverging. Therefore, the requirement for spiral stability is satisfied.

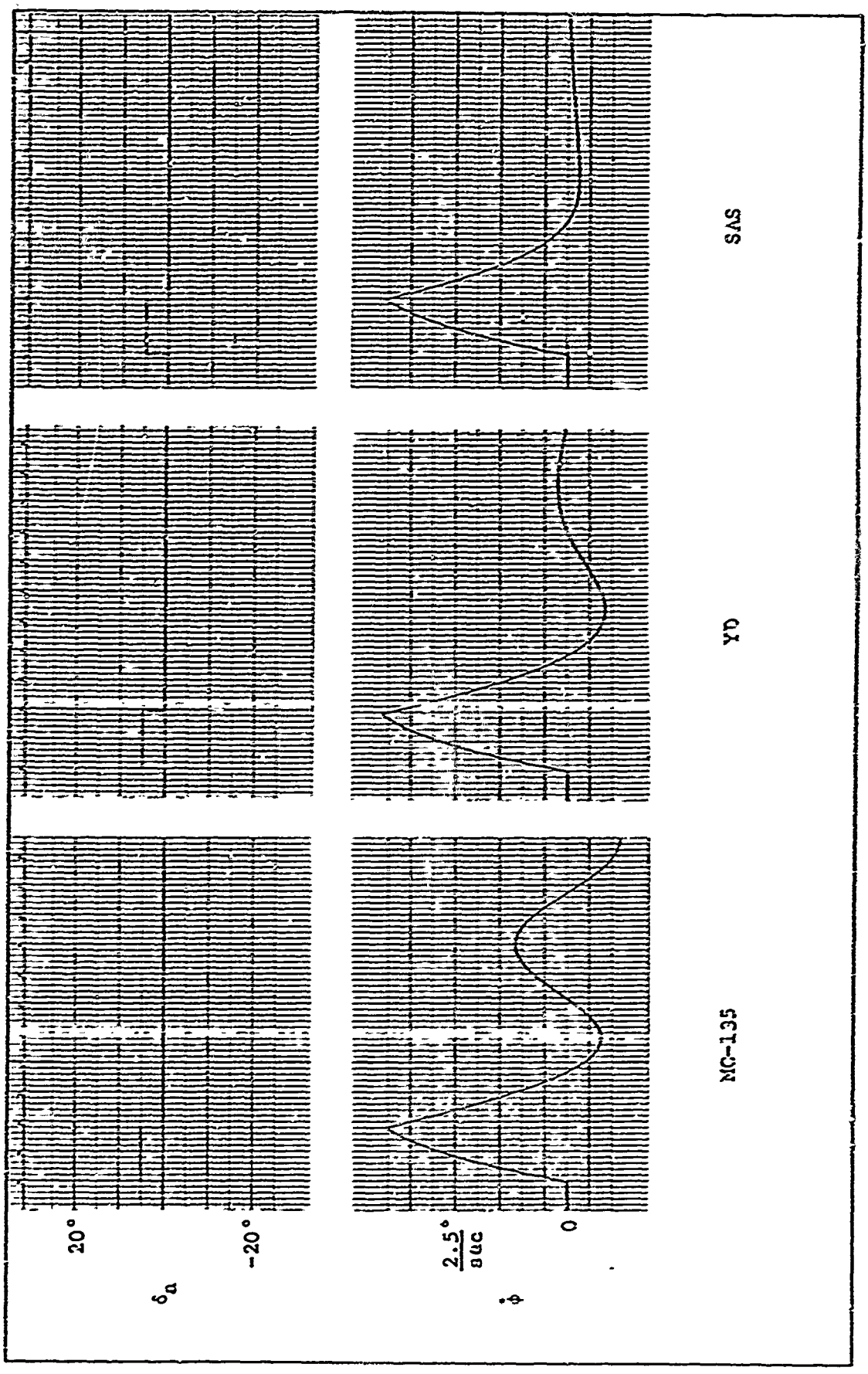

Figure 28. Roll Mode Time Constant - Cruise 1

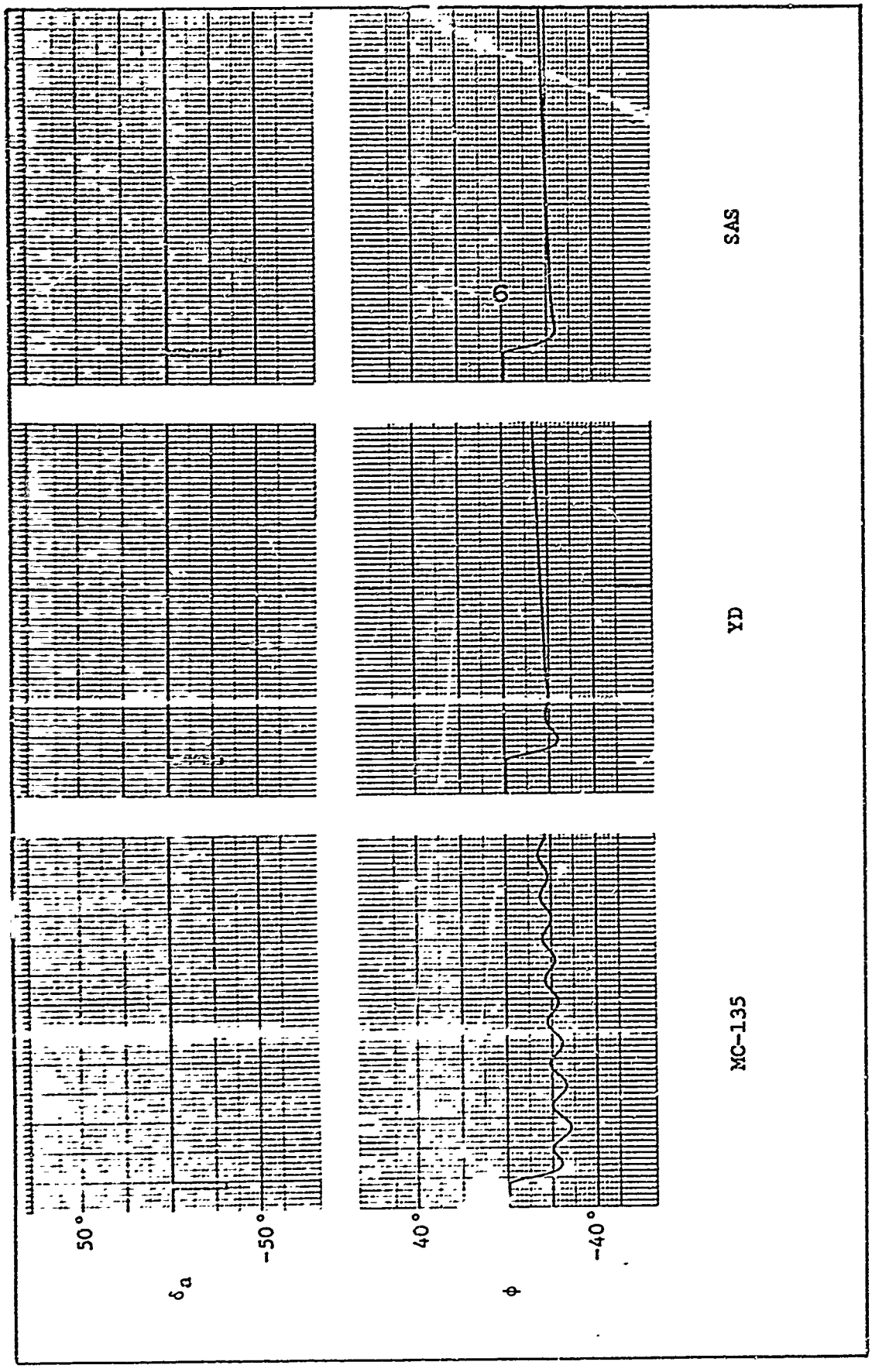

Figure 29. Spiral Stability - Cruise 1

Figures 30 and 31 are used to check the requirements concerning large aileron inputs. A twenty degree step aileron is shown in Fig. 30 while a fifteen degree aileron is shown in Fig. 31. The specifications for large aileron inputs require a bank angle change of ninety degrees. To keep the small angle approximation equations valid, the aircraft is first banked to minus forty-five degrees. When the output traces have stabilized at this condition, the aileron step is applied and the bank angle changes from minus forty-five to plus forty-five degrees. At this point, the input is taken out. From Fig. 30 (SAS), it is seen that the aileron is removed before a distinct minimum occurs in the $\dot{\phi}$ trace. However, the small angle approximation equations dictate the removal of the input and therefore the value of $\dot{\phi}$ at this point is designated as the minimum. It can also be seen from this figure that the rudder is required to move only about one degree.

Figure 31 shows that for this slightly smaller value of aileron step, the $\dot{\phi}$ trace with the SAS on has time to reach a minimum before the input is removed. The bank angle at two seconds after the input is fifteen and thirteen degrees for the step aileron inputs of twenty and fifteen degrees, respectively. This provides a K of .5 for the twenty degree input and a K of .434 for the fifteen degree input. The sideslip measured at the point when the bank angle has changed ninety degrees is within the specifications of Requirement 6 for these two values of K.

Table VI tabulates the measurements taken from Figs. 30 and 31.

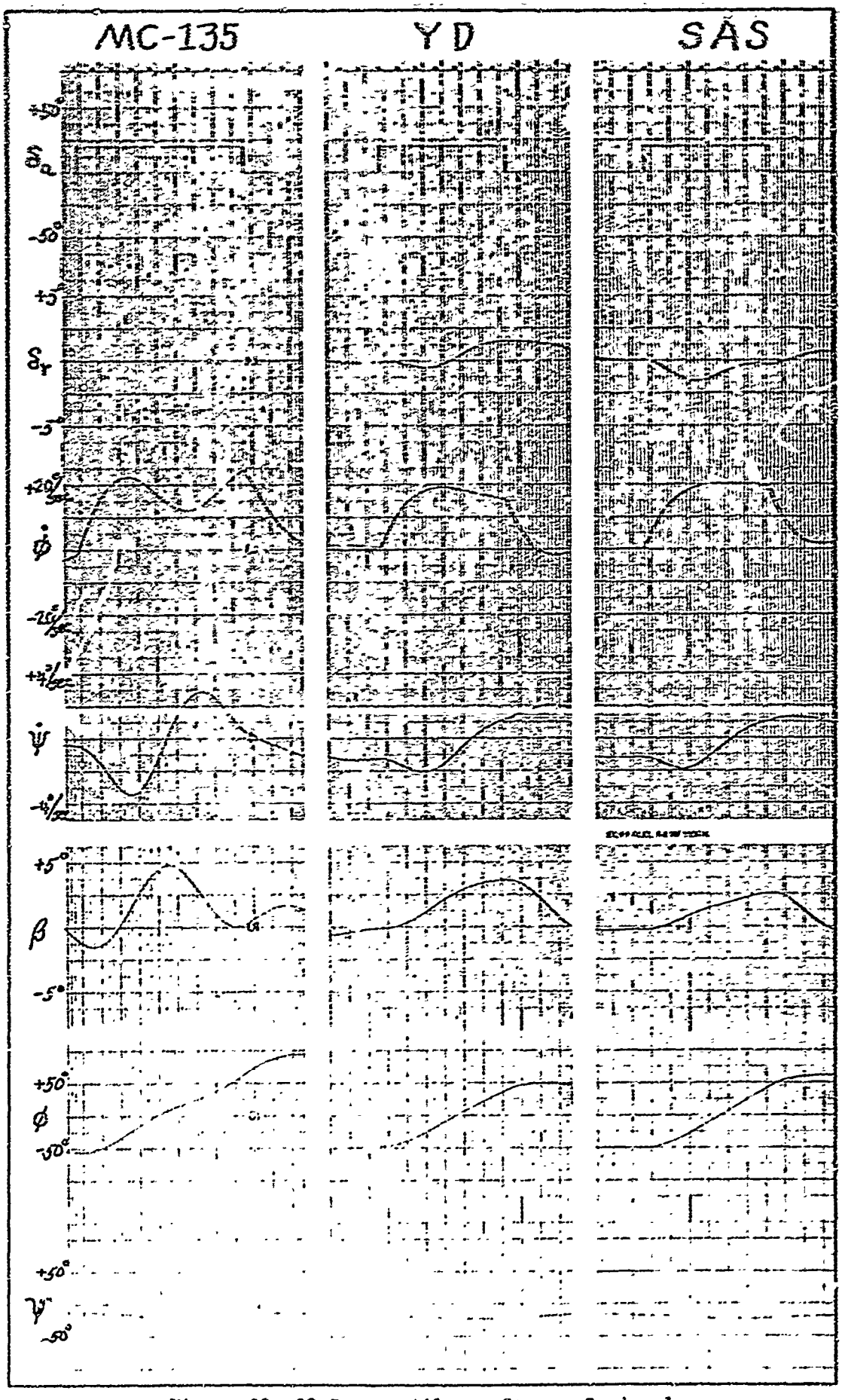

Figure 30. 20 Degree Aileron Step - Cruise 1

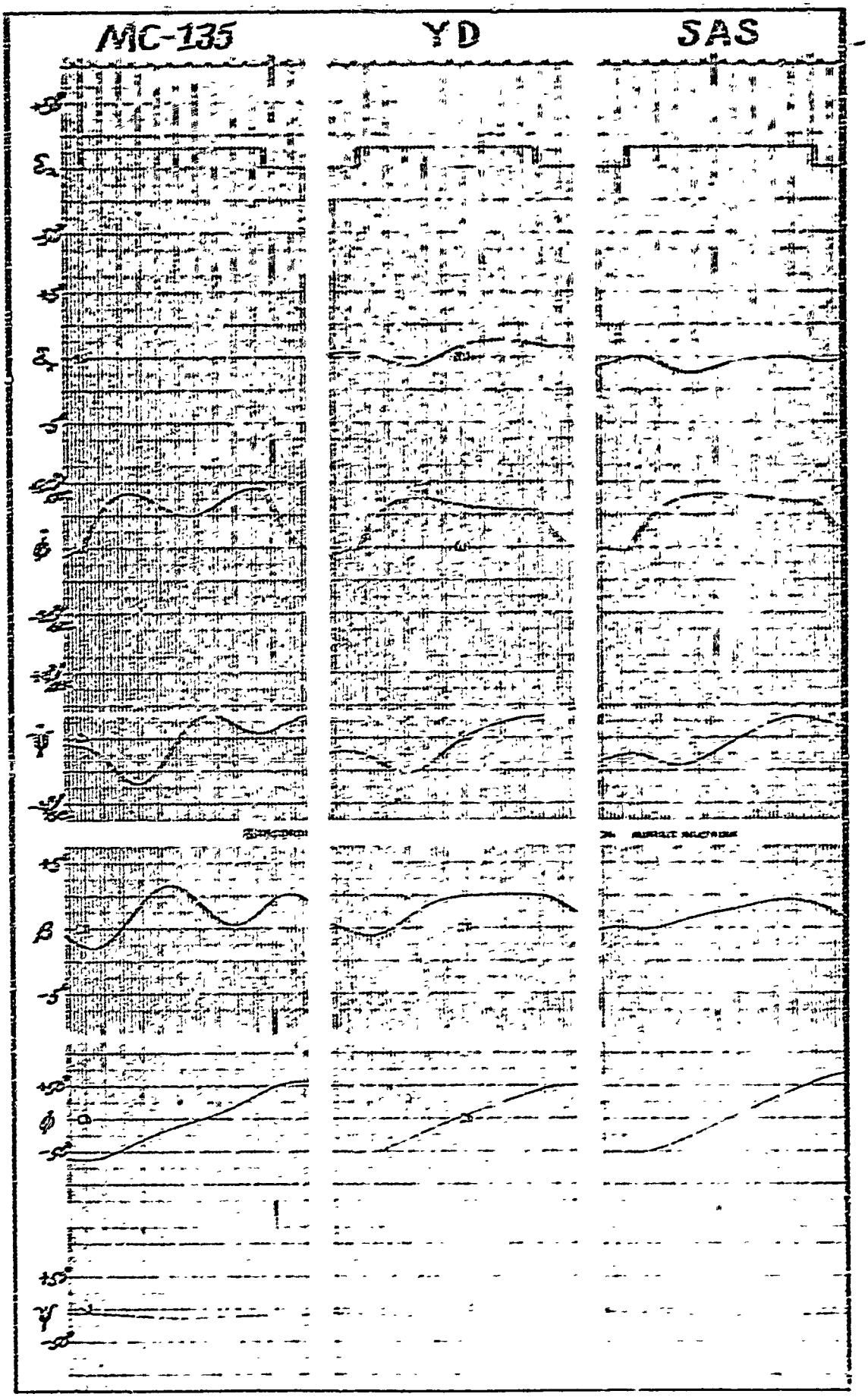

Figure 21. 15 Degree Aileron Step - Cruise 1

Table VI

Large Aileron Inputs – Cruise I

ξ_a (deg)	Configuration	p_2 at ΔP_2	ϕ_{max} (deg)	K	β at 90° roll (deg)
	MC-135	82.5	10.6	.354	3.50 – 10.3K
20	YB	80.5	17.0	.567	3.25 – 5.5K
	SAS	96.5	17.0	.567	2.75 – 4.8K
	MC-135	58.8	13.0	.435	3.25 – 7.4K
15	YB	68.8	14.9	.467	2.50 – 5.2K
	SAS	96.5	13.0	.435	2.10 – 4.8K

Figures 32, 33, and 34 show small aileron inputs of six, four, and two degrees, respectively. For these small inputs, a requirement for a bank angle change of ninety degrees does not exist. Therefore, the bank angle does not first have to be banked to minus forty-five degrees, but rather the aileron step is applied with wings level. These three figures are virtually identical except for the magnitudes of the traces, therefore statements made about Fig. 32 apply equally well to Figs. 33 and 34.

From Fig. 32, it was determined that P_{osc}/P_{av} increased with the yaw damper on but then decreases with SAS on to a value smaller than the MC-135 value of P_{osc}/P_{av}. The P_{osc}/P_{av} values for both MC-135 and yaw damper are satisfactory only if ϕ_β and $\Delta P/\beta$ are of certain values. However, the improvement in P_{osc}/P_{av} with SAS on is sufficient to meet the requirements regardless of the values of ϕ_β and $\Delta P/\beta$.

To determine ϕ_β and $\Delta P/\beta$, the time of the first peak in the β trace is required. Since the oscillations in the β trace are extremely difficult to measure for small inputs with the SAS on (see Fig. 34), it is fortunate that these values of ϕ_β and $\Delta P/\beta$ are not required. From

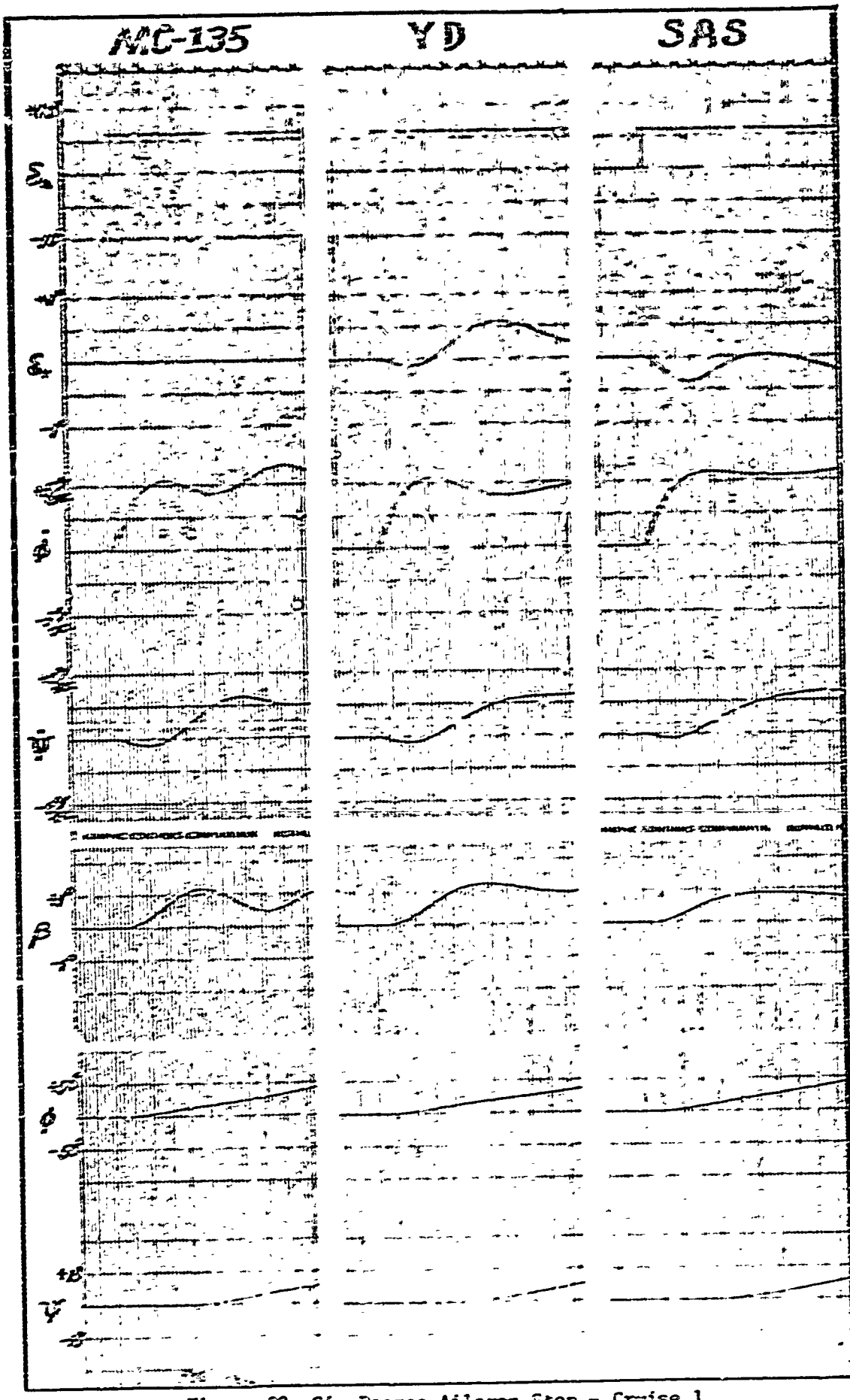

Figure 32. Six Degree Aileron Step - Cruise 1

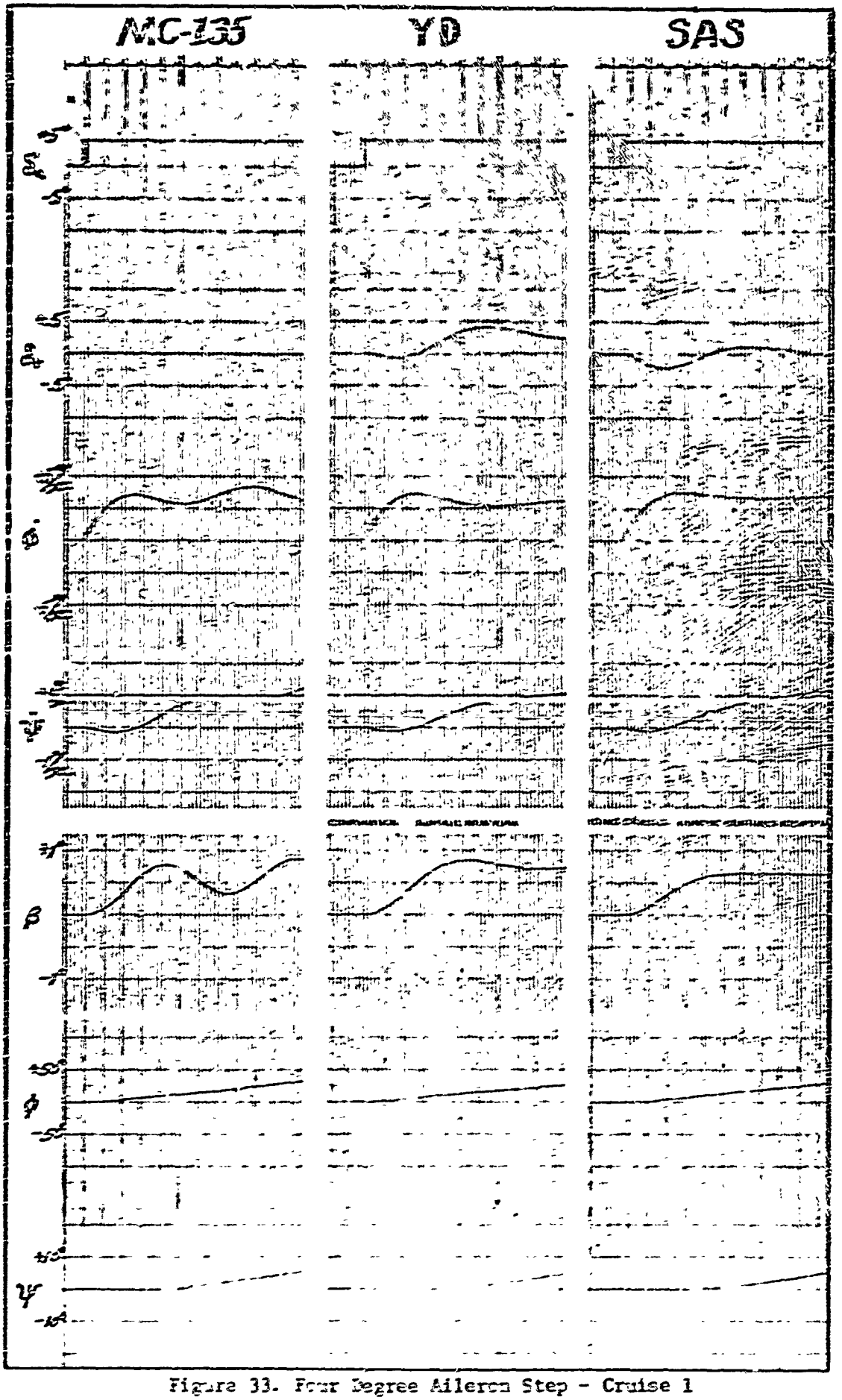

Figure 33. Four Degree Aileron Step - Cruise 1

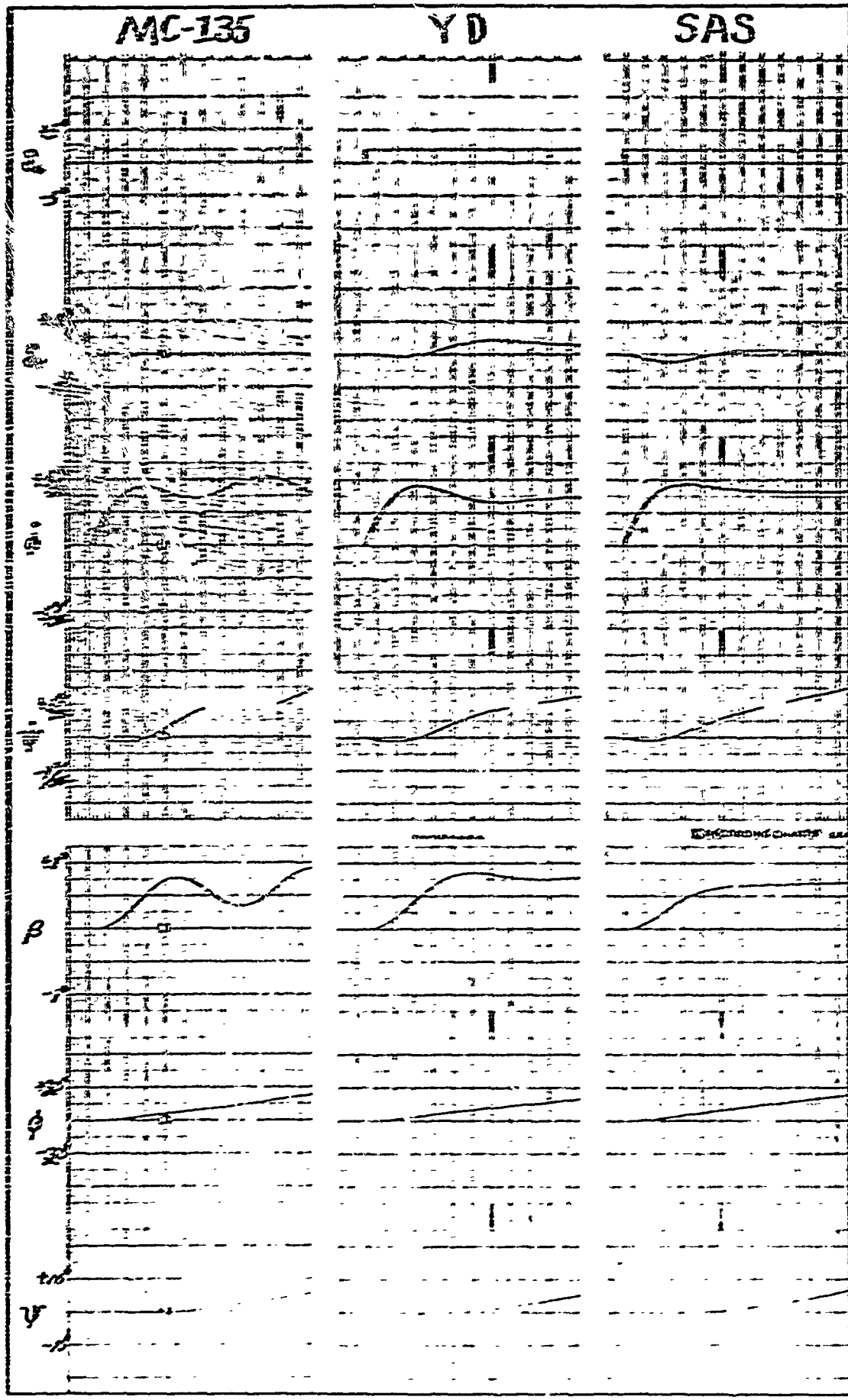

Figure 34. Two Degree Aileron Step - Cruise 1

Fig. 33, it is also apparent that more movement is required of the rudder with just the yaw damper than with the SAS on.

The measurements taken from Figs. 32, 33, and 34 are listed in Table VII.

Table VII

Small Aileron Inputs - Cruise 1

δ_a(deg)	Configuration	P_{osc}/P_{av}	ψ_2	ψ_2/β	ϕ_{com}(deg)	K	ΔS_{max} at $\frac{1}{2}T_D$
	MC-135	.111	-226	92	4.0	.333	1.05 = 7.90%
6	YD	.222	-248	128	5.0	.167	1.20 = 7.15%
	SAS	.051	#	#	6.0	.200	.60 = 3.00%
	MC-135	.098	-231	92	3.5	.110	.60 = 5.45%
4	YD	.234	-252	128	4.0	.133	.80 = 6.00%
	SAS	.032	#	#	4.5	.150	.42 = 2.80%
	MC-135	.109	-237	92	2.0	.067	.34 = 5.08%
2	YD	.241	-255	128	2.0	.067	.40 = 5.97%
	SAS	.065	#	#	2.0	.067	.20 = 3.00%

measurement not necessary since parameters meet requirements regardless of value

Cruise 2. The Cruise 1 value of K_A is used for Cruise 2 and this value provides acceptable ζ and ω_n. Therefore, $K_A = 125$ is used to investigate the other requirements in Cruise 2.

Figure 35 compares ζ, ω_n, and $\zeta\omega_n$. From this figure, it is seen that Cruise 2 is unstable for the MC-135 as the oscillations diverge. The yaw damper improves the ζ to an acceptable value as well as $\zeta\omega_n$. This is a noticeable improvement over Cruise 1 where the yaw damper does not provide satisfactory $\zeta\omega_n$. With the SAS on, the ζ actually

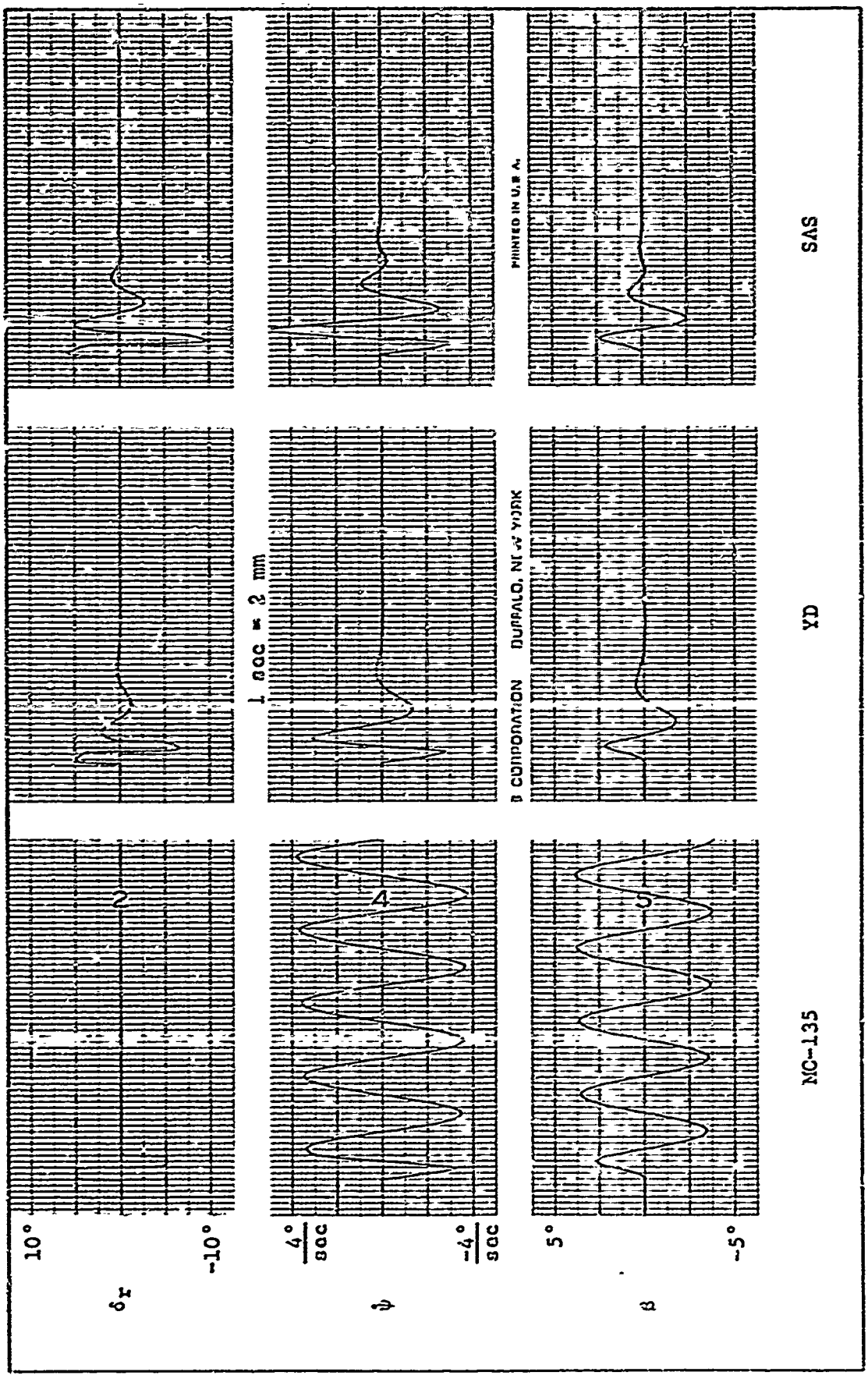

Figure 35. Comparison of ζ And ω_η - Cruise 2

decreases but the ω_n increases by a greater amount, therefore $\zeta\omega_n$ increases.

Table VIII shows that both the yaw damper and the SAS meet the requirements on ζ, ω_n, and $\zeta\omega_n$.

Table VIII

ζ, ω_n, and $\zeta\omega_n$ Versus MC-135, YD, SAS - Cruise 2

Configuration	ζ	ω_n	$\zeta\omega_n$
MC-135	.017	1.04	.018
YD	.450	.94	.421
SAS	.360	1.68	.610

The following figures are used to check the other requirements.

Figure	Requirements	
36	roll mode time constant	(2)
37	spiral stability	(3)
38 and 39	large aileron inputs	(4 and 6)
40, 41, and 42	small aileron inputs	(5 and 7)

Figure 36 illustrates that the roll mode time constant does not change when going to the different configurations. The roll mode time constant is measured as 1.1 seconds which is satisfactory.

Since the spiral mode is convergent, the spiral stability requirement is satisfied and Fig. 37 demonstrates this.

Figures 38 and 39 are twenty and fifteen degree aileron step inputs, respectively. As in Cruise 1, the problem arises in determining the minimum of the roll rate trace for the twenty degree aileron input. The value of $\dot{\phi}$ when the input is discontinued is designated the minimum value. These values of bank angle (fifteen and twelve degrees)

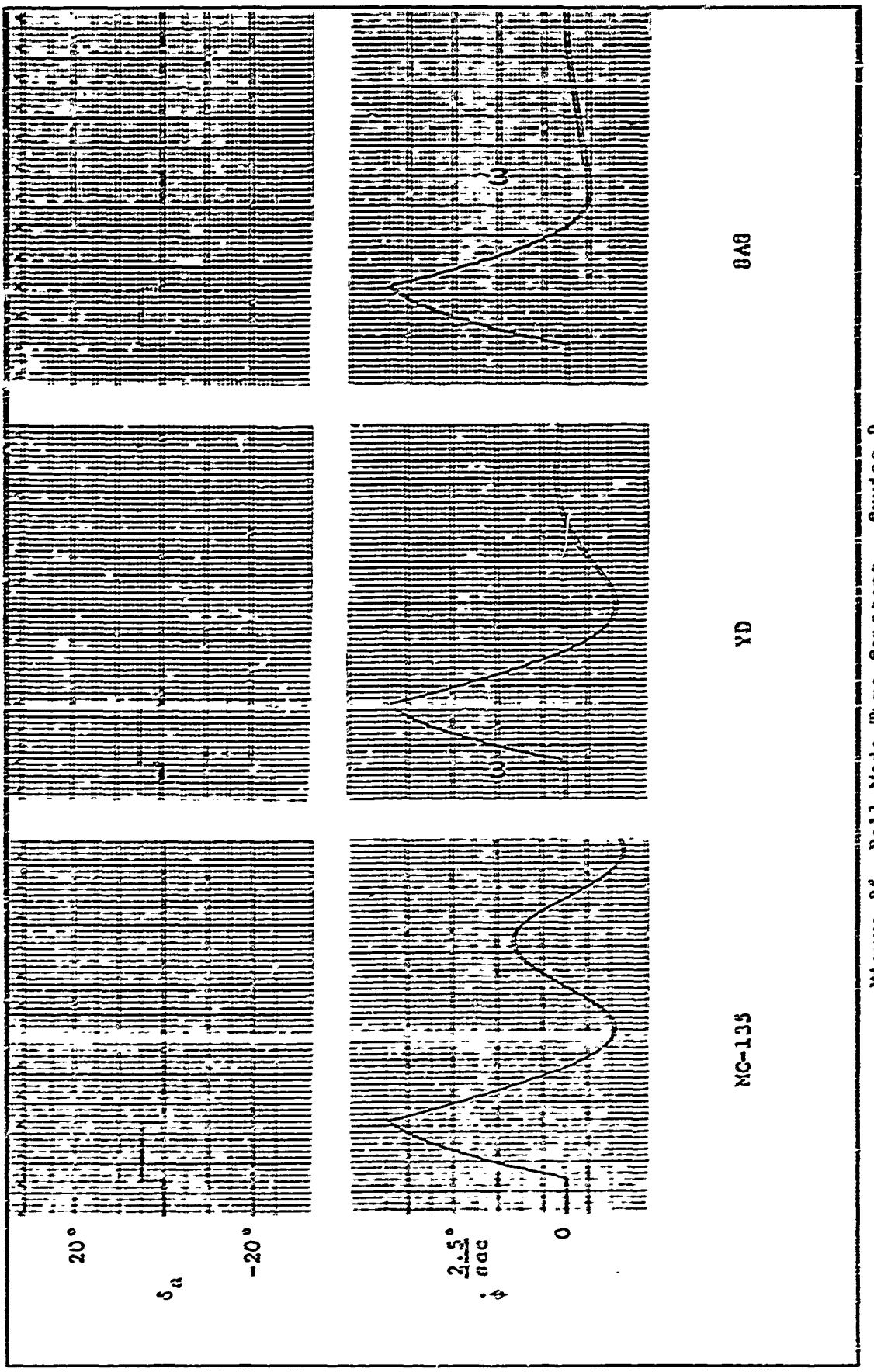

Figure 36. Roll Mode Time Constant - Cruise 2

Figure 37. Spiral Stability - Cruise 2

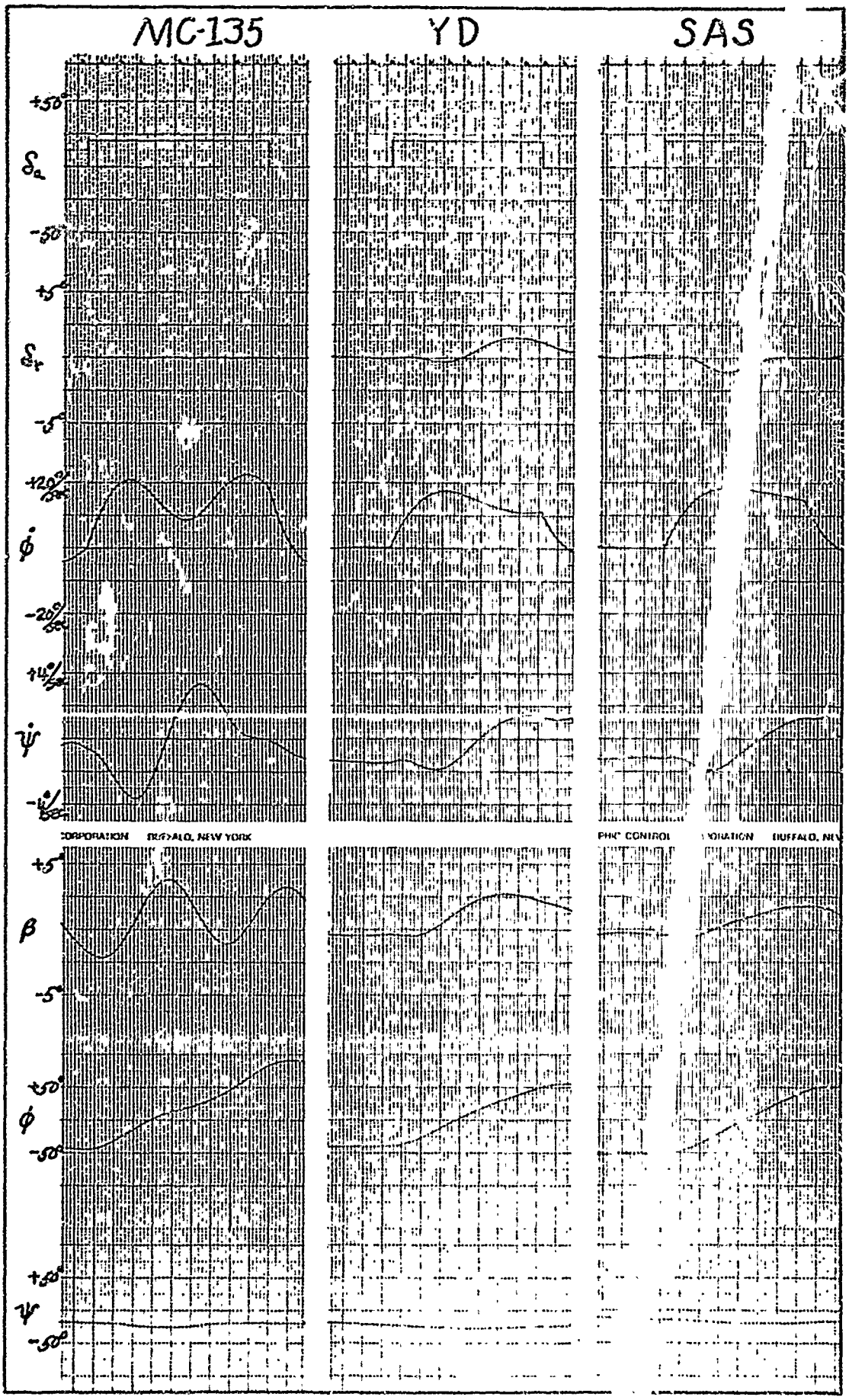

Figure 38. 20 Degree Aileron Step - Cruise 2

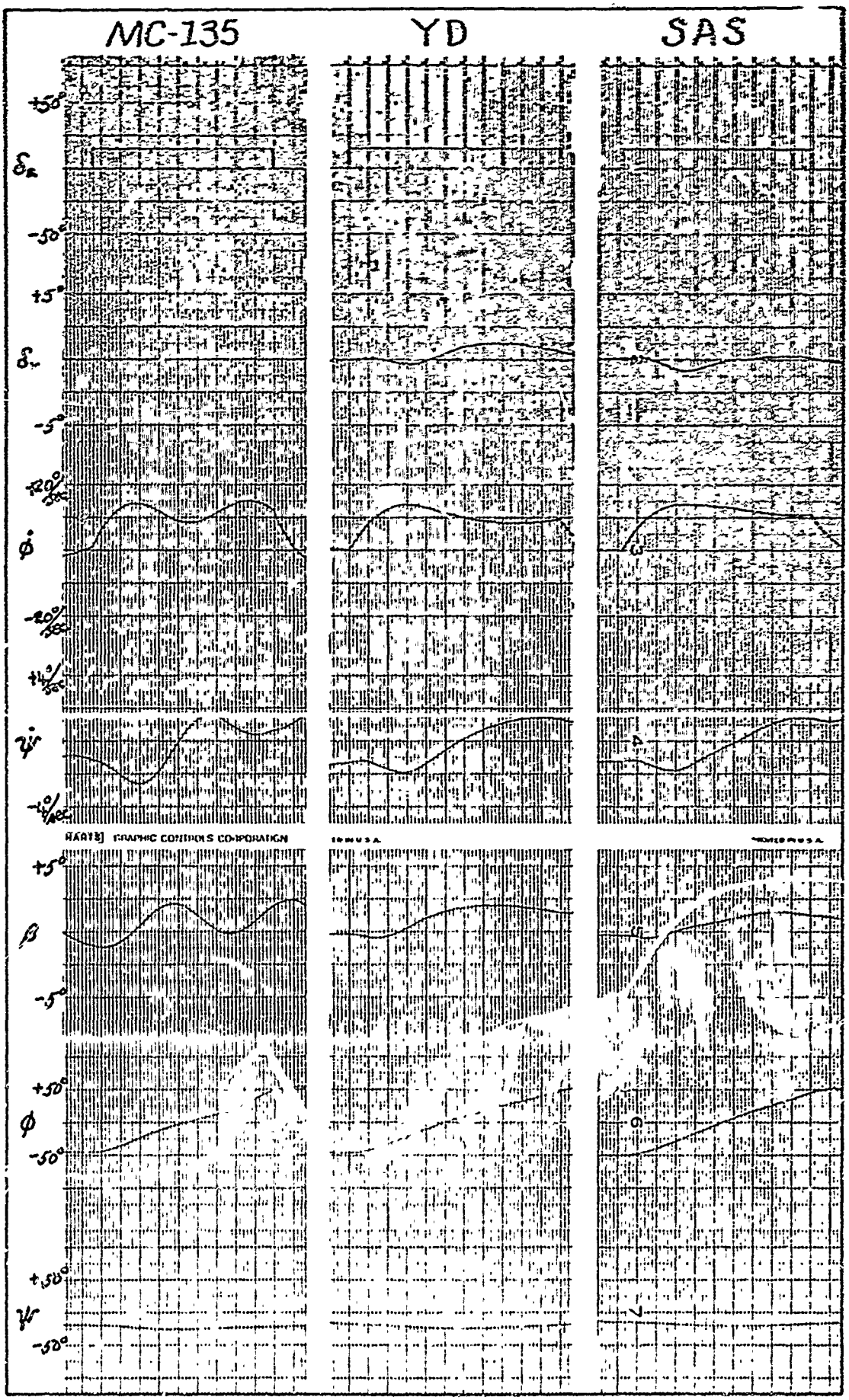

Figure 39. 15 Degree Aileron Step - Cruise 2

measured at two seconds after the input is applied are nearly identical to those measured in Cruise 1 (fifteen and thirteen degrees).

The amount of rudder movement required is reduced with SAS on. However, the rudder is required to move less than two degrees with only the yaw damper which is completely acceptable.

The parameters measured from Figs. 38 and 39 are listed in Table IX

Table IX

Large Aileron Inputs - Cruise 2

δ_a (deg)	Configuration	P_2 as $\%P_1$	ϕ_{com} (deg)	K	β at 90° roll (deg)
	[illegible]-135	66.7	25.0	.835	3.75 = 4.48%
20	YD	61.5	20.0	.667	2.75 = 4.13%
	SAS	81.5	17.0	.564	1.75 = 3.10%
	[illegible]-135	57.7	20.0	.66[illegible]	2.[illegible] = 3.[illegible]%
15	YD	60.7	12.0	.400	2.00 = 5.00%
	SAS	82.0	12.0	.400	1.50 = 3.74%

Step aileron inputs of six, four, and two degrees are shown in Figs. 40, 41, and 42, respectively. There is a significant difference between small aileron inputs of Cruise 1 and of Cruise 2 with SAS on configuration. P_{osc}/P_{av} is of sufficient magnitude that ψ_β and $\%P/\beta$ must be measured to determine if P_{osc}/P_{av} is within specifications. The oscillations in the sideslip trace are more discernible in Cruise 2 than in Cruise 1 and therefore ψ_β and $\%P/\beta$ are measurable. These oscillations are virtually non-existent in Cruise 1 with SAS on. However, ψ_β and $\%P/\beta$ are not required due to the smaller P_{osc}/P_{av} in Cruise 1.

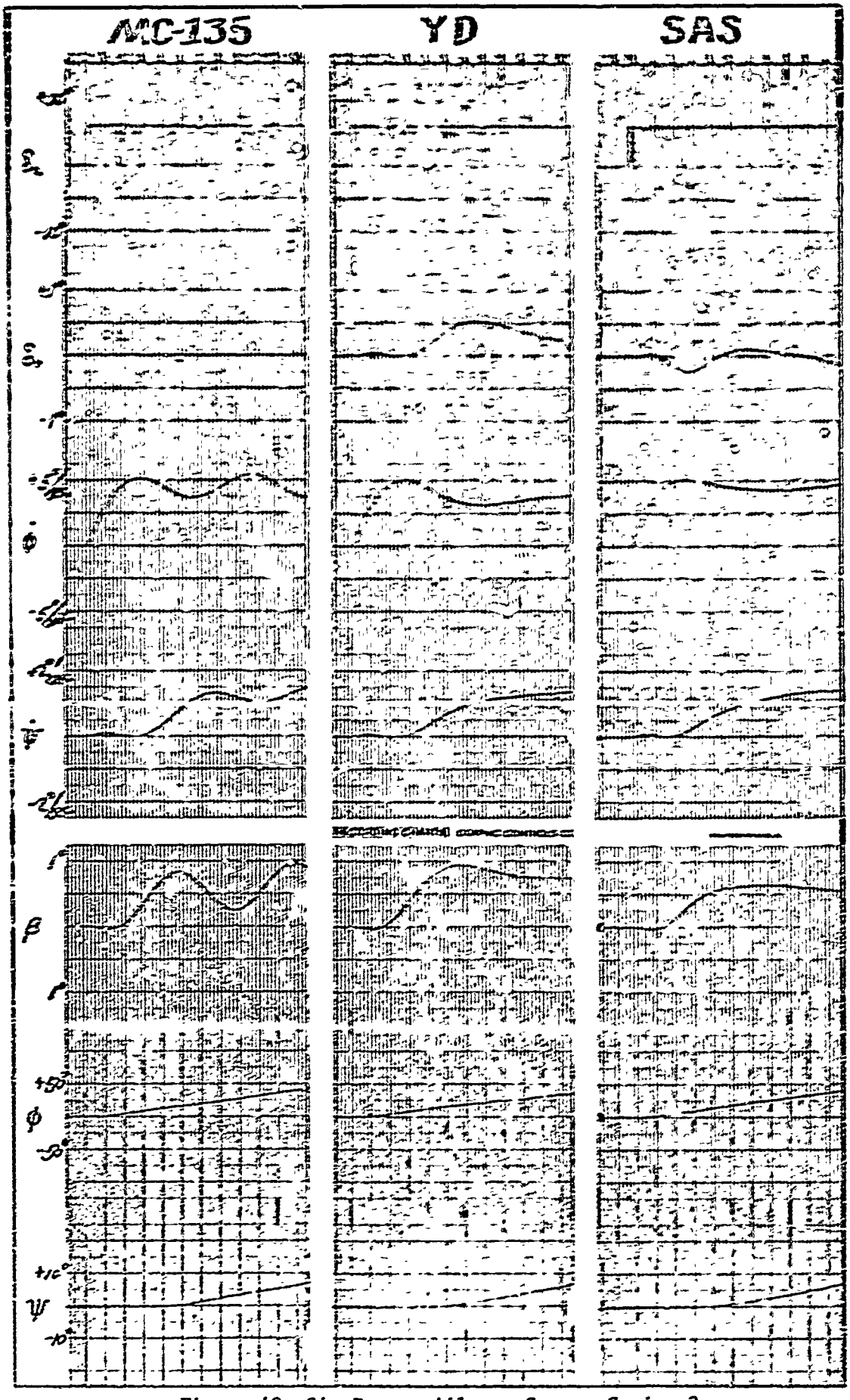

Figure 40. Six Degree Aileron Step - Cruise 2

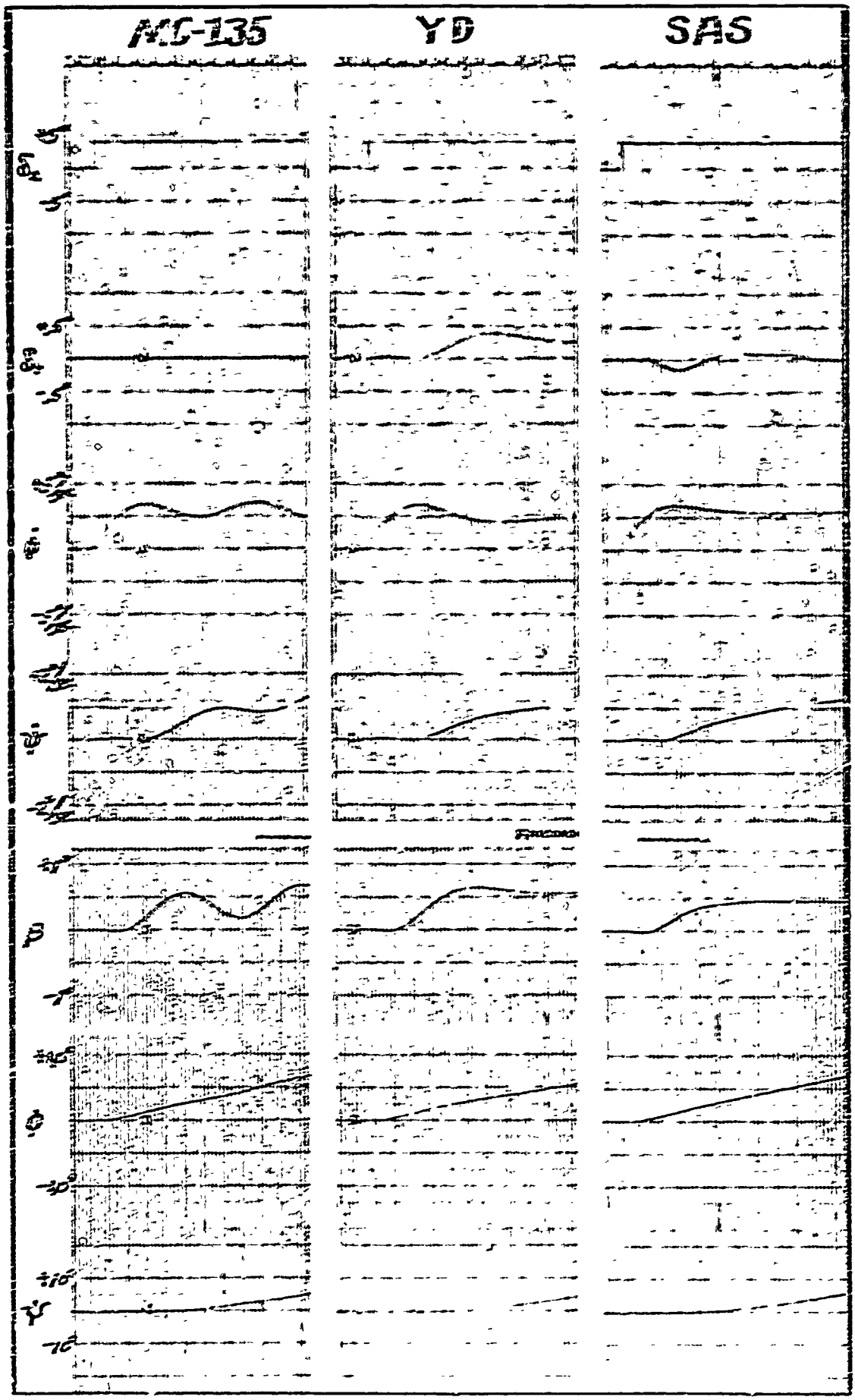

Figure 41. Four Degree Aileron Step - Cruise 2

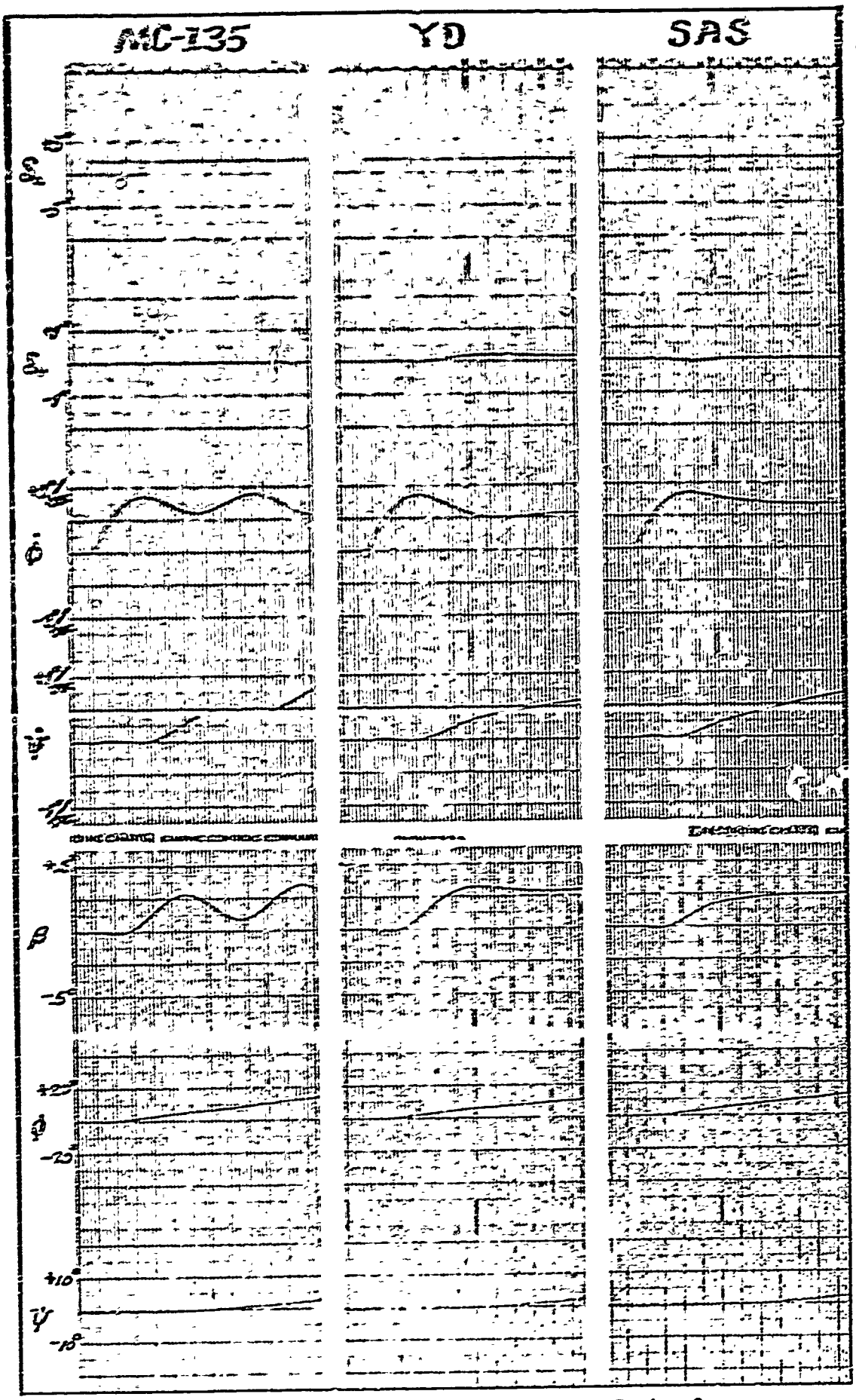

Figure 42. Two Degree Aileron Step - Cruise 2

As before, the yaw damper results in an unwanted increase in P_{osc}/P_{av} and $\Delta\delta_{max}$. The SAS on decreases these two parameters to smaller values than the MC-135 values. The required rudder movement is measured in tenths of degrees rather than in degrees as is the case for large aileron inputs.

Table I correlates the information taken from these small aileron inputs.

Table I

Small Aileron Inputs - Cruise 2

δ_a(deg)	Configuration	P_{osc}/P_{av}	Ψ_β	$\Psi P/\beta$	Φ_{com}(deg)	K	$\Delta\delta_{max}$ at $\frac{1}{2}\tau_D$
	MC-135	.155	-276	108	5.0	.167	.925 = 5.55K
6	YD	.231	-330	168	5.0	.167	.850 = 5.10K
	SAS	.120	-304	120	5.0	.167	.350 = 2.10K
	MC-135	.170	-288	120	3.0	.100	.500 = 5.00K
4	YD	.256	-324	180	3.0	.100	.650 = 6.50K
	SAS	.111	-252	108	4.0	.134	.400 = 3.00K
	MC-135	.172	-276	120	2.0	.067	.288 = 4.29K
2	YD	.259	-336	180	1.5	.050	.267 = 5.35K
	SAS	.116	-264	120	1.6	.060	.180 = 3.00K

Power Approach. Figure 43 illustrates how the optimum value of K_A is determined. By looking at the sideslip trace for a K_A of 125, it becomes obvious that this value of K_A is inadequate for Power Approach. While both ζ and ω_η are above minimum for this value, the $\zeta\omega_\eta$ value is below minimum. Also, the time to steady state is a long twenty-two seconds. The other four K_A values shown all provide acceptable ζ, ω_η, and $\zeta\omega_\eta$ with the time to steady state varying. The value 440 provides

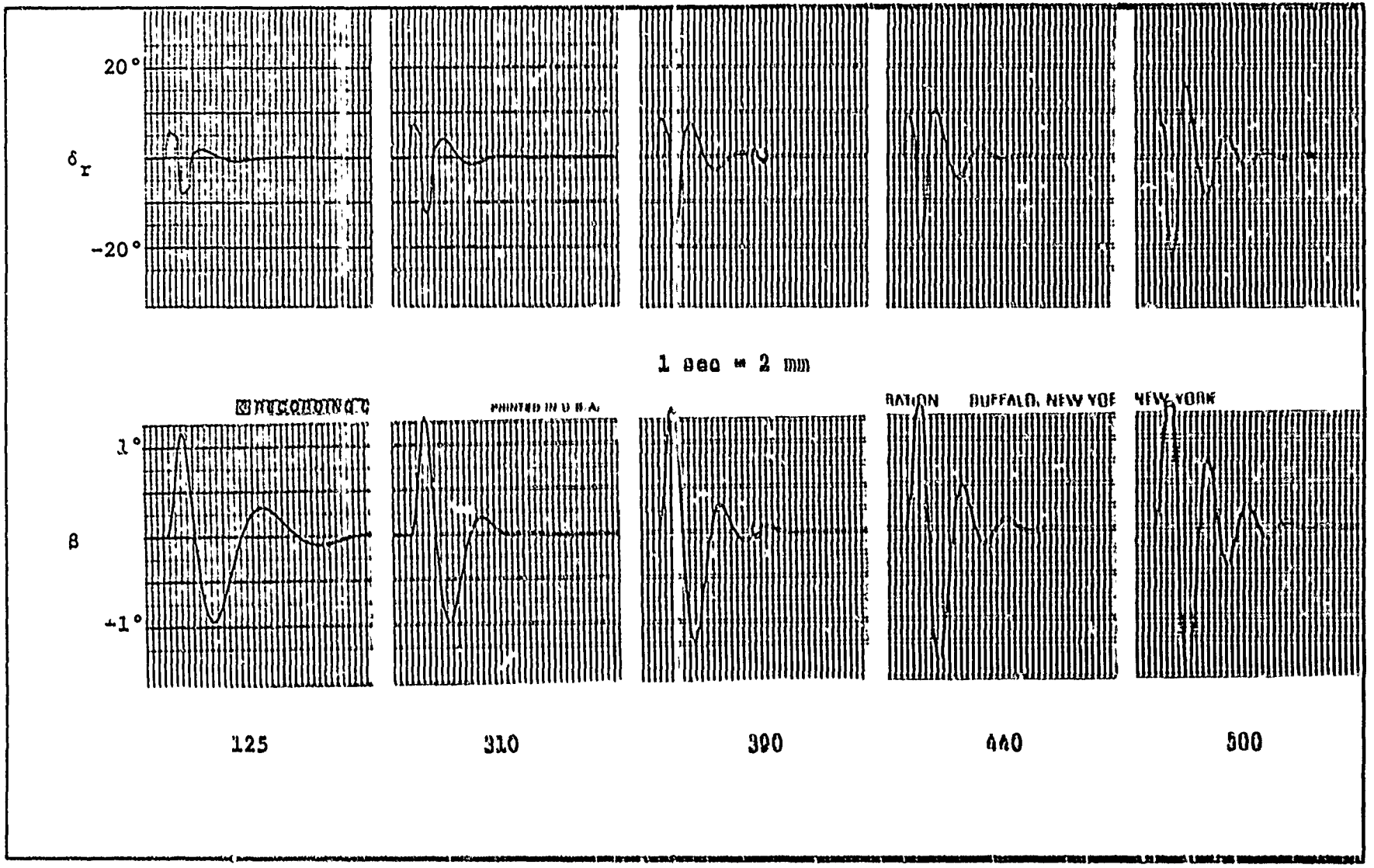

Figure 43. Varying l'_A - Power Approach

the highest $\zeta\omega_n$ of .917 which is .13 larger than the $\zeta\omega_n$ resulting from K_A of 330. This 330 value has the shortest time to steady state of 11.0 seconds, while the 440 value takes 11.5 seconds to reach steady state. The .13 increase in $\zeta\omega_n$ more than compensates for the .5 second slower time to steady state. Therefore, the value of K_A chosen as optimum is 440. This information is tabulated in Table XII.

Table XII

K_A Versus ζ, ω_n, $\zeta\omega_n$ and Time to Steady State – Power Approach

K_A	ζ	ω_n	$\zeta\omega_n$	Time to S.S. (sec)
125	.34	.766	.235	22.0
220	.54	1.333	.720	15.0
330	.48	1.640	.787	11.0
440	.48	1.910	.917	11.5
500	.33	2.050	.677	16.0

Figure 44 compares the ζ, ω_n, and $\zeta\omega_n$ for the three configurations. The MD-135 ζ (.04) is double the value from Cruise 2 (.02). However, it still falls considerably short of the required .19. Also, the ω_n is lower than either cruise condition. Therefore $\zeta\omega_n$ is extremely small. The yaw damper increases the ζ but to a smaller value than the cruise conditions. The decrease in ω_n is also apparent from this figure. For the yaw damper, ζ and ω_n are both above minimum, however $\zeta\omega_n$ is not. Surprisingly, the SAS increases ζ by .2 which compares very favorably to the .2 increase from the yaw damper. The SAS increases the ω_n substantially, thereby causing $\zeta\omega_n$ to be satisfactory.

Table XII compares ζ, ω_n, and $\zeta\omega_n$ for the three configurations.

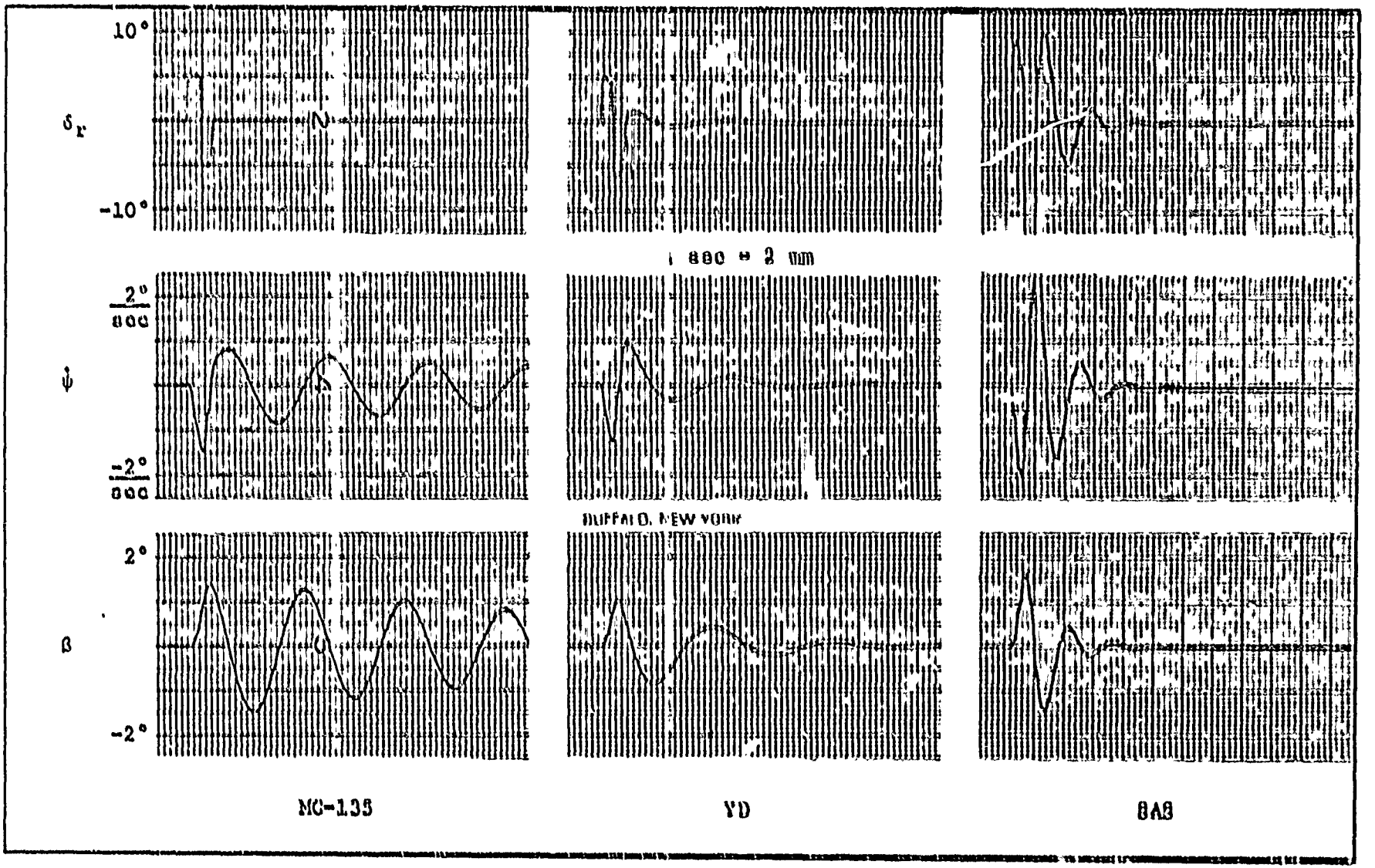

Figure 44. Comparison of ζ And ω_n - Power Approach

Table XIII

ζ, ω_n, and $\zeta\omega_n$ Versus EC-135, ED, SIS – Power Approach

Configuration	ζ	ω_n	$\zeta\omega_n$
EC-135	.046	.742	.034
ED	.230	.585	.134
SIS	.435	2.010	.875

The other requirements are checked by use of the following figures:

Figure	Requirements	
45	roll mode time constant	(2)
46	spiral stability	(3)
47 and 48	large aileron inputs	(4 and 6)
49, 50, and 51	small aileron inputs	(5 and 7)

The roll mode time constant is measured to be .75 seconds from Fig. 45. This is smaller than the 1.1 seconds in the cruise conditions and is approximately half the maximum allowed of 1.4 seconds. This indicates that the roll angle at two seconds after the input will be considerably larger in Power Approach than in cruise conditions for the same aileron inputs.

The spiral stability is measured from Fig. 46. The Power Approach spiral mode is divergent as opposed to the convergent spiral mode for the cruise conditions. However, the time it takes for the bank angle to double is almost forty seconds, well beyond the twenty second requirement.

Figures 47 and 48 show the large aileron inputs of twenty and fifteen degrees, respectively. Due to the small roll mode time constant, the roll angle changes so fast that the input has to be removed

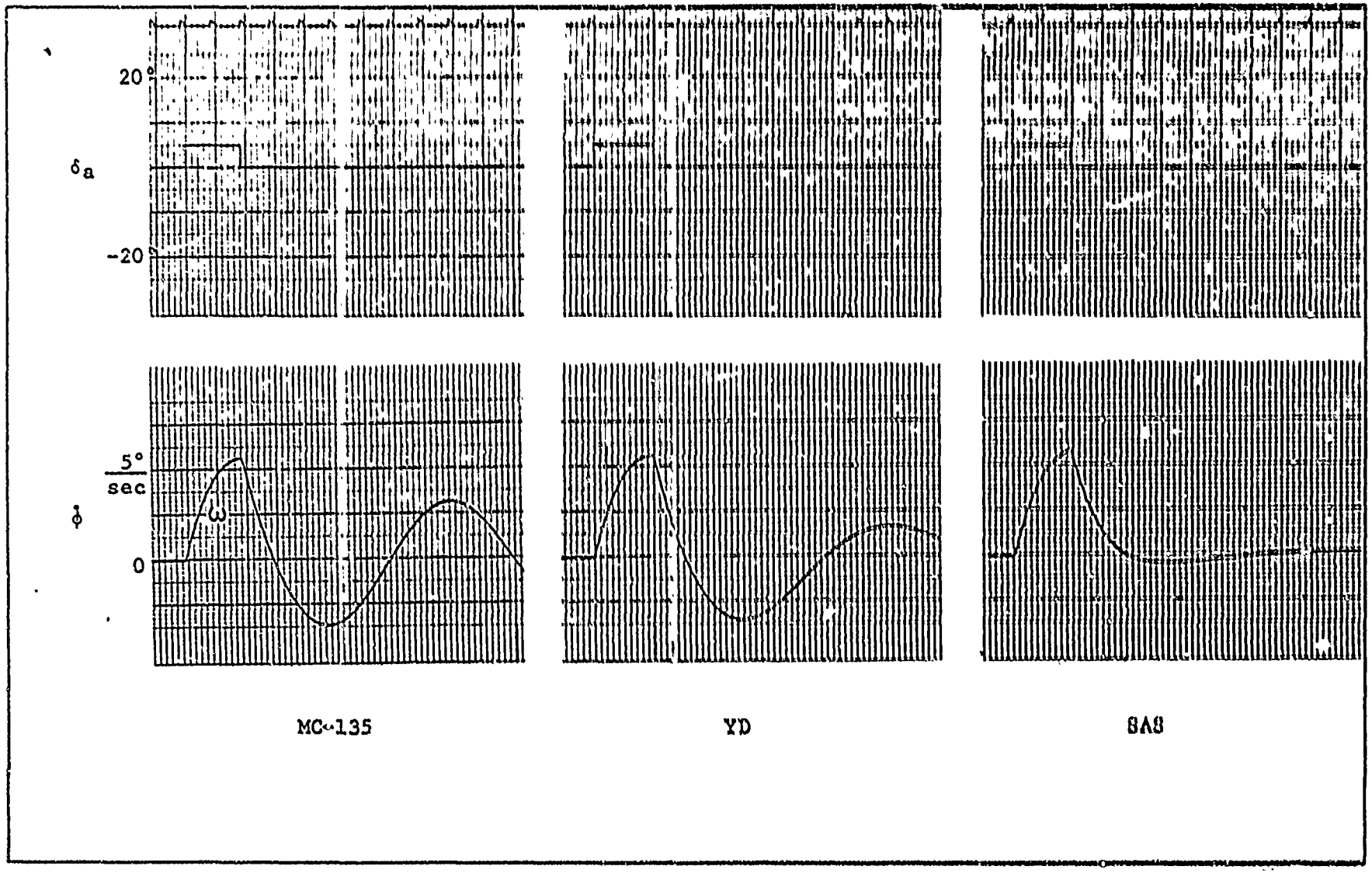

Figure 45. Roll Mode Time Constant - Power Approach

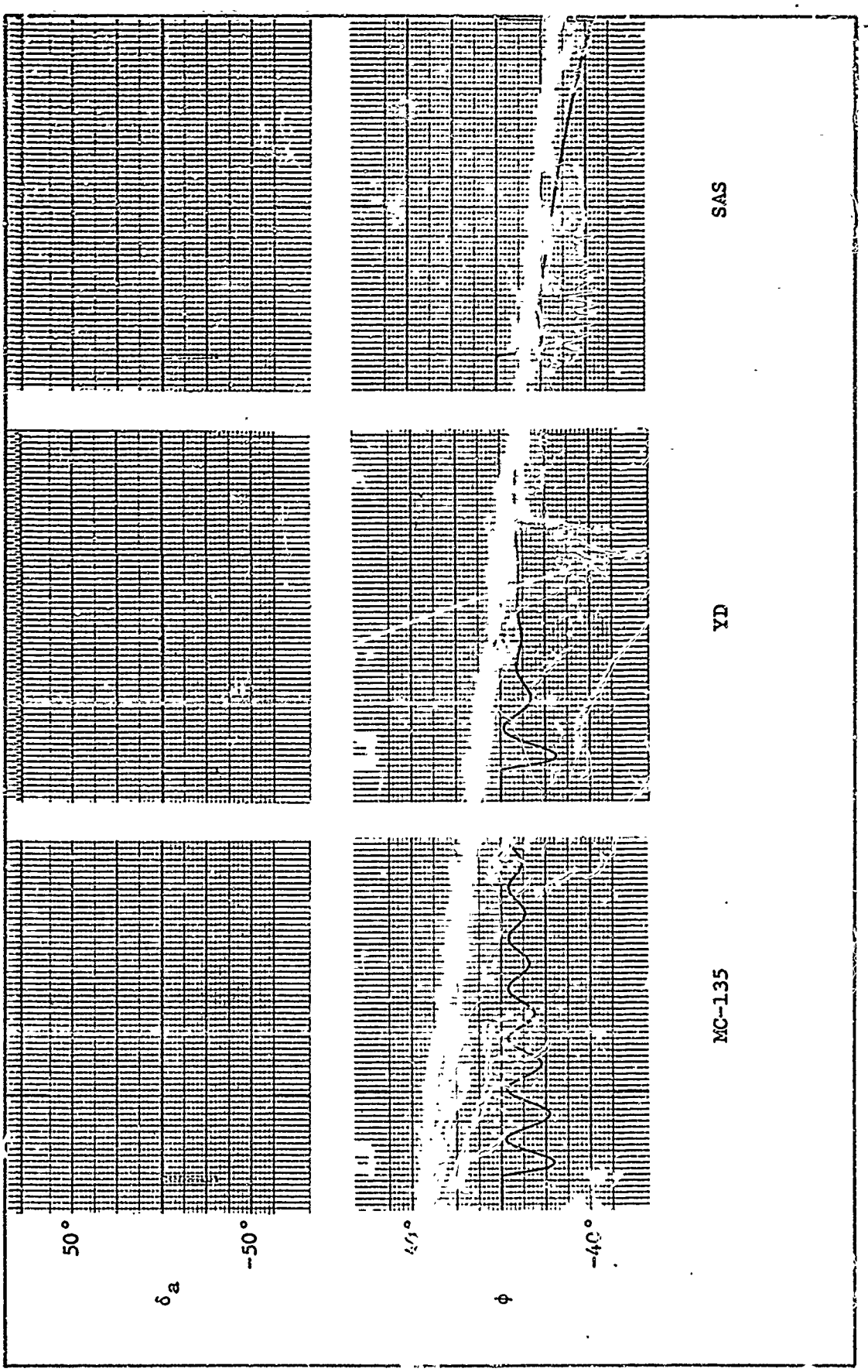

Figure 46. Spiral Stability - Power Approach

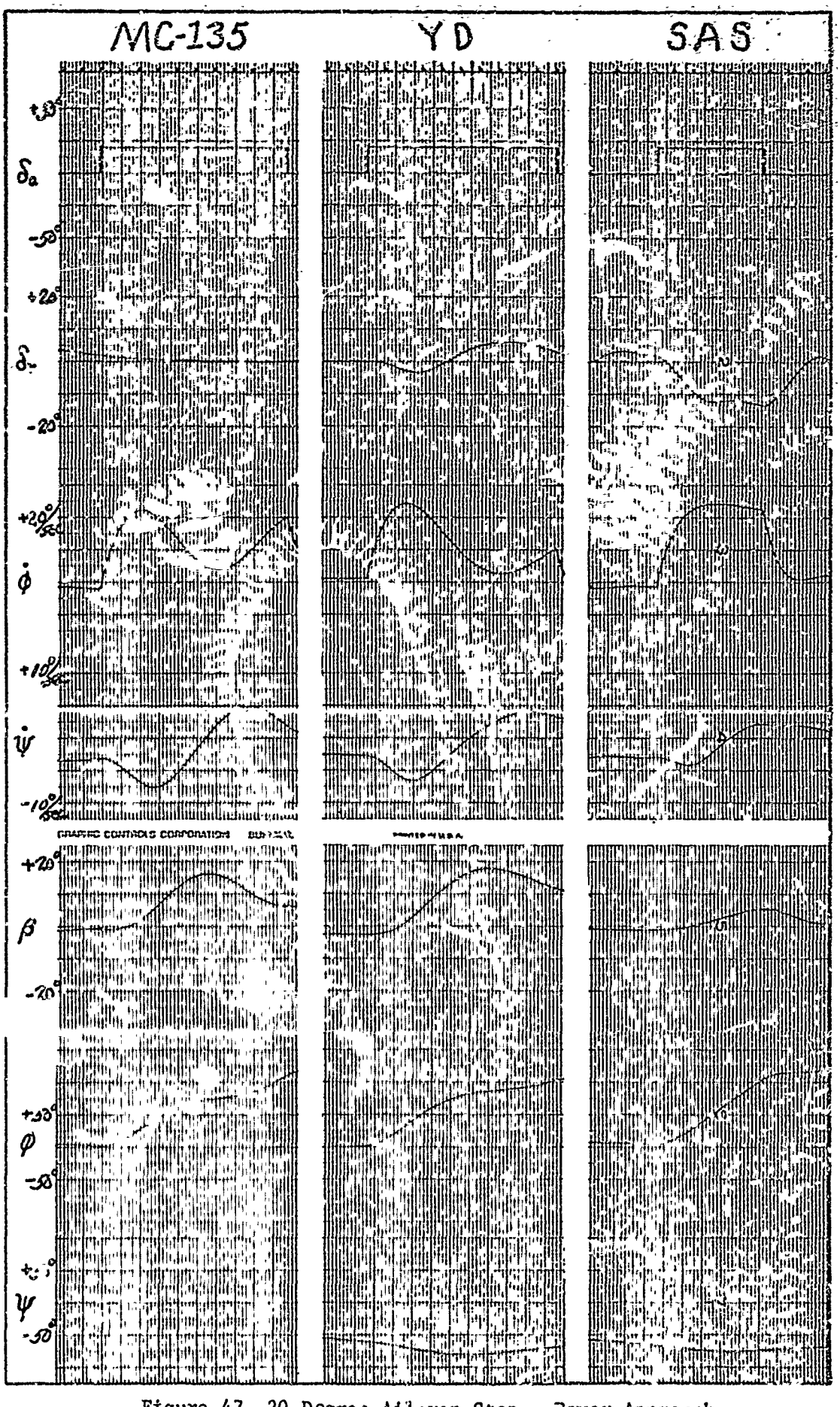

Figure 47. 20 Degree Aileron Step - Power Approach

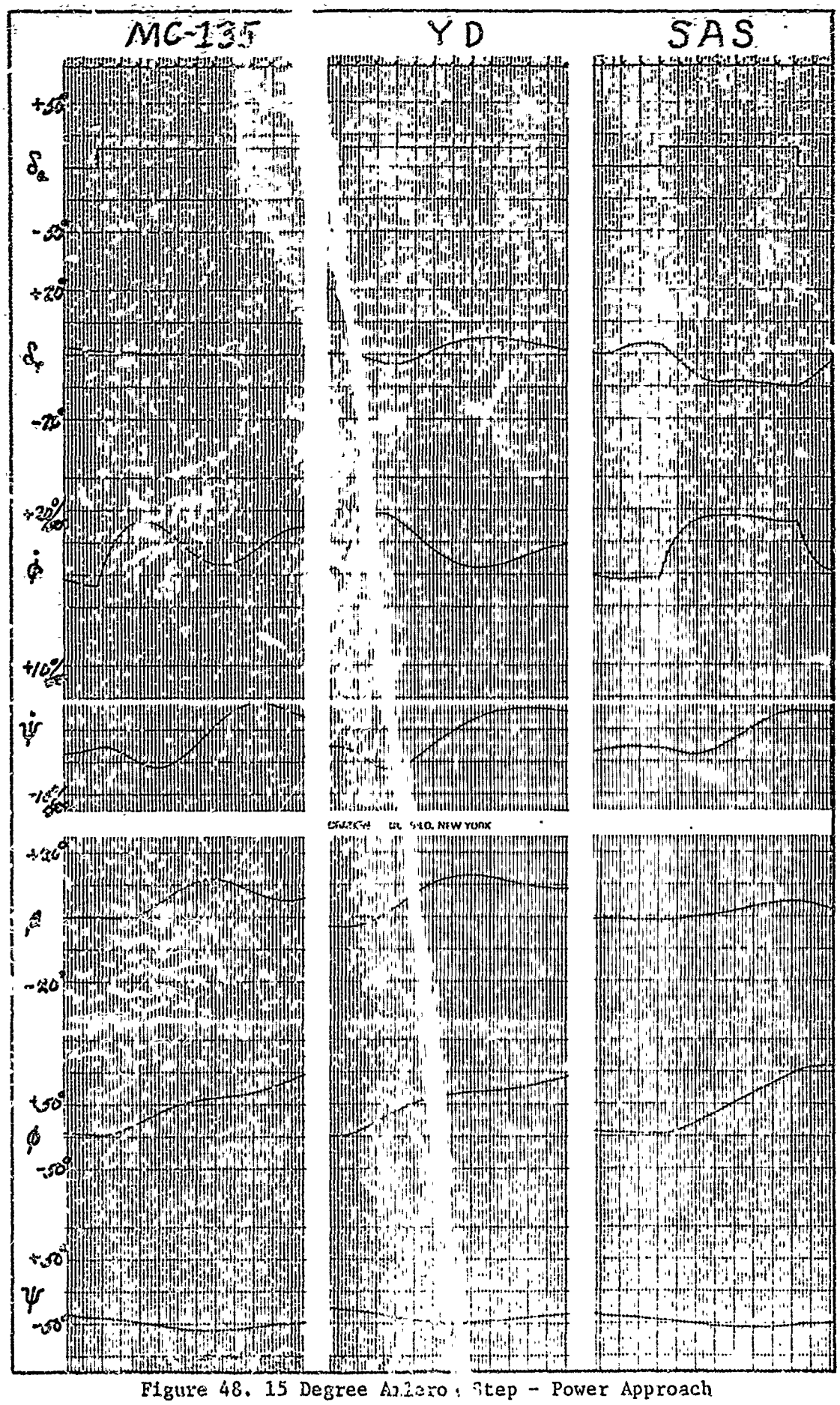

Figure 48. 15 Degree Aileron Step - Power Approach

before a minimum in the roll rate trace occurs for the fifteen as well as the twenty degree input. The roll angle after two seconds is twenty-two degrees as compared to thirteen degrees in Cruise 1 and twelve degrees in Cruise 2 for a fifteen degree aileron input.

Further, an important difference between Power Approach and the cruise conditions is the rudder movement required. Even with the SAS on, the twenty degree aileron input requires the rudder to move about fifteen degrees while the fifteen degree aileron input requires the rudder to move eleven degrees. This is considerably beyond the four degree limit that is presently being used on the C-135B. This point is discussed in more detail under the section entitled "Limiter".

Table XIII lists the measurements taken from Figs. 47 and 48.

Table XIII

Large Aileron Inputs - Power Approach

δ_a (deg)	Configuration	P_2 as $\%P_1$	ϕ_{com} (deg)	K	β at 90° roll (deg)
	MC-135	25.0	22.0	.734	16.50 = 22.2K
20	YD	7.3	30.0	1.000	17.00 = 17.0K
	SAS	93.5	25.0	.834	6.25 = 7.5K
	MC-135	32.5	17.0	.568	12.50 = 22.0K
15	YD	2.9	25.0	.834	13.00 = 15.6K
	SAS	96.7	22.0	.735	5.50 = 7.5K

The small aileron inputs of six, four, and two degrees are shown in Figs. 49, 50, and 51, respectively. The MC-135 has an extremely poor P_{osc}/P_{av}. Even so, the yaw damper further degrades this parameter almost to the point of roll rate reversal. The SAS decreases P_{osc}/P_{av} to values small enough that ψ_β and $\not P/\beta$ are not necessary to show

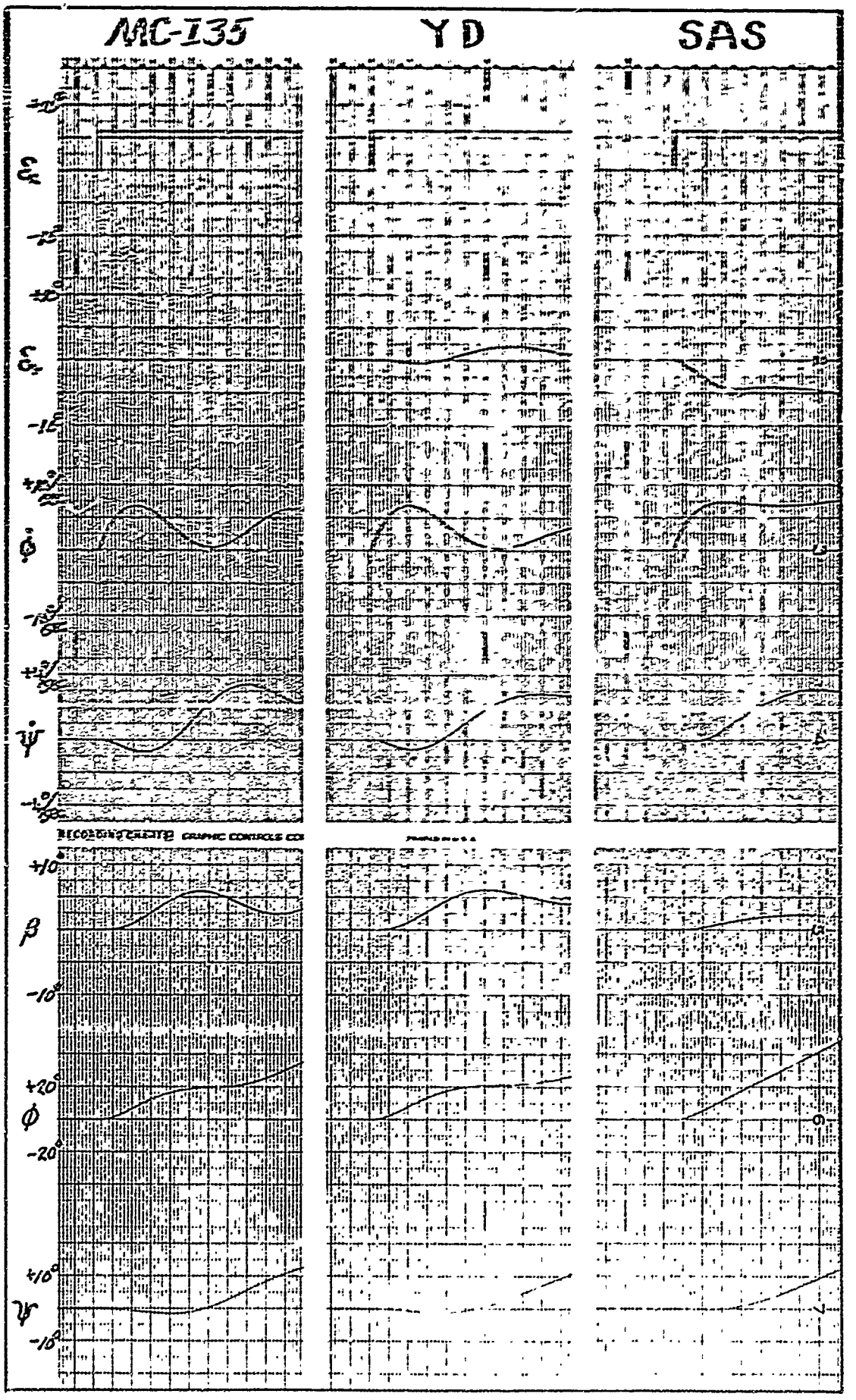

Figure 49. Six Degree Aileron Step - Power Approach

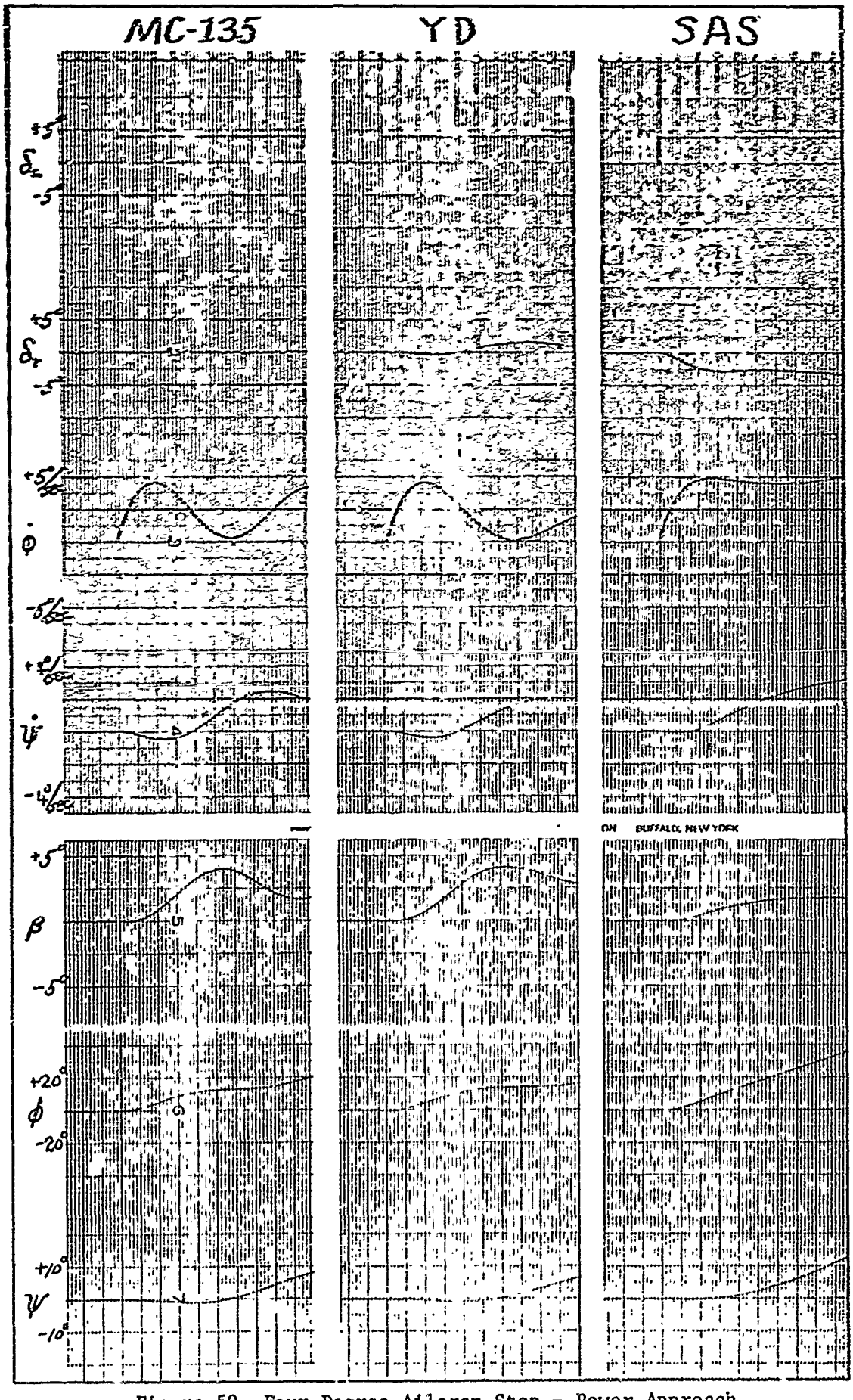

Figure 50. Four Degree Aileron Step - Power Approach

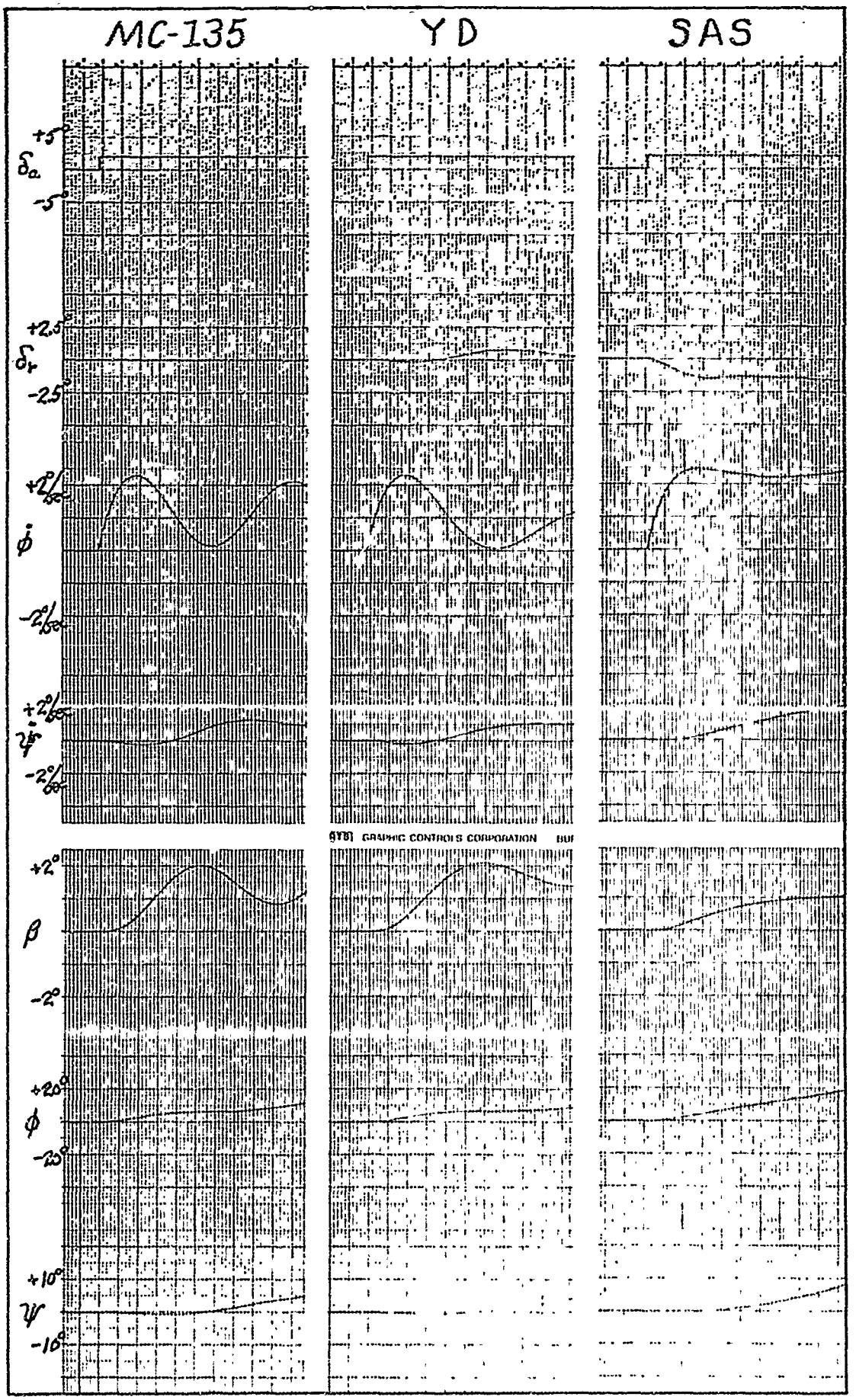

Figure 51. Two Degree Aileron Step - Power Approach

compliance with the requirements. As in Cruise 1, this is fortunate since the oscillations of the sideslip trace are very difficult to measure.

From the rudder trace, it is seen the six, four, and two degree aileron inputs require rudder movement of five, three, and one and a half degrees, respectively.

The measurements taken from these three figures are shown in Table XIV.

Table XIV

Small Aileron Inputs - Power Approach

δ_a(deg)	Configuration	P_{osc}/P_{av}	ψ_β	$\dot{\psi}P/\beta$	ϕ_{com}(deg)	K	$\Delta\beta_{max}$ at $\frac{1}{2}T_D$
	MC-135	.862	-158	326	8.0	.267	3.0 = 11.2K
6	YD	.892	-196	4	7.8	.260	3.0 = 11.5K
	SAS	053	#	#	9.5	.316	.9 = 2.9K
	MC-135	.895	-138	307	5.0	.167	1.0 = 6.0K
4	YD	.948	-216	23	5.0	.167	1.0 = 6.0K
	SAS	.053	#	#	7.0	.234	.6 = 2.8K
	MC-135	.878	-158	326	3.0	.100	1.0 = 10.0K
2	YD	.957	-216	23	3.0	.100	1.0 = 10.0K
	SAS	.053	#	#	4.0	.134	.3 = 2.2K

measurement not necessary since parameters meet requirements regardless of value

Discussion

Damping and Frequency. It can be seen from Tables V, VIII, and XII that the increase in ζ is largely due to the yaw damper while the increase in ω_n is a result of the acceleration feedback. The success of this design is a direct result of this effect.

Roll Mode Time Constant. Due to the analog scale involved, it was difficult to measure any change in the roll mode time constant. The root locus computer printout indicates a slight shift of value, but it is of little significance as the time constant was within requirements for all conditions.

Large Aileron Inputs. The requirement for large aileron inputs states the input must be held until the bank angle changes ninety degrees. Small angle approximation theory provides erratic results at large angles because the equations become invalid. Therefore, the aircraft was set at a minus forty-five degree bank angle and then the step aileron input (for measurement) was applied. This requires the angle to change from minus forty-five degrees to plus forty-five degrees as opposed to changing from zero degrees to ninety degrees and is a standard simulation technique used to avoid large angles.

With an initial minus forty-five degree bank angle, sideslip also has an initial value. As the parameters involved are concerning with relative change of values instead of absolute values, the initial magnitudes are of no significance. However, it is important (for accurate results) that bank angle and sideslip have reached steady state values before applying the input.

As a point of interest, trim was incorporated in some sample runs to compare with the runs (without trim) used in this study. The trim

consisted of the small values of rudder and aileron required to bring the steady state sideslip back to zero for a minus forty-five degree bank angle. The comparison showed negligible difference.

Small Aileron Inputs. For small inputs, the bank angle changes at a much slower rate. Since the amount of time required to measure the parameters remains fairly constant, the slower rate means that large bank angles do not occur within the time of interest. Therefore, the initial bank angle can start at zero.

In both the basic aircraft and yaw damper, the value of ϕ_β determines whether the requirements are satisfactory or not. In these two cases, ϕ_β is measurable (see Fig. 42 'HC-135'). However, it is virtually impossible to measure ϕ_β for these small inputs with the SAS on as oscillations on the sideslip trace are not observable (see Fig. 42 'SAS'). But, any value of ϕ_β meets the requirements for the overall system because of the small values of P_{osc}/P_{av} and $\Delta\beta_{max}$. Therefore, it is not required to measure ϕ_β in this case.

Additional Comments

With the SAS on, it can be seen that the Dutch roll is almost completely eliminated for any kind of aileron input. To demonstrate this, a thirty degree aileron doublet was applied to the system in an effort to excite the Dutch roll oscillation. The results for each flight configuration are shown in Figs. 52, 53, and 54.

Since the Dutch roll excitation from an aileron input is virtually eliminated, even with a very large input, it seems reasonable to assume that no oscillation and thus no P_{osc}/P_{av} should be present in any of the roll rate traces for SAS on when subject to the various aileron

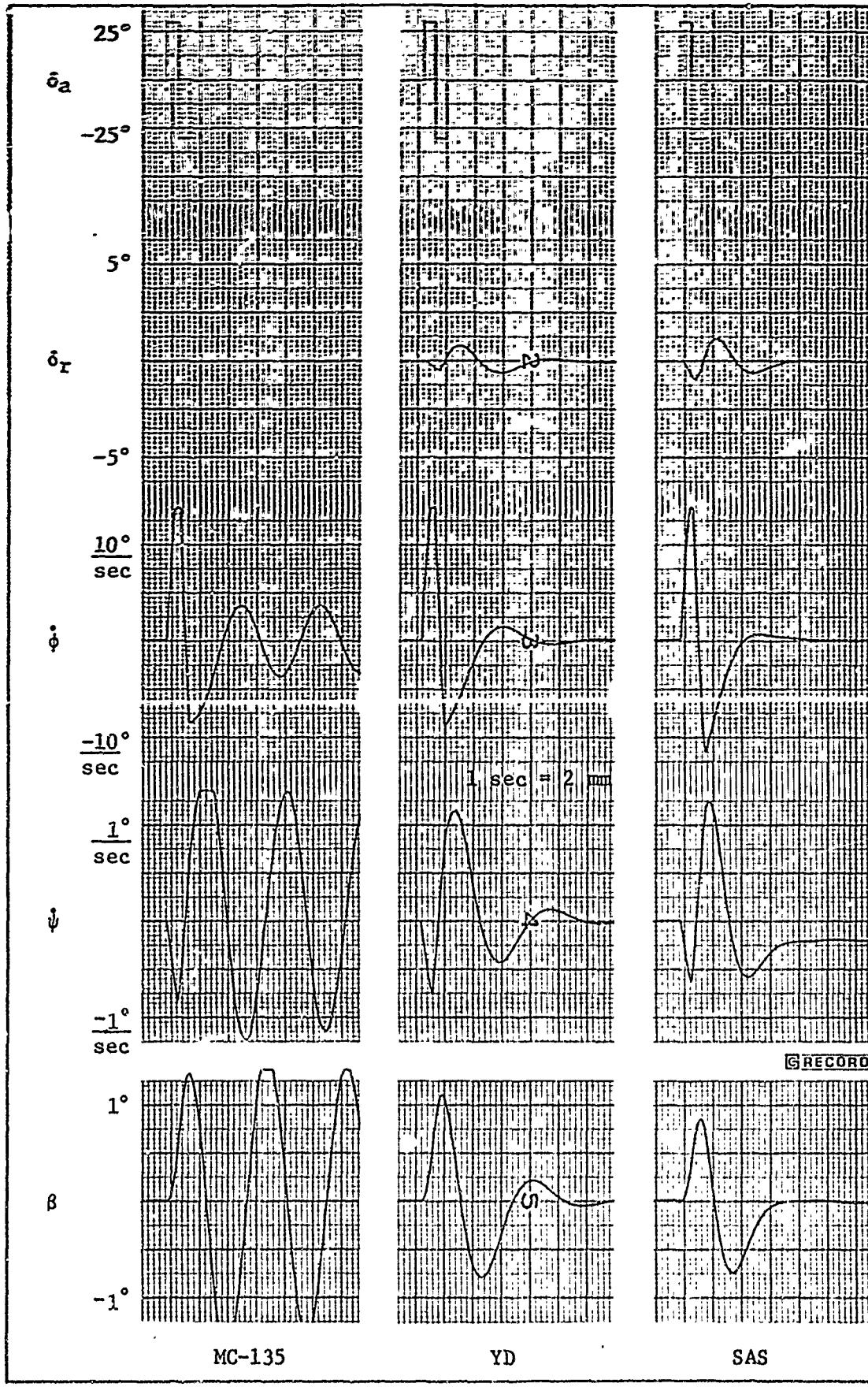

Figure 52. 30 Degree Aileron Doublet - Cruise 1

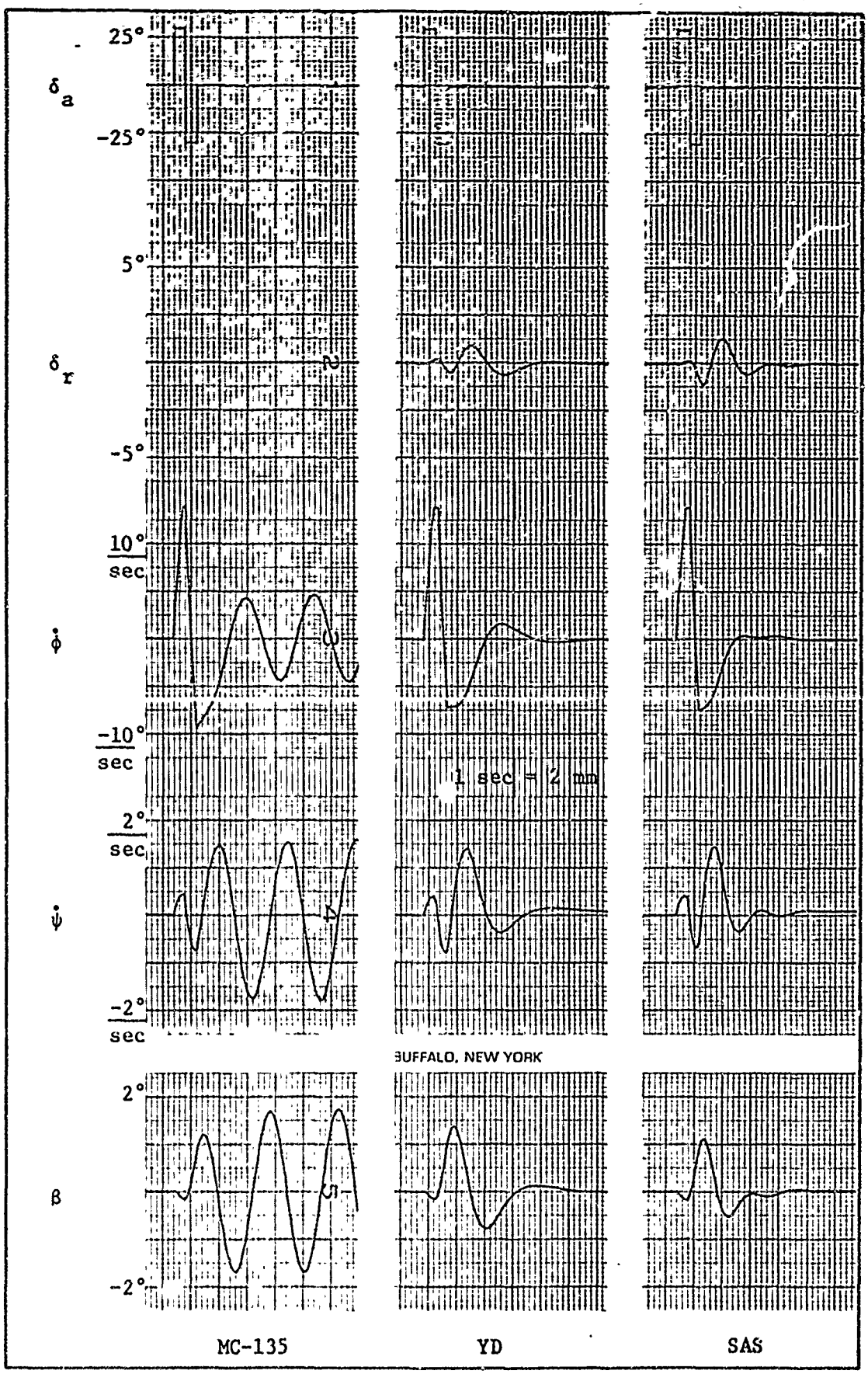

Figure 53. 30 Degree Aileron Doublet - Cruise 2

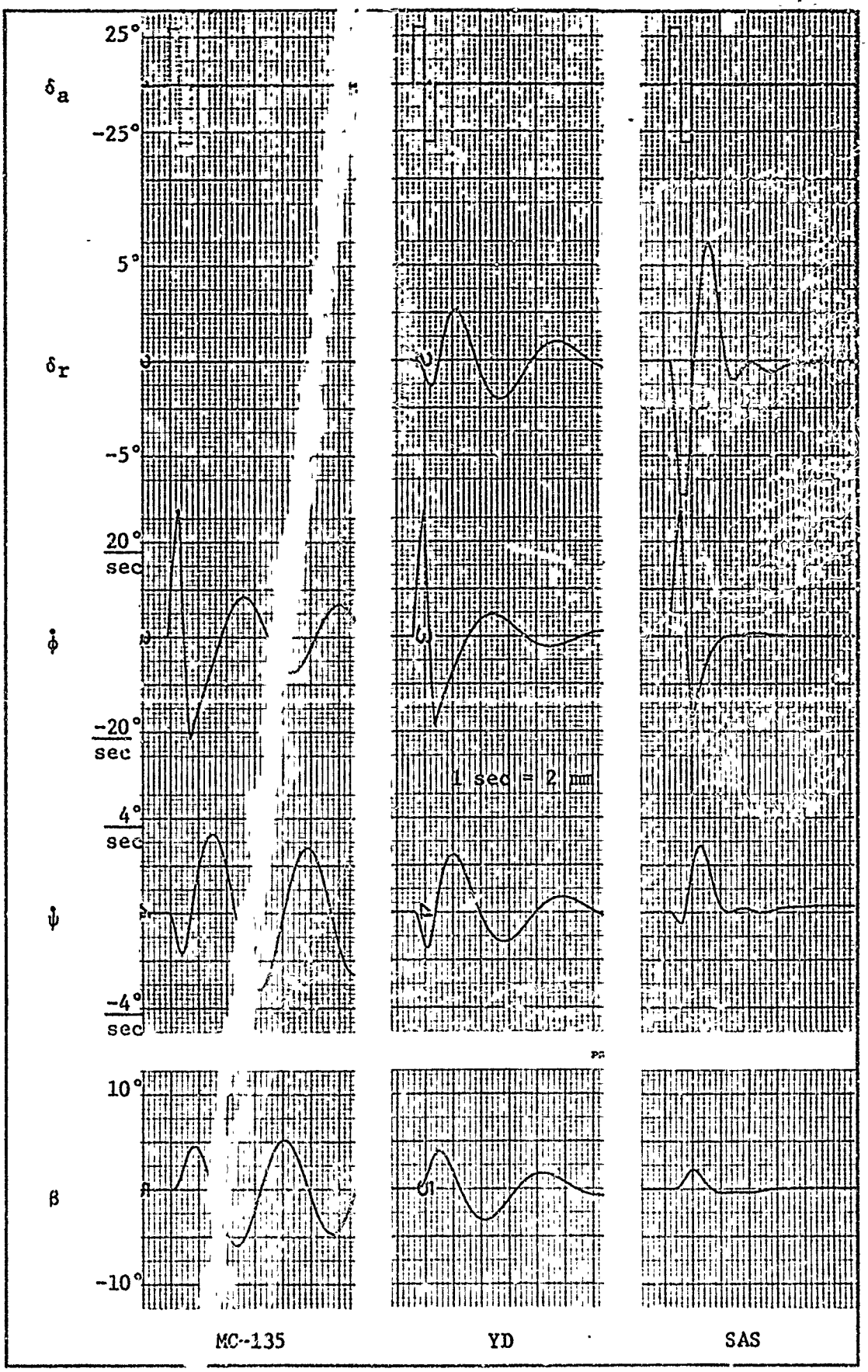

Figure 54. 30 Degree Aileron Doublet - Power Approach

step inputs. However, it can be seen that there is a definite variation or fluctuation present in these roll rate traces thus constituting a measurable P_{osc}/P_{av}. This effect is caused simply by the resulting action of the SAS and thus the rudder during the rolling maneuver. Further, one can see that this action is not created by the addition of acceleration feedback but rather is a characteristic of the original yaw damper itself. In fact, the addition of acceleration feedback helps to correct the action and thus decrease the P_{osc}/P_{av} which in either case is within the specified tolerance.

Limiter

The SAS design performs its designated purpose extremely well by assuming full rudder authority. Full rudder authority means the augmentation system can move the rudder to the stops if required.

At present, the MC-135 contains a limiter which prevents the SAS fror moving the rudder past four degrees. This limiter would reduce the effectiveness of the SAS whenever a rudder larger than four degrees is required. There is no effect in the two cruise conditions because the SAS does not require the rudder to move more than four degrees. Power Approach is affected, but only at the larger inputs.

The limiter prevents "hard-over" in the event the SAS fails at a point where it was requiring large amounts of rudder. Four degrees was designated as the value not to exceed if a failure occurred.

In Power Approach, the roll response is quite small as a four degree rudder input changes roll angle by only eight tenths of a degree in two seconds. Due to this small response, a much larger limit can be used for Power Approach. Because of the large roll response to aileron

inputs, relatively large aileron would, in all probability, not be used in Power Approach.

For twenty degree aileron (aircraft limit) input, the SAS requires the rudder to move fifteen degrees and smaller inputs require corresponding smaller rudder movement. This fifteen degree limit is deemed acceptable for Power Approach and allows the SAS to perform as intended. Therefore, the limiter value is changed from four degrees in cruise to fifteen degrees in Power Approach.

If subsequent test flights indicate a lower limit is desired for Power Approach, a reduced limit could be used with slight degradation of performance and then only at larger aileron inputs.

V. Conclusions and Recommendations

From root locus analysis, it was determined that cascade compensation techniques were inadequate to produce the required ζ and ω_η. In every case tried, the compensated system provided either insignificant changes in ζ or actually reduced ζ instead of increasing it. These systems were verified through analog simulation.

A technique commonly used in cascade compensation is to cancel system poles and zeros with compensator zeros and poles. In this system, however, certain poles can not be cancelled. For instance, to retain the same filtering characteristics, the rate filter poles must remain unchanged. Also, exact cancellation of any aircraft poles or zeros is not possible since the location of these poles and zeros varies from one flight condition to the next. In this system, the aircraft poles and zeros that needed to be cancelled were so close to the imaginary axis and in some cases even unstable, thus undesirable results could exist if exact cancellation was not realized.

The ζ of the basic system was increased to an acceptable value by using the Boeing series yaw damper. However, the yaw damper caused a decrease in ω_η. Other parameters such as P_{osc}/P_{av} , and $\Delta\beta_{max}$ were also degraded when the yaw damper was used.

Since a large roll rate is produced by a yaw or sideslip disturbance, it was felt that a SAS which used $\dot{\phi}$ feedback, in addition to $\dot{\psi}$ feedback, would be very effective in improving the handling qualities over that of the yaw damper alone. However, root locus analysis and subsequent analog simulation indicated that this was not the case. In every case tried, the $\dot{\psi}$ feedback alone produced a better performance

than did the blended $\dot{\phi}$ and $\dot{\psi}$ feedback.

Acceleration feedback was then incorporated into the system to improve the response. In all cases, ω_η, P_{osc}/P_{av}, and $\Delta\beta_{max}$ were improved over that of the basic aircraft. As noted from the analog runs, when the system was disturbed by a rudder deflection the time required to damp the resultant Dutch roll was significantly improved. Moreover, the Dutch roll was almost totally suppressed when the system was disturbed with the ailerons.

Location of the accelerometer was investigated as discussed in Appendix B. It was determined that adequate performance could be obtained with the accelerometer located at the aircraft c.g. In that position, the accelerometer measures only acceleration in the lateral or Y direction which is precisely the quantity that needed to be reduced. An accelerometer located forward or aft of the c.g. measures the yaw angular (tangential) acceleration in addition to the acceleration at the c.g. This tangential acceleration either adds to or subtracts from the lateral acceleration. Final analysis showed that essentially all that this addition or subtraction changes is the sensitivity required of the accelerometer. Since no apparent advantage was noted by moving the accelerometer, it was located at the c.g. in the final design. If it becomes necessary to locate the accelerometer at some point other than the c.g., it can be done simply by using an accelerometer with a different sensitivity.

Of the cruise conditions, Cruise 1 showed the least acceptable handling qualities for the basic unaugmented aircraft. Therefore, the design was based primarily on this flight condition. As a result, the optimum value of loop gain for Cruise 1 was also used for Cruise 2.

The final analog verification showed this approach to be quite adequate for both cruise conditions. However, at that particular setting of loop gain, the handling qualities for Power Approach were not acceptable. Since the transition to Power Approach begins when flaps are lowered, two flap switches were used to change the gain and achieve the optimum value.

It was determined that the four degree rudder limiter, which is used in the standard yaw damper, would prevent the SAS from performing to its full capability while operating in Power Approach. Due to the small response of roll rate to a rudder input, when in Power Approach, the four degree limit was considered as unnecessarily restrictive. From repeated simulation of rudder hardovers while varying the rudder limit, it was concluded that a limit of as much as fifteen degrees could be used for Power Approach. Since the four degree rudder limit is still required for cruise, it would be necessary to switch from a four degree to a fifteen degree limit when entering Power Approach. This can be done by using another flap switch.

The SAS designed in this study is considered to be quite successful in meeting all the required specifications. Further, the other objectives of simplicity and low cost are adequately fulfilled. The design requires, in addition to the standard series yaw damper, only an accelerometer and two flap switches.

This system has shown significant improvement. However, only three flight conditions were analyzed. It is therefore recommended that further studies include analysis of several additional flight conditions. Further studies should also investigate the effects of turbulence (wind gusts) and unsymmetrical thrust (one engine out) on

this system.

Even though this SAS was designed to correct a problem encountered with a particular modified C-135B aircraft, it could be used to improve the flying qualities of other similar aircraft whose lateral-directional handling qualities have been degraded because of external modifications that change the aircraft aerodynamic characteristics.

Bibliography

1. Blakelock, Col. J. H. Automatic Control of Aircraft and Missiles. New York: John Wiley and Sons, Inc., 1966.

2. Bureau of Aeronautics, Navy Department. Dynamics of the Airframe. Report AE-61-4II. Washington: BuAer, September 1952.

3. D'Azzo, J. J., and C.H. Houpis. Feedback Control System Analysis and Synthesis. New York: McGraw-Hill Book Co., Inc., 1960.

4. Etkin, Bernard. Dynamics of Flight. New York: John Wiley and Sons, Inc., 1962.

5. Fisher, J. D. Root Locus Computing Routine. Unpublished Report. Wright-Patterson AFB, Ohio: Air Force Institute of Technology, June 1969.

6. Griffin, J. M. Analog Simulation of a Modified C-135 Aircraft Having a Series Yaw Damper. Aeronautical Systems Division Technical Report ASD-TR-69-97. Wright-Patterson AFB, Ohio: Air Force Systems Command, January 1970.

7. Griffin, J. M. Digital Computer Solution of Aircraft Longitudinal and Lateral-Directional Dynamic Characteristics. Aeronautical Systems Division, Deputy for Engineering Technical Report SEG-TR-66-52. Wright-Patterson AFB, Ohio: Air Force Systems Command, December 1967.

8. Kuo, B.C. Automatic Control Systems. Englewood Cliffs, New Jersey: Prentice-Hall, Inc., 1962.

9. MIL-F-008785A (USAF). Flying Qualities of Piloted Airplanes. Military Specification. October 1968.

10. Woodcock, R. J., et al. Background Information and User Guide for MIL-F-8785B (ASG). Air Force Flight Dynamics Laboratory Technical Report AFFDL-TR-69-72. Wright-Patterson AFB, Ohio: Air Force Systems Command, August 1969.

Appendix A

Development of the Lateral Acceleration Transfer Function

Substituting equations (2-4), (2-5), and (2-6) into equation (2-1) and rearranging, the Y-force equation, ΣF_y, becomes

$$U_o\dot{\beta} - Y_\beta\beta + U_o\dot{\psi} - Y_r\dot{\psi} - Y_p\dot{\phi} - g\psi\sin\Theta_o - g\phi\cos\Theta_o - Y_{\dot{\beta}}\dot{\beta} = Y_{\delta_a}\delta_a + Y_{\delta_r}\delta_r \tag{A-1}$$

Since $\Theta_o = 0$, for straight and level flight, (A-1) becomes

$$U_o\dot{\beta} - Y_\beta\beta + (U_o - Y_r)\dot{\psi} - Y_p\dot{\phi} - g\phi - Y_{\dot{\beta}}\dot{\beta} = Y_{\delta_a}\delta_a + Y_{\delta_r}\delta_r \tag{A-2}$$

From Table II, it is seen that Y_{δ_a} and $Y_{\dot{\beta}}$ are both equal to zero. Neglecting these terms and rearranging, (A-2) becomes

$$U_o\dot{\beta} - g\phi + U_o\dot{\psi} - Y_\beta\beta - Y_r\dot{\psi} - Y_p\dot{\phi} = Y_{\delta_r}\delta_r \tag{A-3}$$

Looking at the dimensions on (2-1) and (A-3), it can be seen that, as written, these equations are really a summation of lateral acceleration along the Y-axis rather than lateral force, ΣF_y. This is true because (2-1) has been divided by the vehicle mass, m. Therefore

$$a_y = U_o\dot{\beta} - g\phi + U_o\dot{\psi} = Y_\beta\beta + Y_r\dot{\psi} + Y_p\dot{\phi} + Y_{\delta_r}\delta_r \tag{A-4}$$

Using only the RHS of (A-4) and dividing by δ_r, the transfer function for lateral acceleration to rudder deflection is obtained.

$$\frac{a_y}{\delta_r} = Y_\beta \frac{\beta}{\delta_r} + Y_r \frac{\dot{\psi}}{\delta_r} + Y_p \frac{\dot{\phi}}{\delta_r} + Y_{\delta r} \qquad \text{(A-5)}$$

Note that (A-4) is an exprssion for lateral acceleration along the vehicle's Y-axis which is lateral acceleration of the c.g. only, as opposed to total acceleration in the XY-plane. A more general expression can be developed which represents not only the lateral acceleration of the c.g. but also the acceleration due to rotation about the c.g. The expression of (A-5) can then be written as

$$\frac{a_{yt}}{\delta_r} = Y \frac{\beta}{\delta_r} + Y_r \frac{\dot{\psi}}{\delta_r} + Y_p \frac{\dot{\phi}}{\delta_r} + Y_{\delta r} + \ell_x \ddot{\psi} \qquad \text{(A-6)}$$

where a_{yt} - total lateral acceleration

ℓ_x - distance of the c.g. to the point of measurement (forward is positive)

Appendix B

Accelerometer Location

So far all the analysis of acceleration feedback has been done with the accelerometer located at the center of gravity (c.g.) of the airframe. As can be seen from Eq (2-19), when the accelerometer is located away from the c.g. it measures not only lateral acceleration of the c.g., $a_{y_{cg}}$, but also the yaw angular acceleration, $\ell_x\ddot{\psi}$. From Fig. 2 it can be seen that $a_{y_{cg}}$ and $\ell_x\ddot{\psi}$ act in opposite directions. This means that if the accelerometer is located aft of the c.g., $-\ell_x$, that it will sense a higher acceleration for a given yawing motion. This means in effect that the accelerometer is more sensitive. Conversely, if it is located forward of the c.g. it will be less sensitive. The transfer functions of four accelerometer locations (including c.g.) in all three flight conditions are listed in Table XV. The resulting root locus sketches of the acceleration feedback system for the different accelerometer locations are shown in Fig. 55.

Note that in each case, a shift in zero location is apparent. However, since the location of the poles remains the same, the resultant root locus is altered very little in the areas of interest. Therefore, the location of the roots and thus the closed loop response should remain virtually unchanged. It can then be concluded that accelerometer location has an effect primarily on accelerometer sensitivity. For example, the design here requires an accelerometer with a

Table XV
Acceleration Transfer Functions for Different ℓ_x

ℓ_x (ft)	Cruise 1	Cruise 2	Power Approach
-47	$\frac{a_y}{\delta_r} = \frac{41.3(s+.074)(s+.80)(s-.19\pm j.128)}{(s+.009)(s+.62)(s+.009\pm j.89)}$	$\frac{a_y}{\delta_r} = \frac{58.12(s+.276)(s+1.1)(s-.047)(s-.624)}{(s+.011)(s+.886)(s-.0045\pm j1.026)}$	$\frac{a_y}{\delta_r} = \frac{26.29(s+1.14)(s+.172\pm j.064)(s-.251\pm j.81)}{s(s+.024)(s+1.14)(s+.026\pm j.74)}$
0	$\frac{a_{yco}}{\delta_r} = \frac{16.68(s+.193)(s+.967)(s-.068)(s-.61)}{(s+.009)(s+.62)(s+.009\pm j.89)}$	$\frac{a_{yco}}{\delta_r} = \frac{18.73(s+.534)(s+1.51)(s-.032)(s-1.29)}{(s+.011)(s+.886)(s-.0045\pm j1.026)}$	$\frac{a_{yco}}{\delta_r} = \frac{10.55(s+.111)(s+.489)(s+1.18)(s-.234)(s-.635)}{s(s+.024)(s+1.14)(s+.026\pm j.74)}$
20	$\frac{a_y}{\delta_r} = \frac{6.2(s+.282)(s+1.35)(s-.048)(s-1.14)}{(s+.009)(s+.62)(s+.009\pm j.89)}$	$\frac{a_y}{\delta_r} = \frac{1.96(s+.517)(s+3.82)(s-.028)(s-4.65)}{(s+.011)(s+.886)(s-.0045\pm j1.026)}$	$\frac{a_y}{\delta_r} = \frac{3.85(s+.10)(s+.778)(s+1.34)(s-.17)(s-1.32)}{s(s+.024)(s+1.14)(s+.026\pm j.74)}$
30	$\frac{a_y}{\delta_r} = \frac{.964(s+.336)(s+3.03)(s-.041)(s-3.19)}{(s+.009)(s+.62)(s+.009\pm j.89)}$	$\frac{a_y}{\delta_r} = \frac{-6.42(s+.558)(s-.027)(s+.264\pm j2.3)}{(s+.011)(s+.886)(s-.0045\pm j1.026)}$	$\frac{a_y}{\delta_r} = \frac{.50(s+.096)(s+.96)(s+2.61)(s-.177)(s-4.93)}{s(s+.024)(s+1.14)(s+.026\pm j.74)}$

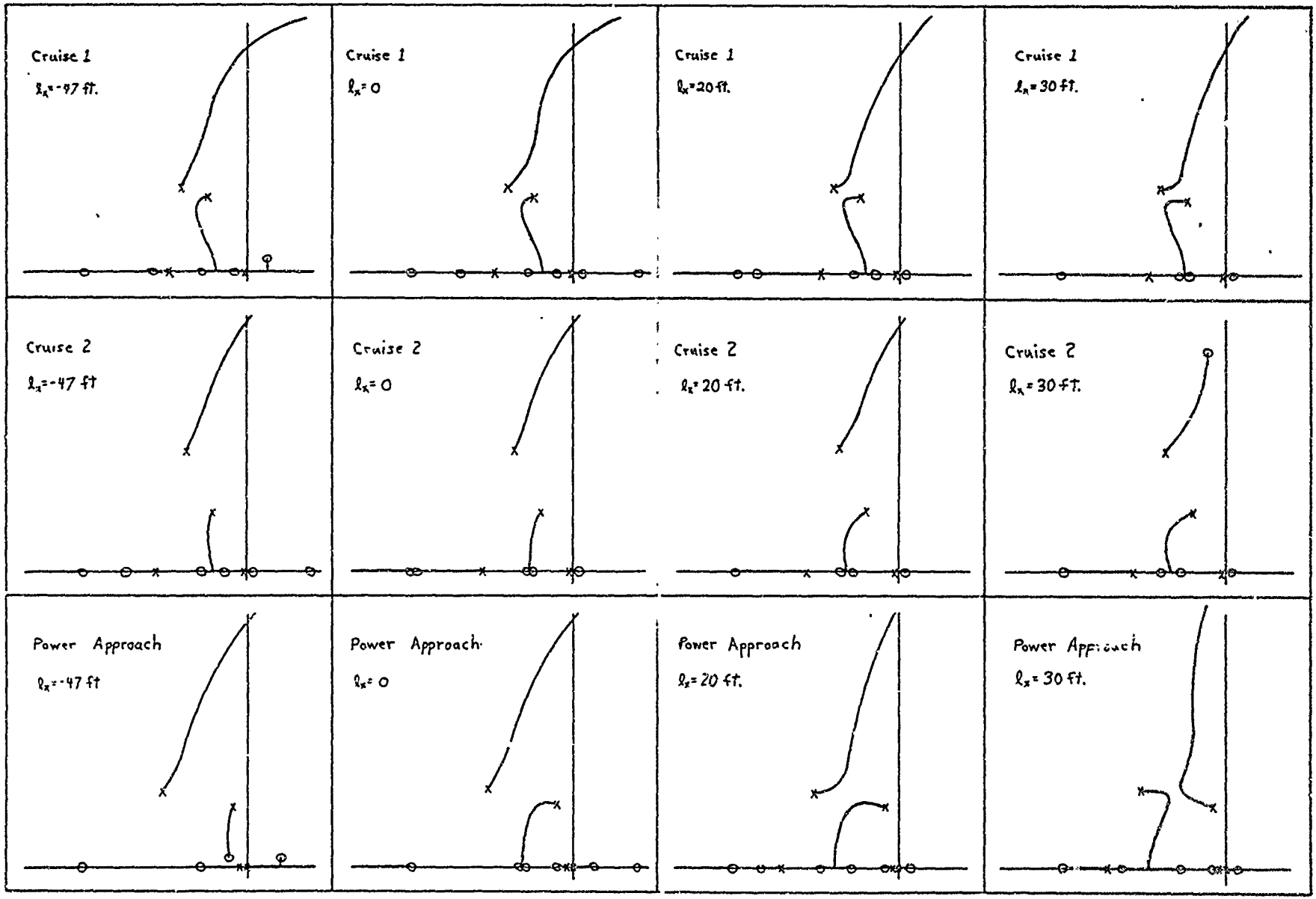

Figure 55. Root Loci of Acceleration System for Varying Locations of Accelerometer

gain (sensitivity) of about .008. An accelerometer with a sensitivity of say .01 v/g will give the same results provided it is located four feet forward of the c.g.

Appendix C

Other Design Considerations

Cascade Compensation. As can be seen from the root locus of the original series yaw damper (Fig. 6, Chapter II, the system response was undesireable mainly because the one pair of second order roots remain too close to the $j\omega$-axis as K_g is increased from zero to infinity. Early attempts to modify the existing yaw damper included a rather intensive search for a cascade compensator that would draw the troublesome branch of the root locus further into the LHP, thus making it possible to choose a more desireable pair of closed loop roots, i.e. a pair with a higher $\zeta\omega_n$. Several lead compensators were tried but in every case the compensation caused the other dominant branch to be drawn to the left. Then, because of the symmetry of a root locus, the branch which was expected to be drawn to the left was actually drawn to the right, thus resulting in a less desireable root location than before.

Other, more elaborate types of passive cascade compensators were tried - primarily compensators that generate complex poles and zeros. Probably the simplest and most practical of these is the bridged-T network which has a transfer function of

$$G_c(s) = \frac{1 + B\,\_\_\_\_}{1 + Ds + Cs^2}$$

Such a compensator could be used to cancel the complex pair of poles or zeros of the airframe. However, since the location of the airframe poles and zeros are constant only for a particular flight condition, exact cancellation would be possible only at one flight condition. Use of such a compensator then results in closed loop roots which, even though are close to respective zeros, lie in very undesireable positions in the s-plane. In fact, in this case, such roots could very well be unstable. Such a design would require a very extensive study of all possible flight conditions in order to best locate the compensator roots. Even then, the resultant effect of these roots on the overall response is questionable, since the system would now be predominantly sixth order. Therefore, it was decided that a multiloop feedback system, although more difficult to analyze, would, in the end, result in a more simplified and probably a more acceptable design.

Roll Rate Feedback. Analog computer simulation revealed that the aircraft exhibited a substantially larger roll component than yaw or sideslip component of the Dutch roll. Further, the rudder is almost as effective in rolling the aircraft as in yawing the aircraft. It was, therefore, thought that a SAS which controlled not only $\dot{\psi}$ but also $\dot{\phi}$ through a combined feedback of both quantities, would be very effective in damping the Dutch roll. Such a system was analyzed [illegible] plotted, one for positive feedback (Fig. 56) and one for negative feedback (Fig. 57). Looking at Figs. 56 and 57, it is immediately evident that roll rate feedback, when blended into the system, results in a degradation of performance. This is the case no matter how much roll rate is fed back. These conclusions were verified on the analog computer.

Since the results of using lateral acceleration feedback were quite encouraging, efforts were concentrated on that rather than on any other forms of feedback or cascade compensation.

MC-135 POSITIVE YAW-ROLL RATE FEEDBACK

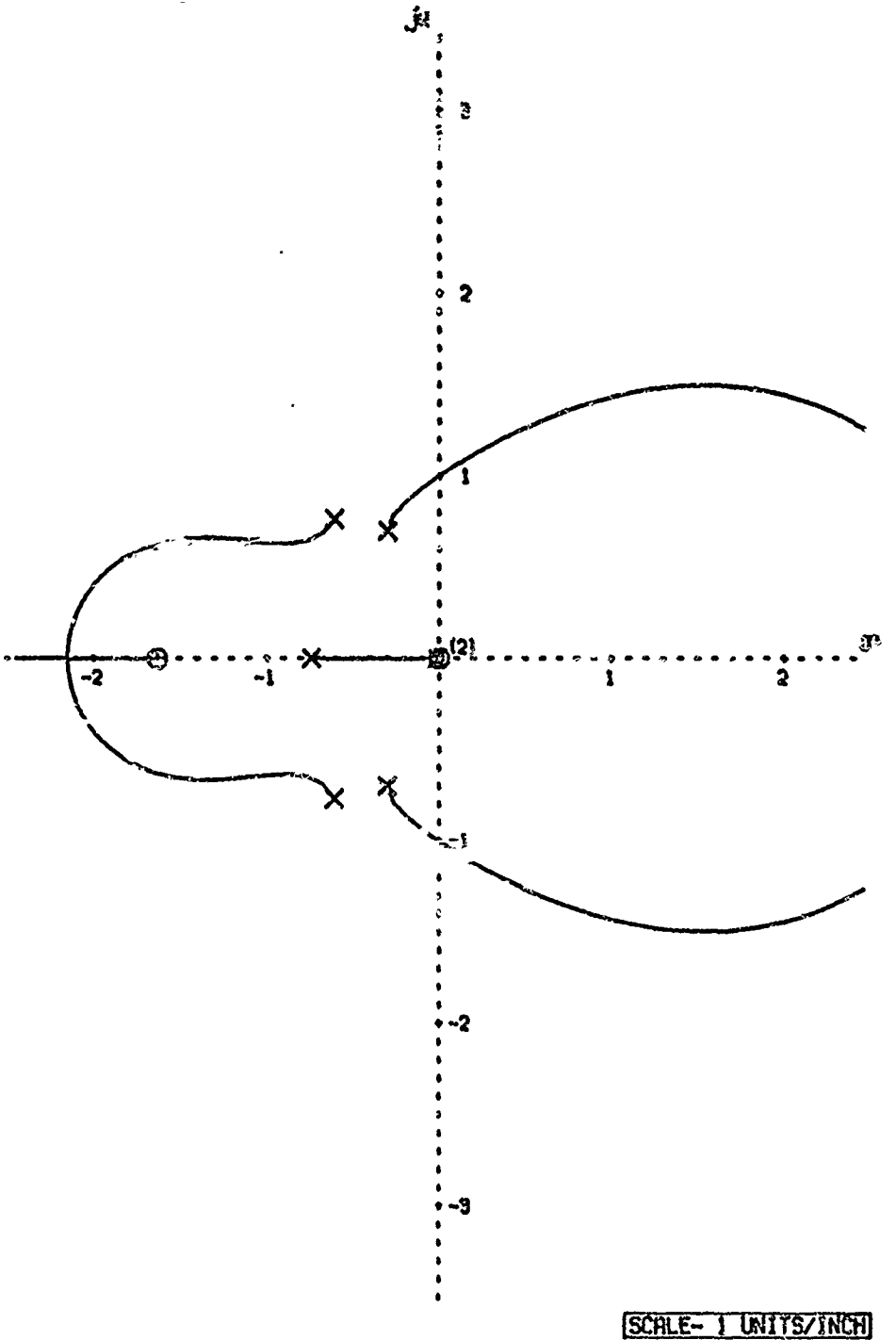

THE OPEN LOOP TRANSFER FUNCTION IS

$$\frac{-K(s^2)(s+1.69)(s-2.04)}{(s+0.008)(s+0.78)(s+20.5)(s+46.2)(s+150)(s^2+0.65s+0.58)(s^2+1.21s+0.858)(s^2+196.3s+18152.100)}$$

FIGURE 56 - ROOT LOCUS

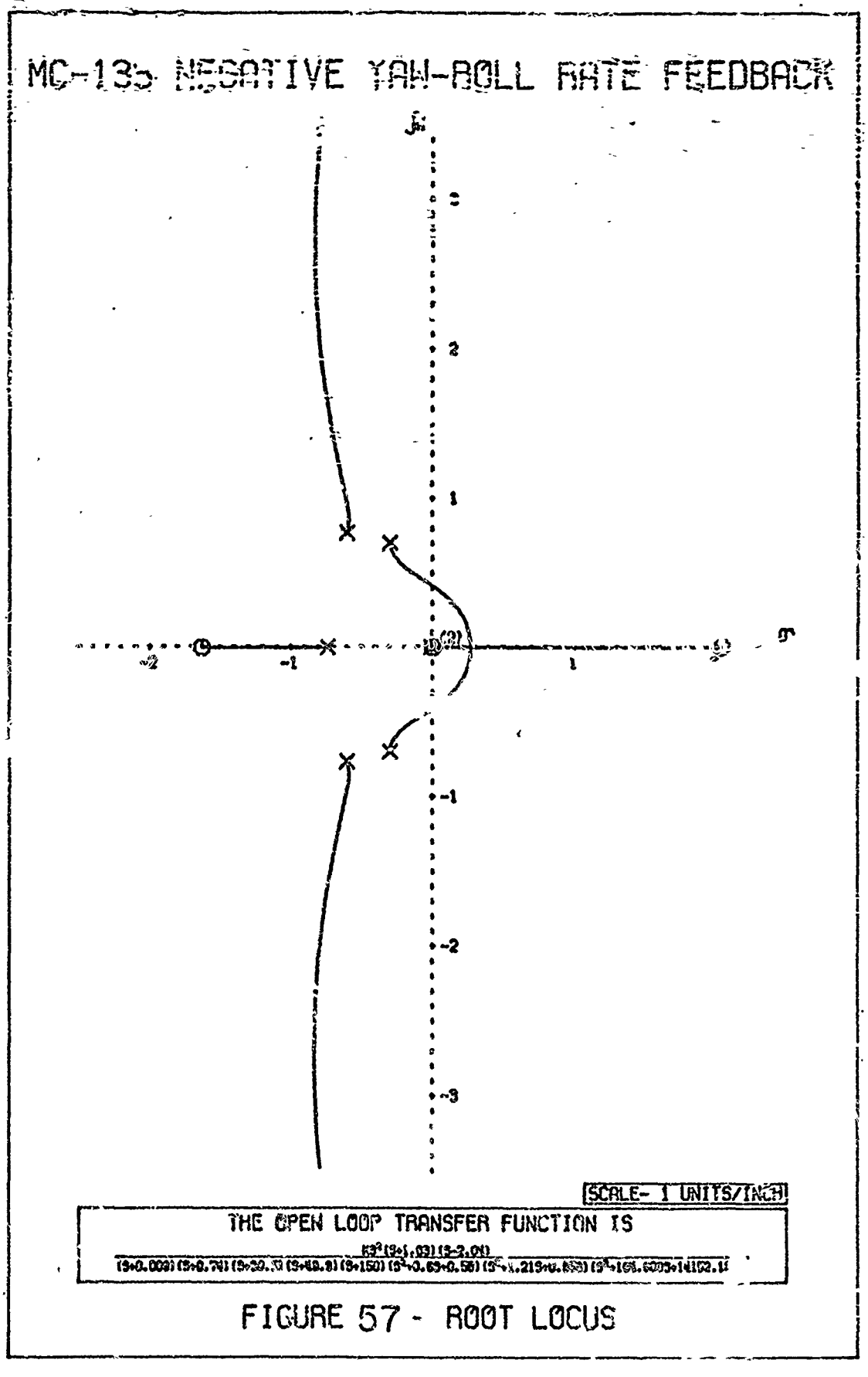

FIGURE 57 - ROOT LOCUS

Appendix D

Output - Lateral-Directional

Computer Program

RCOTS OF A/C LATERAL DIRECTIONAL TRANSFER FUNCTIONS

RUN NO. 3C1

CRUISE 1 MC-135 DAMPER OFF H=42K M=.75 X=190K 3AUG69

INPUT DATA (NON-DIMENSIONAL) PER DEGREE

RHO = 0.5571E-03	U = 0.7265E 03	S = 0.2631E 04	GWT = 0.1900E 06	SPAN = 0.1308E 03	IXB = 0.3500E 07			
IZB = 0.8750E 07	IXZ = 0.	G = 0.3721E 02	ALFI = 0.8000E 01	GAMA = 0.	LX = 0.			
CYB = -0.1203E-01	CYBD = 0.	CYP = -0.4270E-02	CYR = 0.8380E-02	CYDA = 0.	CYDR = 0.4800E-02			
CLB = -0.3210E-02	CLBD = 0.	CLP = -0.7100E-02	CLR = 0.3490E-02	CLDA = 0.9700E-03	CLDR = 0.1300E-01			
CNB = 0.1660E-02	CNBD = 0.3950E-02	CNP = -0.2100E-02	CNR = -0.3320E-02	CNDA = 0.1170E-03	CNDR = -0.1600E-02			
ALFA = -1.	ALFX = -0.							

3 DIMENSIONAL STABILITY DERIVATIVES

YB = -0.4[illegible]E 02	YBD =	YP = -0.1331E 01	YR = 0.2621E 01	YDA = 0.	YDR = 0.1668E 02			
LB = -0.2394E 01	LBD =	LP = -0.4691E-00	LR = 0.2341E-00	LDA = 0.7227E 00	LDR = 0.2[illegible]E-00			
NB = 0.[illegible]E 00	NBD = 0.1105E-01	NP = -0.5[illegible]E-01	NR = -0.9274E-01	NDA = 0.3631E-01	NDR = -0.4[illegible]E-00			

DIMENSIONAL STA[illegible] DERIVATIVES PRIMED

ALFI = 0.8000E 01	ALFA = -0.	ALFX = -0.	IX = 0.3602E 07	IZ = 0.8648E 07	IXZ = -0.7235E 06			
LBP = -0.2529E 01	LBDP = -0.2254E-02	LPP = -0.4651E-00	LRP = 0.2570E-00	LDAP = 0.7277E 00	LDRP = 0.3188E-00			
NBP = 0.7205E 00	NBDP = 0.1122E-01	NPP = -0.1971E-01	NRP = -0.1142E-00	NDAP = -0.2457E-01	NDRP = -0.5240E 00			

LATERAL DIRECTIONAL DENOMINATOR RCOTS

ROOTS (COMPLEX FORM)

0.	0.
-0.9450D-02	0.8901D 00
-0.9450D-02	-0.8901D 00
-0.3348D-02	
-0.6201D 00	

TS = 0.1066675E 03 TR = 0.7312[illegible]E 01 ZRS = 0.1061[illegible]55E-01 WDR = 0.6901[illegible]76E 00 RAD/SEC = 0.1416[illegible]76E-00 CYCLES/SEC WDDR = 0.8901[illegible]26E 00 RAD/SEC = 0.1416[illegible]68E-00 CYCLES/SEC

DUTCH ROLL MODE

TDR = 0.7059[illegible]4E 01	TIME TO HALF AMP. = 0.7335[illegible]2E 02	TIME TO ONE TENTH AMP. = 0.2436[illegible]7E 03
TDDR = 0.7058[illegible]8E 01	CYCLES TO HALF AMP. = 0.1039[illegible]2E 02	CYCLES TO ONE TENTH AMP. = 0.3452[illegible]0E 02
	ONE OVER CYCLES TO HALF AMP. = 0.9623[illegible]2E-01	ONE OVER CYCLES TO ONE TENTH AMP. = 0.2896[illegible]9E-02

COEFFICIENTS

A = 0.10000E 01 B = 0.6483[illegible]6E 00 C = 0.8101[illegible]1E 00 D = 0.4989[illegible]-00 E = 0.4593[illegible]5E-02

PHI TC BETA RATIO = 0.2[illegible]80E 01

PHI TC EQUIV VEL = 0.4[illegible]02E-00

FREQ SQUARED TIMES PHI TO BETA RATIO = 0.2282[illegible] 01

OPTION 2

TIME HISTORY FOR A STEP INPUT

TIME SEC	P(T), ROLL RATE DEG/SEC	PHI(T), ROLL ANGLE DEG	BETA(T), SIDESLIP DEG
0.	-0.6985E-00	0.	-0.4051E-07
0.1	0.7106E-01	0.3581E-02	0.1226E-03
0.2	0.1386E-00	0.1410E-01	0.5170E-03
0.3	0.2032E-00	0.3122E-01	0.1219E-02
0.4	0.2644E-00	0.5463E-01	0.2260E-02
0.5	0.3224E-00	0.8399E-01	0.3608E-02
0.6	0.3774E-00	0.1190E-00	0.5463E-02
0.7	0.4293E-00	0.1594E-00	0.7663E-02
0.8	0.4781E-00	0.2046E-00	0.1028E-01
0.9	0.5240E 00	0.2549E-00	0.1338E-01
1.0	0.5669E 00	0.3095E-00	0.1679E 01
1.1	0.6070E 00	0.3682E-00	0.2064E-01
1.2	0.6441E 00	0.4308E-00	0.2500E-01
1.3	0.6784E 00	0.4969E-00	0.2972E-01
1.4	0.7099E 00	0.5663E 00	0.3482E-01
1.5	0.7386E 00	0.6388E 00	0.4030E-01
1.6	0.7646E 00	0.7140E 00	0.4613E-01
1.7	0.7879E 00	0.7916E 00	0.5228E-01
1.8	0.8086E 00	0.8715E 00	0.5871E-01
1.9	0.8268E 00	0.9533E 00	0.6540E-01
2.0	0.8425E 00	0.1037E 01	0.7231E-01
2.1	0.8558E 00	0.1122E 01	0.7940E-01
2.2	0.8667E 00	0.1208E 01	0.8662E-01
2.3	0.8755E 00	0.1295E 01	0.9394E-01
2.4	0.8820E 00	0.1383E 01	0.1013E-00
2.5	0.8866E 00	0.1471E 01	0.1087E-00
2.6	0.8892E 00	0.1560E 01	0.1160E-00
2.7	0.8900E 00	0.1649E 01	0.1233E-00
2.8	0.8891E 00	0.1738E 01	0.1304E-00
2.9	0.8867E 00	0.1827E 01	0.1374E-00
3.0	0.8828E 00	0.1915E 01	0.1441E-00
3.1	0.8776E 00	0.2003E 01	0.1506E-00
3.2	0.8712E 00	0.2091E 01	0.1568E-00
3.3	0.8639E 00	0.2178E 01	0.1626E-00
3.4	0.8556E 00	0.2264E 01	0.1681E-00
3.5	0.8466E 00	0.2349E 01	0.1732E-00
3.6	0.8370E 00	0.2433E 01	0.1777E-00
3.7	0.8270E 00	0.2516E 01	0.1818E-00
3.8	0.8167E 00	0.2598E 01	0.1856E-00
3.9	0.8062E 00	0.2679E 01	0.1887E-00
4.0	0.7958E 00	0.2759E 01	0.1913E-00
4.1	0.7854E 00	0.2839E 01	0.1934E-00
4.2	0.7752E 00	0.2917E 01	0.1950E-00
4.3	0.7653E 00	0.2994E 01	0.1960E-00
4.4	0.7562E 00	0.3070E 01	0.1965E-00
4.5	0.7475E 00	0.3145E 01	0.1964E-00
4.6	0.7396E 00	0.3219E 01	0.1958E-00
4.7	0.7324E 00	0.3293E 01	0.1946E-00
4.8	0.7261E 00	0.3366E 01	0.1930E-00
4.9	0.7207E 00	0.3438E 01	0.1909E-00
5.0	0.7164E 00	0.3510E 01	0.1883E-00
5.1	0.7132E 00	0.3581E 01	0.1852E-00
5.2	0.7111E 00	0.3653E 01	0.1818E-00
5.3	0.7102E 00	0.3724E 01	0.1780E-00

5.4	0.7105E 00	0.3795E 01	0.1729E-00
5.5	0.7119E 00	0.3885E 01	0.1695E-00
5.6	0.7146E 00	0.3977E 01	0.1648E-00
5.7	0.7195E 00	0.4009E 01	0.1600E-00
5.8	0.7235E 00	0.4081E 01	0.1549E-00
5.9	0.7297E 00	0.4153E 01	0.1498E-00
6.0	0.7370E 00	0.4227E 01	0.1445E-00
6.1	0.7454E 00	0.4301E 01	0.1393E-00
6.2	0.7548E 00	0.4376E 01	0.1341E-00
6.3	0.7651E 00	0.4452E 01	0.1289E-00
6.4	0.7762E 00	0.4529E 01	0.1239E-00
6.5	0.7881E 00	0.4607E 01	0.1190E-00
6.6	0.8007E 00	0.4687E 01	0.1143E-00
6.7	0.8139E 00	0.4767E 01	0.1099E-00
6.8	0.8276E 00	0.4849E 01	0.1057E-00
6.9	0.8417E 00	0.4933E 01	0.1019E-00
7.0	0.8560E 00	0.5018E 01	0.9841E-01
7.1	0.8705E 00	0.5104E 01	0.9532E-01
7.2	0.8850E 00	0.5192E 01	0.9266E-01
7.3	0.8995E 00	0.5281E 01	0.9043E-01
7.4	0.9138E 00	0.5372E 01	0.8867E-01
7.5	0.9278E 00	0.5464E 01	0.8739E-01
7.6	0.9414E 00	0.5557E 01	0.8660E-01
7.7	0.9544E 00	0.5652E 01	0.8632E-01
7.8	0.9669E 00	0.5748E 01	0.8655E-01
7.9	0.9787E 00	0.5845E 01	0.8730E-01
8.0	0.9896E 00	0.5944E 01	0.8855E-01
8.1	0.9997E 00	0.6043E 01	0.9031E-01
8.2	0.1009E 01	0.6144E 01	0.9257E-01
8.3	0.1017E 01	0.6245E 01	0.9530E-01
8.4	0.1024E 01	0.6347E 01	0.9850E-01
8.5	0.1030E 01	0.6450E 01	0.1021E-00
8.6	0.1034E 01	0.6553E 01	0.1062E-00
8.7	0.1037E 01	0.6657E 01	0.1106E-00
8.8	0.1039E 01	0.6760E 01	0.1154E-00
8.9	0.1040E 01	0.6864E 01	0.1205E-00
9.0	0.1040E 01	0.6968E 01	0.1259E-00

PQSC/PAV = 0.1522E-00	DBMAX = 0.7231E-01	ANGLE P/B = 0.1220E 03
PSIP = -0.9725E 02	PSIB = -0.2193E 03	KC/KSS = 0.1843E-00
KP = 0.	KB = 0.7405E 00	PHI QSC/PHI AV = 0.1522E-00
KPR = -0.9369E 00	KBR = -0.5330E-01	PSIBP = -0.3993E 03
KPS = 0.9583E 00	KBS = -0.6330E 00	P2/P1 = 0.7979E 00
MKPPCR = 0.1767E-00	MKBPOR = 0.7005E-01	

RUN NO. 301 RUDDER NUMERATOR ROOTS

SIDESLIP TO CONTROL DEFLECTION

ROOTS (COMPLEX FORM)

0.	0.
0.15700-01	
-0.52380 00	
-0.22790 02	

1/TB1 = 0.156959E-01 1/TB2 = -0.523755E 00 1/TB3 = -0.227905E 02

AB = 0.2295E-01 BB = 0.5348E 00 CB = -0.2656E-00 DB = -0.4301E-02

ROLL ANGLE TO CONTROL DEFLECTION

0.
0.20330 01
-0.16310 01

1/TP1 = 0. 1/TP2 = 0.203758E 01 1/TP3 = -0.163073E 01

AP = 0.3287E-00 BP = -0.1337E-00 CP = -0.1095E 01 DP = -0.

YAW RATE TO CONTROL DEFLECTION

ROOTS (COMPLEX FORM)

0.	0.
0.9234D-01	-0.3537D-00
0.9234D-01	0.3537D-00
-0.6884D 00	

ZR = -0.252570E-00 WR = 0.365588E-00 1/TR = -0.688445E 00

AR = -0.52373E 00 BR = -0.26384E-00 CR = -0.34153E-02 DR = -0.48190E-01

ROOTS OF A/C LATERAL DIRECTIONAL TRANSFER FUNCTIONS

RUN NO. 1C2

CRUISE 2 MC-135 DAMPER OFF H=25K M=.65 W=250K 26 AUG 69

INPUT DATA (NON-DIMENSIONAL) PER DEGREE

RHO = 0.1065E-02	U = 0.6600E 03	S = 0.2433E 04	GWT = 0.2500E 06	SPAN = 0.1308E 03	IXB = 0.4000E 07			
IZB = 0.8750E 07	IXZB = 0.	G = 0.3217E 02	ALFI = 0.3000E 01	GAMA = 0.	LX = 0.			
CYB = -0.1500E-01	CYBD = 0.	CYP = -0.3840E-02	CYR = 0.7770E-02	CYDA = 0.	CYDR = 0.4500E-02			
CLB = -0.2950E-02	CLBD = 0.	CLP = -0.6110E-02	CLR = 0.3110E-02	CLDA = 0.6750E-03	CLDR = 0.3000E-03			
CNB = 0.1600E-02	CNBD = 0.	CNP = -0.1920E-02	CNR = -0.3140E-02	CNDA = 0.1240E-03	CNDR = -0.1710E-02			
ALFA = -0.	ALFX = -0.							

DIMENSIONAL STABILITY DERIVATIVES

YB = -0.6242E 02	YBD = 0.	YP = -0.1583E 01	YR = 0.3204E 01	YDA = 0.	YDR = 0.1873E 02			
LB = -0.3109E 01	LBD = 0.	LP = -0.6381E 00	LR = 0.3248E-00	LDA = 0.7114E 00	LDR = 0.3162E-00			
NB = 0.7745E 00	NBD = 0.	NP = -0.9210E-01	NR = -0.1506E-00	NDA = 0.6003E-01	NDR = -0.8276E 00			

DIMENSIONAL STABILITY DERIVATIVES PRIMED

ALFI = 0.3000E 01	ALFA = -0.	ALFX = -0.	IX = 0.4013E 07	IZ = 0.8737E 07	IXZ = -0.2483E 06			
LBP = -0.3163E 01	LBDP = -0.	LPP = -0.6335E 00	LRP = 0.3347E-00	LDAP = 0.7089E 00	LDRP = 0.3680E-00			
NBP = 0.8644E 00	NBDP = -0.	NPP = -0.7410E-01	NRP = -0.1601E-00	NDAP = 0.3988E-01	NDRP = -0.8382E 00			

LATERAL DIRECTIONAL DENOMINATOR ROOTS

ROOTS (COMPLEX FORM)

0.	0.
0.4499E-02	0.1026D 01
0.4499E-02	-0.1026D 01
-0.1136E-01	
-0.8859D 00	

TS = 0.880568E 02 TR = 0.112885E 01 ZDR = -0.438671E-02 WDR = 0.102563E 01 RAD/SEC = 0.163235E-00 CYCLES/SEC WDDR = 0.102562E 01 RAD/SEC = 0.163233E-00 CYCLES/SEC

DUTCH ROLL MODE

TDR = 0.61261E 01	TIME TO DOUBLE AMP. = 0.15406E 03	TIME TO TEN TIMES AMP. = 0.51178E 03
TDDR = 0.61262E 01	CYCLES TO DOUBLE AMP. = 0.25148E 02	CYCLES TO TEN TIMES AMP. = 0.83540E 02

COEFFICIENTS

A = 0.10000E 01 B = 0.88822E 00 C = 0.10539E 01 D = 0.94371E 00 E = 0.10582E-01

PHI TO BETA RATIO = 0.2615E 01

PHI TO EQUIV VEL = 0.3392E-00

FREQ SQUARED TIMES PHI TO BETA RATIO = 0.2751E 01

OPTION 2

TIME HISTORIES FOR A STEP INPUT

TIME SEC	P(T), ROLL RATE DEG/SEC	PHI(T), ROLL ANG.E DEG	BETA(T), SIDESLIP DEG
0.	0.	0.	-0.3437E-07
0.1	0.6870E-01	0.3474E-02	-0.1900E-03
0.2	0.1336E-00	0.1362E-01	-0.6995E-03
0.3	0.1946E-00	0.3006E-01	-0.1436E-02
0.4	0.2523E-00	0.5243E-01	-0.2307E-02
0.5	0.3067E-00	0.8041E-01	-0.3235E-02
0.6	0.3582E-00	0.1137E-00	-0.4140E-02
0.7	0.4067E-00	0.1520E-00	-0.4950E-02
0.8	0.4526E-00	0.1949E-00	-0.5590E-02
0.9	0.4957E-00	0.2424E-00	-0.6023E-02
1.0	0.5363E 00	0.2940E-00	-0.6172E-02
1.1	0.5744E 00	0.3496E-00	-0.5996E-02
1.2	0.6100E 00	0.4088E-00	-0.5454E-02
1.3	0.6431E 00	0.4715E-00	-0.4512E-02
1.4	0.6738E 00	0.5373E 00	-0.3143E-02
1.5	0.7021E 00	0.6062E 00	-0.1326E-02
1.6	0.7280E 00	0.6777E 00	0.9499E-03
1.7	0.7515E 00	0.7517E 00	0.3692E-02
1.8	0.7726E 00	0.8279E 00	0.6900E-02
1.9	0.7913E 00	0.9061E 00	0.1057E-01
2.0	0.8076E 00	0.9861E 00	0.1467E-01
2.1	0.8216E 00	0.1068E 01	0.1921E-01
2.2	0.8332E 00	0.1150E 01	0.2414E-01
2.3	0.8426E 00	0.1234E 01	0.2943E-01
2.4	0.8497E 00	0.1319E 01	0.3506E-01
2.5	0.8546E 00	0.1404E 01	0.4097E-01
2.6	0.8574E 00	0.1490E 01	0.4712E-01
2.7	0.8582E 00	0.1575E 01	0.5347E-01
2.8	0.8571E 00	0.1661E 01	0.5996E-01
2.9	0.8540E 00	0.1747E 01	0.6654E-01
3.0	0.8493E 00	0.1832E 01	0.7315E-01
3.1	0.8430E 00	0.1917E 01	0.7974E-01
3.2	0.8351E 00	0.2000E 01	0.8624E-01
3.3	0.8260E 00	0.2084E 01	0.9261E-01
3.4	0.8156E 00	0.2166E 01	0.9870E-01
3.5	0.8043E 00	0.2247E 01	0.1047E-00
3.6	0.7920E 00	0.2326E 01	0.1103E-00
3.7	0.7791E 00	0.2404E 01	0.1156E-00
3.8	0.7656E 00	0.2482E 01	0.1205E-00
3.9	0.7518E 00	0.2558E 01	0.1249E-00
4.0	0.7378E 00	0.2633E 01	0.1289E-00
4.1	0.7239E 00	0.2706E 01	0.1323E-00
4.2	0.7100E 00	0.2777E 01	0.1353E-00
4.3	0.6965E 00	0.2848E 01	0.1376E-00
4.4	0.6833E 00	0.2917E 01	0.1394E-00
4.5	0.6712E 00	0.2984E 01	0.1406E-00
4.6	0.6596E 00	0.3051E 01	0.1412E-00
4.7	0.6494E 00	0.3116E 01	0.1412E-00
4.8	0.6393E 00	0.3181E 01	0.1406E-00
4.9	0.6300E 00	0.3244E 01	0.1394E-00
5.0	0.6230E 00	0.3307E 01	0.1377E-00
5.1	0.6177E 00	0.3369E 01	0.1355E-00
5.2	0.6132E 00	0.3431E 01	0.1327E-00
5.3	0.6102E 00	0.3492E 01	0.1295E-00

5.4	0.60866E 00	0.38532E 01	0.12598E-00
5.5	0.60866E 00	0.38614E 01	0.12198E-00
5.6	0.61008E 00	0.38748E 01	0.11758E-00
5.7	0.61298E 00	0.38930E 01	0.11298E-00
5.8	0.61738E 00	0.39178E 01	0.10808E-00
5.9	0.62318E 00	0.39498E 01	0.10308E-00
6.0	0.63038E 00	0.39228E 01	0.97908E-01
6.1	0.63878E 00	0.39058E 01	0.92738E-01
6.2	0.64838E 00	0.40508E 01	0.87668E-01
6.3	0.65908E 00	0.41138E 01	0.82478E-01
6.4	0.67078E 00	0.41018E 01	0.77518E-01
6.5	0.68318E 00	0.42498E 01	0.72748E-01
6.6	0.69638E 00	0.43108E 01	0.68328E-01
6.7	0.71018E 00	0.43888E 01	0.64008E-01
6.8	0.72428E 00	0.44608E 01	0.60138E-01
6.9	0.73868E 00	0.46338E 01	0.56668E-01
7.0	0.75318E 00	0.46088E 01	0.53648E-01
7.1	0.76758E 00	0.46048E 01	0.51098E-01
7.2	0.78178E 00	0.47618E 01	0.49088E-01
7.3	0.79558E 00	0.48408E 01	0.47568E-01
7.4	0.80888E 00	0.49208E 01	0.46638E-01
7.5	0.82148E 00	0.50028E 01	0.46208E-01
7.6	0.83328E 00	0.50858E 01	0.46328E-01
7.7	0.84418E 00	0.51688E 01	0.47358E-01
7.8	0.85388E 00	0.52038E 01	0.48178E-01
7.9	0.86248E 00	0.53398E 01	0.50708E-01
8.0	0.86978E 00	0.54268E 01	0.53358E-01
8.1	0.87568E 00	0.55138E 01	0.56478E-01
8.2	0.88018E 00	0.56018E 01	0.60118E-01
8.3	0.88318E 00	0.56898E 01	0.64248E-01
8.4	0.88478E 00	0.57778E 01	0.68828E-01
8.5	0.88448E 00	0.58658E 01	0.73808E-01

POSC/PAV =	0.17708E-00	DDMAX = 0.20088E-01	ANGLE P/B = 0.12708E 03
PSIP =	-0.13088E 03	PSIB = -0.26688E 03	KB/KSS = 0.17738E-00
KP =	0.	KB = 0.58448E 00	PHI OSC/PHI AV = 0.17308E-00
KPS =	-0.70178 00	KBR = -0.86408E-01	PSIBR = -0.2668E 03
KPS =	0.60098E 00	KBS = -0.82468E 00	PB/PI = 0.70898E 00
HKPPDR =	0.14308E-00	HKBRDR = 0.59698E-01	

RUN NO. 102 RUDDER NUMERATOR ROOTS

SIDESLIP TO CONTROL DEFLECTION

ROOTS (COMPLEX FORM)

0. 0.
0.10210-01
-0.70940 00
-0.29470 02

1/TB1 = 0.1020930E-01 1/TB2 = -0.7094038E 00 1/TB3 = -0.2947138E 02

AB = 0.20378-01 BB = 0.85568 00 CB = 0.87776E 00 DB = -0.10808-01

ROLL ANGLE TO CONTROL DEFLECTION

0.
0.29300 01
-0.21700 01

1/TP1 = 0. 1/TP2 = 0.2929600E 01 1/TP3 = -0.2170826E 01

AP = 0.3680E-00 BP = -0.2765E-00 CP = -0.2349E 01 DP = -0.

YAW RATE TO CONTROL DEFLECTION

ROOTS (COMPLEX FORM)

0. 0.
0.7161D-01 -0.30730-00
0.71610-01 0.30730-00
-0.67446 00

ZR = -0.191827E-00 WR = 0.3938346-00 1/TR = -0.0745018 00

AR = -0.838246 00 BR = -0.61305E 00 CR = -0.250208-01 DR = -0.11371?-00

ROOTS OF A/C LATERAL DIRECTIONAL TRANSFER FUNCTIONS

RUN NO. 1PA

POWER APPROACH MC-135 DAMPER OFF V=165K 25AUG69

INPUT DATA (NON-DIMENSIONAL) PER DEGREE

RHO =	0.2377E-02	U =	0.2750E 03	S =	0.2433E 04	GWT =	0.1605E 06	SPAN =	0.1308E 03	IXB =	0.2800E 07
IZB =	0.7700E 07	IXZB =	0.	G =	0.3217E 02	ALFI =	0.3000E 01	GAMA =	-0.3000E 01	LX =	0.
CYB =	-0.1400E-01	CYBD =	0.	CYP =	-0.3840E-02	CYR =	0.7160E-02	CYDA =	0.	CYDR =	0.4200E-02
CLB =	-0.2800E-02	CLBD =	0.	CLP =	-0.6550E-02	CLR =	0.4290E-02	CLDA =	0.2460E-02	CLDR =	0.2100E-03
CNB =	0.1100E-02	CNBD =	0.3200E-03	CNP =	-0.2550E-02	CNR =	-0.2965E-02	CNDA =	0.1890E-03	CNDR =	-0.1550E-02
ALFA =	-0.	ALFX =	-0.								

DIMENSIONAL STABILITY DERIVATIVES

YB =	-0.3516E 02	YBD =	0.	YP =	-0.2294E 01	YR =	0.4277E 01	YDA =	0.	YDR =	0.1055E 02
LB =	-0.1631E 01	LBD =	0.	LP =	-0.9074E 00	LR =	0.5943E 00	LDA =	0.1433E 01	LDR =	0.1223E-00
NB =	0.2345E-00	NBD =	0.1623E-01	NP =	-0.1293E-00	NR =	-0.1503E-00	NDA =	0.4030E-01	NDR =	-0.3305E-00

DIMENSIONAL STABILITY DERIVATIVES PRIMED

ALFI =	0.3000E 01	ALFA =	-0.	ALFX =	-0.	IX =	0.2813E 07	IZ =	0.7687E 07	IXZ =	-0.2561E 06
LBP =	-0.1657E 01	LBDP =	-0.1481E-02	LPP =	-0.8983E 00	LRP =	0.6098E 00	LDAP =	0.1434E 01	LDRP =	0.1529E-00
NBP =	0.2397E-00	NBDP =	0.1627E-01	NPP =	-0.9937E-01	NRP =	-0.1707E-00	NDAP =	-0.7469E-02	NDRP =	-0.3356E-00

LATERAL DIRECTIONAL DENOMINATOR ROOTS

ROOTS (COMPLEX FORM)

0.	0.
-0.2595D-01	0.7407D 00
-0.2595D-01	-0.7407D 00
-0.2402D-01	
-0.1137D 01	

TS = 0.416320E 02 TR = 0.879544E 00 ZDR = 0.350074E-01 WDR = 0.741179E 00 RAD/SEC = 0.117962E-00 CYCLES/SEC WDDR = 0.740724E 00 RAD/SEC = 0.117890E-00 CYCLES/SEC

DUTCH ROLL MODE

TDR =	0.84773E 01	TIME TO HALF AMP. =	0.26714E 02	TIME TO ONE TENTH AMP. =	0.88743E 02
TDCR =	0.84825E 01	CYCLES TO HALF AMP. =	0.31494E 01	CYCLES TO ONE TENTH AMP. =	0.10462E 02
		ONE OVER CYCLES TO HALF AMP. =	0.31753E-00	ONE OVER CYCLES TO ONE TENTH AMP. =	0.95585E-01

COEFFICIENTS

A = 0.10000E 01 B = 0.12129E 01 C = 0.63690E 00 D = 0.63919E 00 E = 0.15002E-01

PHI TO BETA RATIO = 0.2027E 01

PHI TO EQUIV VEL = 0.4224E-00

FREQ SQUARED TIMES PHI TO BETA RATIO =, 0.1114E 01

OPTION 2

TIME HISTORIES FOR A STEP INPUT

TIME SEC	P(T), ROLL RATE DEG/SEC	PHI(T), ROLL ANGLE DEG	BETA(T), SIDESLIP DEG
0.	-0.7451E-06	0.	-0.1043E-06
0.1	0.1371E-00	0.6957E-02	0.2639E-04
0.2	0.2622E-00	0.2702E-01	0.3087E-03
0.3	0.3764E-00	0.5904E-01	0.1108E-02
0.4	0.4803E-00	0.1020E-00	0.2664E-02
0.5	0.5746E 00	0.1549E-00	0.5182E-02
0.6	0.6600E 00	0.2166E-00	0.8841E-02
0.7	0.7370E 00	0.2865E-00	0.1379E-01
0.8	0.8060E 00	0.3637E-00	0.2017E-01
0.9	0.8676E 00	0.4474E-00	0.2807E-01
1.0	0.9221E 00	0.5370E 00	0.3757E-01
1.1	0.9697E 00	0.6316E 00	0.4872E-01
1.2	0.1011E 01	0.7307E 00	0.6162E-01
1.3	0.1046E 01	0.8336E 00	0.7622E-01
1.4	0.1075E 01	0.9397E 00	0.9255E-01
1.5	0.1099E 01	0.1048E 01	0.1106E-00
1.6	0.1117E 01	0.1159E 01	0.1303E-00
1.7	0.1130E 01	0.1272E 01	0.1517E-00
1.8	0.1139E 01	0.1385E 01	0.1746E-00
1.9	0.1141E 01	0.1499E 01	0.1990E-00
2.0	0.1140E 01	0.1613E 01	0.2248E-00
2.1	0.1134E 01	0.1727E 01	0.2520E-00
2.2	0.1125E 01	0.1840E 01	0.2803E-00
2.3	0.1111E 01	0.1952E 01	0.3097E-00
2.4	0.1094E 01	0.2062E 01	0.3401E-00
2.5	0.1074E 01	0.2170E 01	0.3713E-00
2.6	0.1050E 01	0.2277E 01	0.4032E-00
2.7	0.1024E 01	0.2380E 01	0.4357E-00
2.8	0.9969E 00	0.2481E 01	0.4685E-00
2.9	0.9[illegible]E 00	0.2579E 01	0.5016E 00
3.0	0.9297E 00	0.2[illegible]E 01	0.5348E 00
3.1	0.8941E 00	0.2[illegible]E 01	0.5680E 00
3.2	0.8568E 00	0.2853E 01	0.6009E 00
3.3	0.8192E 00	0.2937E 01	0.6334E 00
3.4	0.7784E 00	0.3016E 01	0.6655E 00
3.5	0.7377E 00	0.3092E 01	0.6968E 00
3.6	0.6963E 00	0.3164E 01	0.7274E 00
3.7	0.6546E 00	0.3231E 01	0.7570E 00
3.8	0.6128E 00	0.3295E 01	0.7855E 00
3.9	0.5711E 00	0.3354E 01	0.8128E 00
4.0	0.5298E 00	0.3409E 01	0.8388E 00
4.1	0.4890E-00	0.3460E 01	0.8633E 00
4.2	0.4492E-00	0.3507E 01	0.8862E 00
4.3	0.4103E-00	0.3550E 01	0.9075E 00
4.4	0.3728E-00	0.3589E 01	0.9271E 00
4.5	0.3367E-00	0.3624E 01	0.9448E 00
4.6	0.3023E-00	0.3656E 01	0.9606E 00
4.7	0.2698E-00	0.3685E 01	0.9745E 00
4.8	0.2394E-00	0.3710E 01	0.9864E 00
4.9	0.2111E-00	0.3733E 01	0.9963E 00
5.0	0.1851E-00	0.3753E 01	0.1004E 01
5.1	0.1617E-00	0.3770E 01	0.1010E 01
5.2	0.1408E-00	0.3785E 01	0.1013E 01
5.3	0.1226E-00	0.3798E 01	0.1015E 01

5.4	0.1071E-00	0.3010E 01	0.1015E 01
5.5	0.9452E-01	0.3820E 01	0.1012E 01
5.6	0.8402E-01	0.3829E 01	0.1008E 01
5.7	0.7803E-01	0.3837E 01	0.1001E 01
5.8	0.7420E-01	0.3844E 01	0.9931E 00
5.9	0.7331E-01	0.3852E 01	0.9831E 00
6.0	0.7535E-01	0.3859E 01	0.9714E 00
6.1	0.8030E-01	0.3867E 01	0.9580E 00
6.2	0.8810E-01	0.3875E 01	0.9432E 00
6.3	0.9870E-01	0.3885E 01	0.9269E 00
6.4	0.1120E-00	0.3895E 01	0.9093E 00
6.5	0.1280E-00	0.3907E 01	0.8905E 00
6.6	0.1464E-00	0.3921E 01	0.8708E 00
6.7	0.1673E-00	0.3937E 01	0.8500E 00
6.8	0.1904E-00	0.3954E 01	0.8285E 00
6.9	0.2157E-00	0.3975E 01	0.8064E 00
7.0	0.2429E-00	0.3998E 01	0.7837E 00
7.1	0.2720E-00	0.4023E 01	0.7606E 00
7.2	0.3027E-00	0.4052E 01	0.7374E 00
7.3	0.3348E-00	0.4084E 01	0.7140E 00
7.4	0.3682E-00	0.4119E 01	0.6908E 00
7.5	0.4027E-00	0.4158E 01	0.6677E 00
7.6	0.4380E-00	0.4200E 01	0.6450E 00
7.7	0.4740E-00	0.4245E 01	0.6228E 00
7.8	0.5105E 00	0.4294E 01	0.6012E 00
7.9	0.5472E 00	0.4347E 01	0.5803E 00
8.0	0.5840E 00	0.4404E 01	0.5604E 00
8.1	0.6206E 00	0.4464E 01	0.5414E 00
8.2	0.6568E 00	0.4528E 01	0.5236E 00
8.3	0.6925E 00	0.4595E 01	0.5070E 00
8.4	0.7274E 00	0.4666E 01	0.4917E-00
8.5	0.7613E 00	0.4741E 01	0.4779E-00
8.6	0.7941E 00	0.4819E 01	0.4655E-00
8.7	0.8256E 00	0.4900E 01	0.4547E-00
8.8	0.8556E 00	0.4984E 01	0.4456E-00
8.9	0.8839E 00	0.5071E 01	0.4382E-00
9.0	0.9104E 00	0.5160E 01	0.4329E-00
9.1	0.9350E 00	0.5253E 01	0.4296E-00
9.2	0.9575E 00	0.5347E 01	0.4285E-00
9.3	0.9778E 00	0.5444E 01	0.4296E-00
9.4	0.9958E 00	0.5543E 01	0.4329E-00
9.5	0.1011E 01	0.5643E 01	0.4383E-00
9.6	0.1024E 01	0.5745E 01	0.4458E-00
9.7	0.1035E 01	0.5848E 01	0.4556E-00
9.8	0.1043E 01	0.5952E 01	0.4676E-00
9.9	0.1048E 01	0.6057E 01	0.4820E-00
10.0	0.1051E 01	0.6162E 01	0.4987E-00
10.1	0.1051E 01	0.6267E 01	0.5178E-00
10.2	0.1049E 01	0.6372E 01	0.5394E 00

PDSC/PAV =	-0.8747E 00	DDMAX =	0.2240E-00	AJDLE P/B =	0.1510E 01
PSIP =	-0.7020E 02	PSIA =	-0.2216E 03	KD/KBS =	0.1315E 01
KP =	0.1645E-00	KB =	0.1931E 01	PHI GSC/PHI AV =	0.8747E 00
KPR =	-0.8925E 00	KDR =	-0.1472E-00	PSIDP =	-0.4016E 03
KPS =	0.5150E 00	KDS =	-0.1463E 01	P2/P1 =	0.6419E-01
MXPPDR =	0.6267E 00	MKUPDR =	0.4206E-00		

RUN NO. 1P4 RUDDER NUMERATOR ROOTS

SIDESLIP TO CONTROL DEFLECTION

ROOTS (COMPLEX FORM)

0. 0.
0.52436-01
-0.10936 01
-0.86076 01

1/TP1 = 0.3264139E-01 1/TP2 = -0.1092688 01 1/TP3 = -0.8607128 01

AP = 0.38536E-01 BP = 0.37018E-00 CP = 0.34118E-00 DP = -0.10928E-01

ROLL ANGLE TO CONTROL DEFLECTION

-0.59196-02
0.27210 01
-0.12746 01

1/TP1 = -0.5918618E-02 1/TP2 = 0.2720738 01 1/TP3 = -0.1272658 01

AP = 0.15208E-00 BP = -0.22028E-00 CP = -0.53018 00 DP = -0.31348E-02

YAW RATE TO CONTROL DEFLECTION

ROOTS (COMPLEX FORM)

0. 0.
0.44206-01 -0.39956-00
0.44206-01 0.39956-00
-0.11276-01

ZR = -0.1111064E-00 MR = 0.3900638E-00 1/TR = -0.1127038 01

AR = -0.334948E-00 BR = -0.347088E-00 CR = -0.1961BE-01 DR = -0.897988E-01

Appendix E

Sample Output - Fisher's Root Locus Computer Program

GGC/EE/7C-8

MC-135 BASIC YAW DAMPER SYSTEM CRUISE 1

FIGURE 6

ROOT LOCI USING OPTION NUMBER 2

CODE
0-LOCUS PT. 2-ZERO 4-IMAGINARY AXIS
1-POLE 3-BREAK PT. 5-SENSITIVITY PT.

11 POLES AT

X =	-0.00935	Y =	0.
X =	-0.43500	Y =	0.
X =	-0.62000	Y =	0.
X =	-1.54000	Y =	0.
X =	-30.30000	Y =	0.
X =	-50.00000	Y =	0.
X =	-150.00000	Y =	0.
X =	-0.00945	Y =	0.89000
X =	-0.00945	Y =	-0.89000
X =	-82.30000	Y =	85.90000
X =	-82.30000	Y =	-85.90000

4 ZEROS AT

X =	0.	Y =	0.
X =	-0.68840	Y =	0.
X =	0.09230	Y =	0.35400
X =	0.09230	Y =	-0.35400

TIME DELAY = 0.

GAIN CONSTANT = 1.00000000

REGION OF CALCULATION-REAL -2.500 TO 2.500
IMAG -3.500 TO 3.500

BRANCH NUMBER 1

STEP SIZE= 0.0050

LOCUS REAL	LOCUS IMAG	DISTANCE TO ORIGIN	SENSITIVITY	DAMPING FACTOR	CODE
-0.00535	0.	0.00935	0.	1.00000	1
-0.00435	0.	0.00435	12938922.4E 03	1.00000	0
-0.00248	0.	0.00248	31455064.2E 03	1.00000	0
-0.00061	0.	0.00061	16410052.1E 04	1.00000	0
0.	0.	0.	0.	1.00000	2

BRANCH NUMBER 2

STEP SIZE= 0.0200

LOCUS REAL	LOCUS IMAG	DISTANCE TO ORIGIN	SENSITIVITY	DAMPING FACTOR	CODE
-0.42500	0.	0.42500	0.	1.00000	1
-0.45500	0.	0.45500	10905794.2E 01	1.00000	0
-0.47500	0.	0.47500	19900409.5E 01	1.00000	0
-0.49500	0.	0.49500	26975555.2E 01	1.00000	0
-0.51500	0.	0.51500	32038622.5E 01	1.00000	0
-0.53500	0.	0.53500	34869147.5E 01	1.00000	0
-0.54632	0.	0.54632	35330720.5E 01	1.00000	3
-0.54721	0.01398	0.54758	36831055.0E 01	0.99933	0
-0.54987	0.03980	0.55130	41210328.5E 01	0.99739	0
-0.55421	0.05933	0.55738	48124118.0E 01	0.99432	0
-0.56015	0.07843	0.56561	57061866.0E 01	0.99034	0
-0.56753	0.09701	0.57576	67423983.0E 01	0.98570	0
-0.57621	0.11503	0.58758	78601032.0E 01	0.98065	0
-0.58598	0.13248	0.60077	90039271.0E 01	0.97538	0
-0.59665	0.14940	0.61507	10128407.1E 02	0.97005	0
-0.60799	0.16587	0.63021	11199997.7E 02	0.96474	0
-0.61975	0.18204	0.64594	12197163.0E 02	0.95947	0
-0.63169	0.19810	0.66202	13109224.6E 02	0.95418	0
-0.64347	0.21425	0.67821	13934597.4E 02	0.94879	0
-0.65479	0.23075	0.69425	14678841.1E 02	0.94315	0
-0.66524	0.24780	0.70989	15352711.6E 02	0.93710	0
-0.67448	0.26554	0.72487	15970154.2E 02	0.93049	0
-0.68222	0.28398	0.73896	16546224.7E 02	0.92321	0
-0.68825	0.30305	0.75202	17095074.7E 02	0.91521	0
-0.69255	0.32258	0.76399	17628465.7E 07	0.90649	0
-0.69519	0.34240	0.77494	18155109.2E 02	0.89709	0
-0.69633	0.36237	0.78497	18680768.5E 02	0.88707	0
-0.69613	0.38237	0.79423	19208796.7E 02	0.87648	0
-0.69477	0.40233	0.80285	19740737.5E 02	0.86538	0
-0.69241	0.42219	0.81097	20276858.5E 02	0.85381	0
-0.68919	0.44192	0.81871	20816544.2E 02	0.84180	0
-0.68523	0.46153	0.82616	21358578.5E 02	0.82941	0
-0.68063	0.48099	0.83343	21901334.2E 02	0.81666	0
-0.67544	0.50032	0.84059	22442911.5E 02	0.80358	0
-0.66989	0.51952	0.84773	22981233.2E 02	0.79021	0
-0.66392	0.53861	0.85492	23514131.0E 02	0.77659	0
-0.65767	0.55761	0.86224	24039418.2E 02	0.76275	0
-0.65124	0.57654	0.86978	24554976.0E 02	0.74874	0
-0.64471	0.59545	0.87762	25058828.5E 02	0.73462	0
-0.63822	0.61437	0.88588	25549282.2E 02	0.72044	0
-0.63190	0.63334	0.89466	26025062.5E 02	0.70630	0
-0.62591	0.65242	0.90411	26485536.5E 02	0.69229	0
-0.62043	0.67166	0.91437	26930942.5E 02	0.67854	0
-0.61570	0.69109	0.92558	27362699.7E 02	0.66521	0
-0.61192	0.71073	0.93786	27783654.5E 02	0.65246	0
-0.60930	0.73056	0.95130	28198188.5E 02	0.64050	0
-0.60798	0.75052	0.96568	28614012.5E 02	0.62946	0
-0.60800	0.77052	0.98151	29031618.5E 02	0.61945	0
-0.60927	0.79048	0.99803	29463490.2E 02	0.61047	0
-0.61165	0.81033	1.01526	29913419.7E 02	0.60245	0
-0.61454	0.83006	1.03303	30386108.0E 02	0.59527	0
-0.61894	0.84966	1.05119	30885102.0E 02	0.58880	0
-0.62349	0.86913	1.06964	31412932.5E 02	0.58290	0
-0.62842	0.88951	1.08829	31971335.2E 02	0.57744	0
-0.63363	0.90782	1.10708	32561455.5E 02	0.57234	0
-0.63900	0.92709	1.12597	33184024.0E 02	0.56751	0
-0.64448	0.94632	1.14494	33839479.0E 02	0.56289	0
-0.64959	0.96555	1.16395	34529069.0E 02	0.55844	0
-0.65549	0.98478	1.18299	35249902.0E 02	0.55410	0

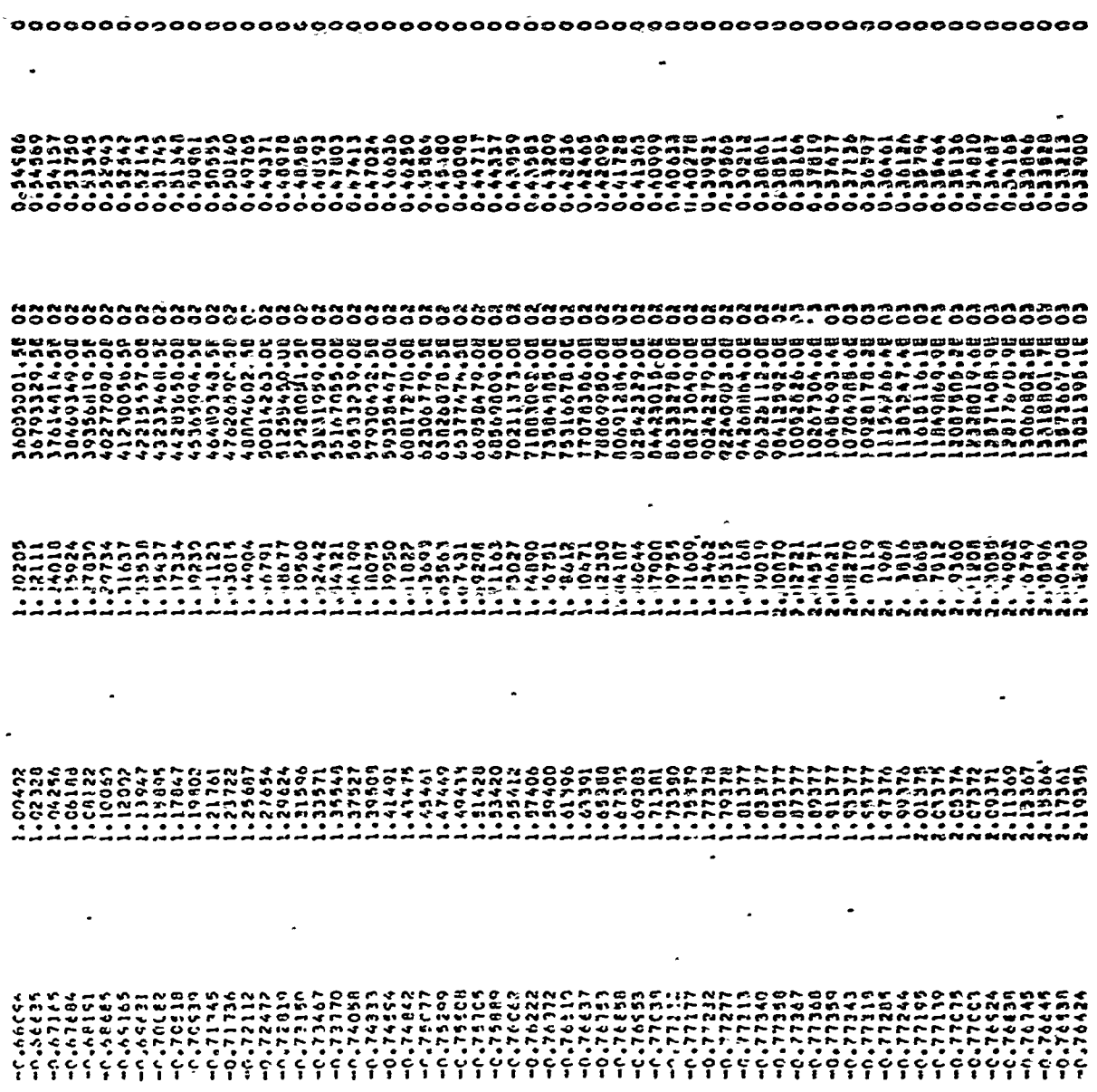

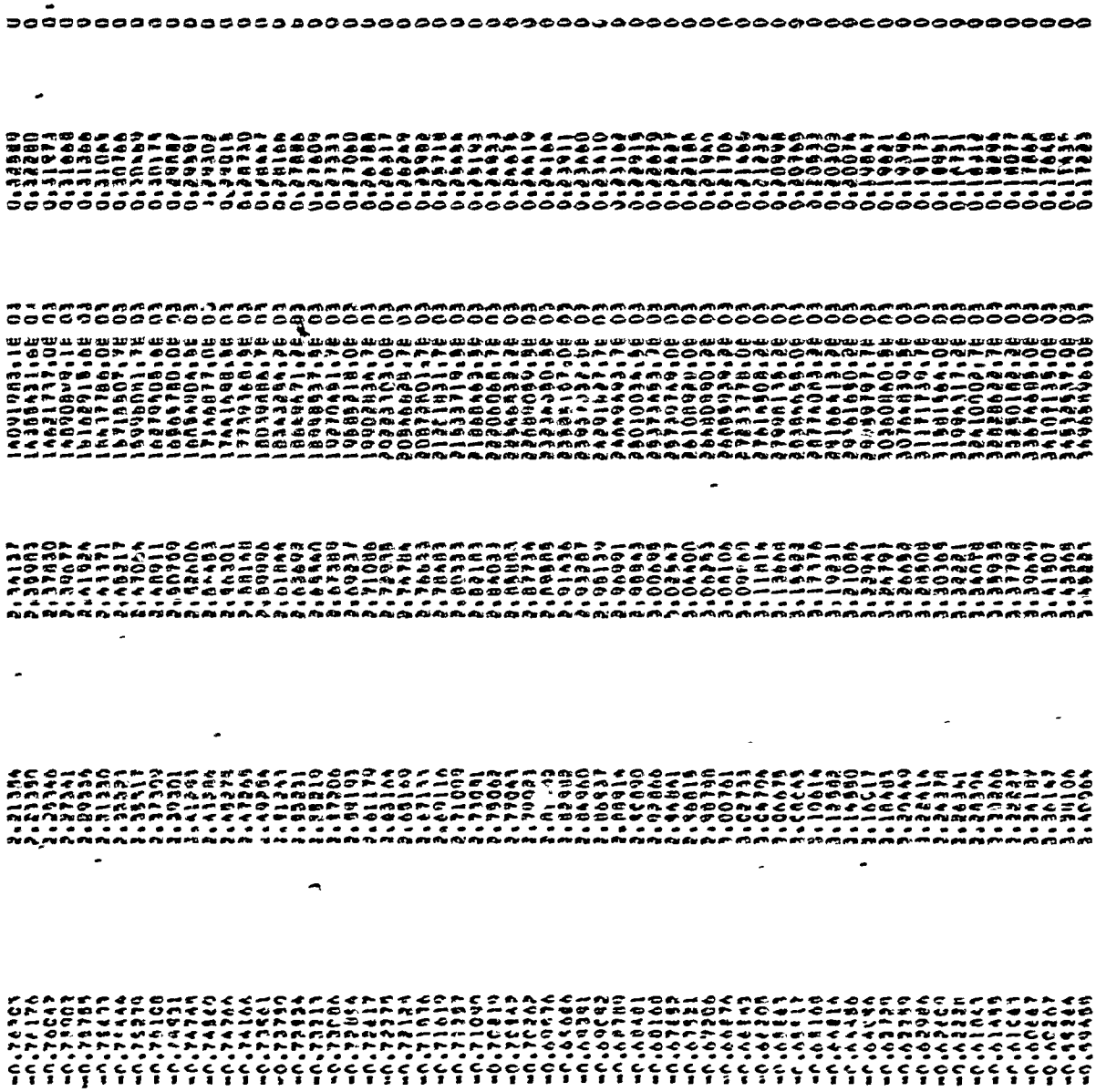

-0.490641	3.447332	3.07001	3540?212.0E 03	0.110613	0
-0.488234	3.441979	3.000945	3688[1492.0E 03	0.108803	0
-0.488217	3.449939	3.00799	3628?3761.0E 03	0.109995	0
-0.487756	3.447590	3.02658	3672?4961.0E 03	0.109389	0
-0.487372	3.449844	3.04817	3717?'84.9E 03	0.110183	0

ROUNDCAPY

BRANCH NUMBER 3

STEP SIZE= 0.0200

LOCUS REAL	LOCUS IMAG	DISTANCE TO ORIGIN	SENSITIVITY	DAMPING FACTOR	CODE
-0.492000	0.	0.03000	0.	1.00000	1
-0.600000	0.	0.00000	2007967[.7E 01	1.00000	0
-0.500000	0.	0.08000	3014?601.0E 01	1.00000	0
-0.560000	0.	0.16000	3487654?.9E 01	1.00000	0
-0.444639	0.	0.14638	3531?772?.1E 01	1.00000	0
-0.941321	-0.61998	0.14788	3683105?.0E 01	0.999133	0
-0.949871	-0.639?0	0.16130	4121?319.9E 01	0.997?39	0
-0.954?31	-0.658?3	0.10738	4811?4101.0E 01	0.994?2?	0
-0.962?19	-0.67843	0.18961	5706[?41.0E 01	0.990?4	0
-0.967?13	-0.69701	0.17573	6742?991.0E 01	0.98?70	0
-0.977?31	-0.71503	0.18750	78?0?992.0E 01	0.980?9	0
-0.981?60	-0.73240	0.20077	900?9226.0E 01	0.97?38	0
-0.89?669	-0.74940	0.21807	101?84?2.1E 02	0.97005	0
-0.6C?99	-0.76587	0.23?81	11?99?92.6E 02	0.?6474	0
-0.61?76	-0.78204	0.24896	12?97158.0E 02	0.959?7	0
-0.63?60	-0.79810	0.26202	13?09?80.4E 02	0.954?8	0
-0.643?7	-0.81425	0.27821	139?4993.2E 02	0.94?79	0
-0.658?9	-0.83079	0.29428	14?78?39.1E 02	0.943?5	0
-0.66?24	-0.84780	0.30989	1535?71?.?E 02	0.937?0	0
-0.674?8	-0.86594	0.32?87	15970154.8E 02	0.?3049	0
-0.68222	-0.88393	0.33?96	16846227.4E 02	0.9?321	0
-0.68?28	-0.90308	0.35208	17099?79.2E 02	0.9?1?1	0
-0.6?285	-0.92286	0.36399	17620?72.2E 02	0.90?49	0
-0.69?10	-0.94240	0.37?94	18158?16.2E 02	0.89?09	0
-0.69?82	-0.96237	0.39?97	18680??8.0E 02	0.88?07	0
-0.69?13	-0.98237	0.41?23	19?08?08.?E 02	0.87?48	0
-0.69?77	-0.?0233	0.42?85	197?0?51.0E 02	0.?6936	0
-0.69?41	-0.?2319	0.44?97	20?76?73.0E 02	0.85?80	0
-0.6?819	-0.?4193	0.46?71	20?16?60.2E 02	0.85?[?	0
-0.6?823	-0.?6183	0.48?16	213?8?95.2E 02	0.8?9??	0
-0.6?843	-0.?8009	0.49?43	21?01?58.?E 02	0.8?4?6	0
-0.67849	-0.?9932	0.51?89	22?4?930.0E 02	0.8?39?	0
-0.6?8?8	-0.?1952	0.53?73	22?8?2?1.?E 02	0.?9?2?	0
-0.6?732	-0.?3861	0.55?92	23?14?60.0E 02	0.?7859	0
-0.6?767	-0.?5761	0.57?24	24?39?39.2E 02	0.?6?7?	0
-0.6?12A	-0.?7654	0.59?78	24?5?49?.5E 02	0.?4?7A	0
-0.6?4?1	-0.?9549	0.61?62	25?8?8?9.2E 02	0.?3?61	0
-0.6?8?2	-0.?1437	0.63?87	26?49?99.?E 02	0.?2?44	0
-0.6?190	-0.?3334	0.65?66	27?2?9?0.?E 02	0.?0?2?	0
-0.6?8?0	-0.?5242	0.67?11	28?8?5?2.?E 02	0.?7???	0
-0.?2?47	-0.?7166	0.69?37	29?3?956.0E 02	0.?7?5A	0
-0.?1?7?	-0.?9109	0.71?98	29?62?13.?E 02	0.?6?2?	0
-0.?11?9	-0.?1073	0.73?86	3??7?A6A.?E 02	0.?5?2A	0
-0.?C?30	-0.?3098	0.75?30	3?1?8197.2E 02	0.?4?3?	0
-0.?C?7A	-0.?5152	0.77?88	32?12?2?.?E 02	0.?3?4?	0
-0.?C?99	-0.?7?8?	0.79?03	329?162A.?E 02	0.?1?45	0
-0.?C?3?	-0.?9?4A	0.81?69	3346?491.0E 02	0.?1?47	0

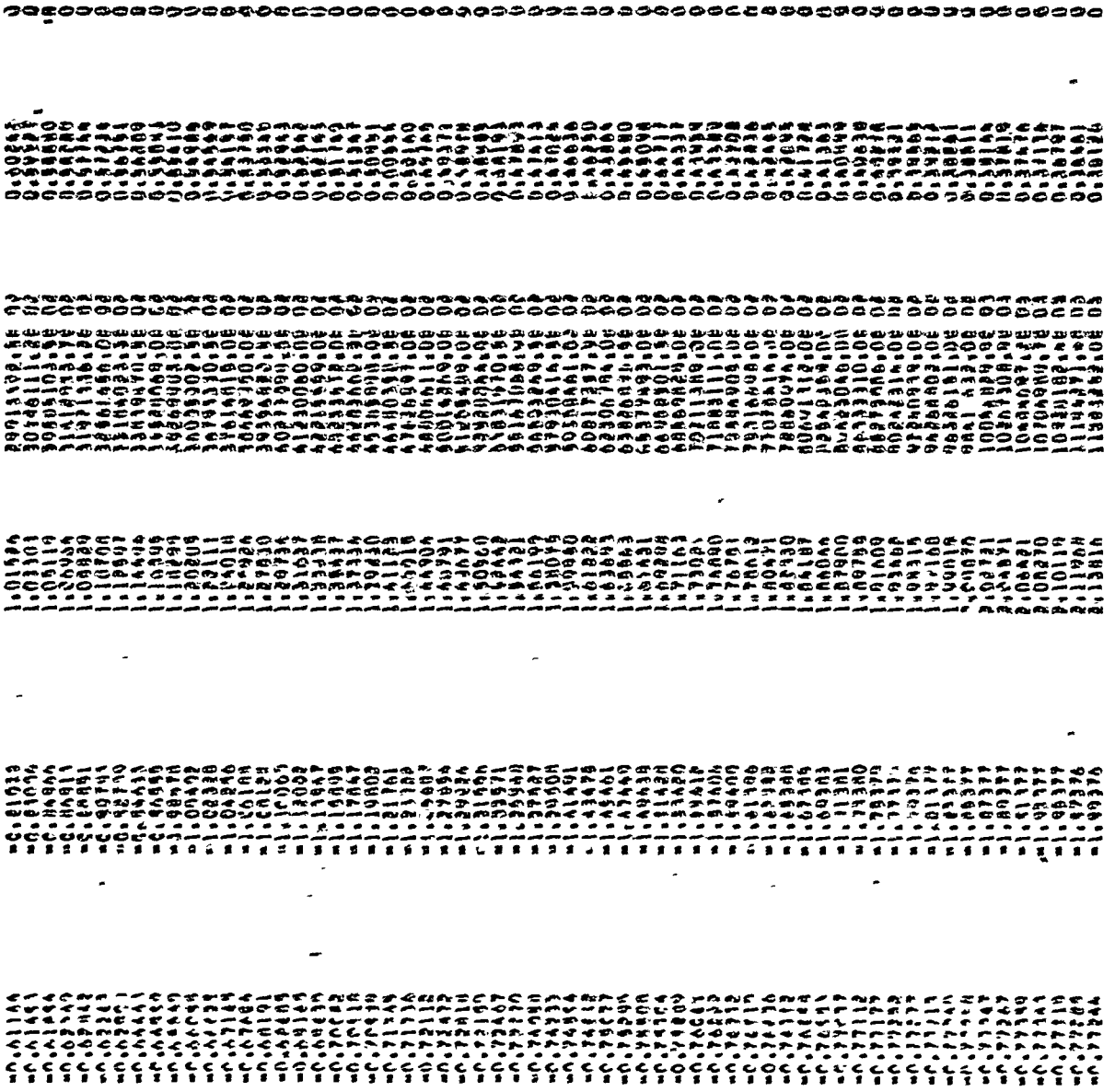

-0.77104	-2.01378	2.19664	11615121.48 03	0.38794	0
-0.77137	-2.03378	2.17913	11869879.38 03	0.38466	0
-0.77174	-2.05374	2.19380	12087510.78 03	0.38134	0
-0.77209	-2.07379	2.21208	12328024.98 03	0.34810	0
-0.77234	-2.09371	2.23086	12571414.98 03	0.34487	0
-0.77259	-2.11369	2.24908	12811676.48 03	0.34165	0
-0.77245	-2.13367	2.26749	13066807.98 03	0.33846	0
-0.77249	-2.15364	2.28596	13318807.98 03	0.33528	0
-0.77277	-2.17361	2.30443	13573677.98 03	0.33213	0
-0.77423	-2.19359	2.32290	13831400.58 03	0.32900	0
-0.77495	-2.21356	2.34137	14091980.48 03	0.32589	0
-0.77574	-2.23380	2.35983	14358438.38 03	0.32280	0
-0.77642	-2.25346	2.37830	14621744.08 03	0.31973	0
-0.77903	-2.27341	2.39677	14889905.48 03	0.31668	0
-0.78159	-2.29336	2.41524	15162922.98 03	0.31366	0
-0.78462	-2.31330	2.43371	15437792.38 03	0.31065	0
-0.78443	-2.33323	2.45217	15715514.68 03	0.30766	0
-0.78279	-2.35317	2.47064	15996088.68 03	0.30469	0
-0.78104	-2.37309	2.48911	16279512.98 03	0.30174	0
-0.74931	-2.39308	2.50759	16565786.08 03	0.29883	0
-0.74744	-2.41303	2.52606	16854910.78 03	0.29591	0
-0.74567	-2.43294	2.54453	17146883.08 03	0.29302	0
-0.74366	-2.45275	2.56301	17441709.78 03	0.29019	0
-0.74166	-2.47265	2.58148	17739378.78 03	0.28730	0
-0.73961	-2.49254	2.59996	18039894.78 03	0.28447	0
-0.73750	-2.51249	2.61844	18343262.78 03	0.28166	0
-0.73434	-2.53231	2.63692	18649479.08 03	0.27886	0
-0.73213	-2.55219	2.65540	18958544.78 03	0.27609	0
-0.73084	-2.57206	2.67389	19270460.88 03	0.27333	0
-0.72854	-2.59193	2.69237	19585226.28 03	0.27059	0
-0.72617	-2.61179	2.71086	19902842.78 03	0.26787	0
-0.72378	-2.63164	2.72935	20223312.78 03	0.26517	0
-0.72128	-2.65149	2.74784	20546634.78 03	0.26249	0
-0.71874	-2.67133	2.76633	20872810.78 03	0.25982	0
-0.71619	-2.69116	2.78483	21201841.58 03	0.25717	0
-0.71357	-2.71099	2.80333	21533727.58 03	0.25454	0
-0.71090	-2.73081	2.82183	21868473.28 03	0.25193	0
-0.70818	-2.75062	2.84033	22206077.58 03	0.24933	0
-0.70542	-2.77043	2.85883	22546542.08 03	0.24675	0
-0.70261	-2.79023	2.87734	22889868.78 03	0.24419	0
-0.69974	-2.81003	2.89584	23236060.58 03	0.24164	0
-0.69686	-2.82982	2.91436	23585117.08 03	0.23911	0
-0.69391	-2.84960	2.93287	23937043.28 03	0.23660	0
-0.69092	-2.86938	2.95139	24291838.08 03	0.23410	0
-0.68788	-2.88914	2.96990	24649504.58 03	0.23162	0
-0.68480	-2.90890	2.98843	25010045.78 03	0.22915	0
-0.68168	-2.92866	3.00695	25373464.28 03	0.22670	0
-0.67851	-2.94841	3.02547	25739761.58 03	0.22427	0
-0.67531	-2.96815	3.04400	26108939.28 03	0.22185	0
-0.67205	-2.98788	3.06253	26481003.08 03	0.21944	0
-0.66876	-3.00761	3.08106	26855951.78 03	0.21705	0
-0.66542	-3.02733	3.09960	27233791.08 03	0.21468	0
-0.66205	-3.04704	3.11814	27614521.58 03	0.21232	0
-0.65863	-3.06675	3.13668	27998140.08 03	0.20998	0
-0.65517	-3.08645	3.15522	28384673.02 03	0.20765	0
-0.65167	-3.10614	3.17376	28774092.78 03	0.20533	0
-0.64814	-3.12582	3.19231	29166427.08 03	0.20303	0
-0.64456	-3.14550	3.21086	29561664.28 03	0.20074	0
-0.64094	-3.16517	3.22941	29959812.08 03	0.19847	0
-0.63728	-3.18483	3.24797	30360874.78 03	0.19621	0
-0.63359	-3.20449	3.26652	30764854.08 03	0.19396	0

-0.62985	-3.22414	3.28508	31111794.7E 03	0.19173	0
-0.62668	-3.24378	3.30365	31581580.2E 03	0.18951	0
-0.62228	-3.26341	3.32221	31994333.7E 03	0.18731	0
-0.61843	-3.28304	3.34078	32410017.7E 03	0.18512	0
-0.61455	-3.30266	3.35935	32828638.2E 03	0.18294	0
-0.61062	-3.32227	3.37792	33250198.7E 03	0.18077	0
-0.60667	-3.34187	3.39649	33674708.5E 03	0.17862	0
-0.60267	-3.36147	3.41507	34102153.0E 03	0.17647	0
-0.59864	-3.38106	3.43365	34532554.0E 03	0.17435	0
-0.59458	-3.40064	3.45223	34965913.0E 03	0.17223	0
-0.59049	-3.42022	3.47082	35402230.5E 03	0.17013	0
-0.58634	-3.43979	3.48940	35841505.0E 03	0.16803	0
-0.58217	-3.45935	3.50799	36283757.0E 03	0.16595	0
-0.57796	-3.47890	3.52658	36728930.0E 03	0.16389	0
-0.57372	-3.49844	3.54517	37177175.5E 03	0.16183	0

BOUNDARY

BRANCH NUMBER 4

STEP SIZE= 0.1000

LOCUS REAL	LOCUS IMAG	DISTANCE TO ORIGIN	SENSITIVITY	DAMPING FACTOR	CODE
-1.54000	0.	1.54000	0.	1.00000	1
-1.44000	0.	1.44000	36226108.5E 01	1.00000	0
-1.34000	0.	1.34000	68241418.0E 01	1.00000	0
-1.24000	0.	1.24000	96138480.0E 01	1.00000	0
-1.14000	0.	1.14000	12013144.9E 02	1.00000	0
-1.04000	0.	1.04000	14075885.1E 02	1.00000	0
-0.94000	0.	0.94000	15964412.0E 02	1.00000	0
-0.84000	0.	0.84000	18353102.7E 02	1.00000	0
-0.74000	0.	0.74000	27690459.0E 02	1.00000	0
-0.68840	0.	0.68840	0.	1.00000	2

BRANCH NUMBER 5

STEP SIZE= 2.0000

LOCUS REAL	LOCUS IMAG	DISTANCE TO ORIGIN	SENSITIVITY	DAMPING FACTOR	CODE
THE POLE AT X =	-30.30000 AND Y =	0.	IS OUTSIDE THE BOUNDARY.		

BRANCH NUMBER 6

STEP SIZE= 2.0000

LOCUS REAL	LOCUS IMAG	DISTANCE TO ORIGIN	SENSITIVITY	DAMPING FACTOR	CODE
THE POLE AT X =	-50.00000 AND Y =	0.	IS OUTSIDE THE BOUNDARY.		

BRANCH NUMBER 7

STEP SIZE= 2.0000

LOCUS REAL	LOCUS IMAG	DISTANCE TO ORIGIN	SENSITIVITY	DAMPING FACTOR	CODE
THE POLE AT X =	-150.00000 AND Y =	0.	IS OUTSIDE THE BOUNDARY.		

BRANCH NUMBER 8

STEP SIZE= 0.0100

LOCUS REAL	LOCUS IMAG	DISTANCE TO ORIGIN	SENSITIVITY	DAMPING FACTOR	CODE
-0.00545	0.89000	0.89005	0.	0.01062	1
-0.01941	0.88906	0.88927	13967592.6E 01	0.02182	0
-0.02934	0.88794	0.88842	27559325.0E 01	0.03303	0
-0.03926	0.88664	0.88759	40771132.5E 01	0.04423	0
-0.04919	0.88515	0.88681	53615263.0E 01	0.05544	0
-0.05901	0.88348	0.88545	66080266.5E 01	0.06664	0
-0.06883	0.88163	0.88431	78170999.0E 01	0.07784	0
-0.07862	0.87958	0.88309	89888626.0E 01	0.08903	0
-0.08837	0.87735	0.88179	10123458.9E 02	0.10022	0
-0.09807	0.87493	0.88041	11221063.2E 02	0.11139	0
-0.10772	0.87231	0.87896	12281479.0E 02	0.12256	0
-0.11732	0.86950	0.87737	13306139.1E 02	0.13372	0
-0.12685	0.86648	0.87572	14294102.4E 02	0.14486	0
-0.13632	0.86326	0.87396	15246059.0E 02	0.15598	0
-0.14572	0.85984	0.87210	16162328.2E 02	0.16709	0
-0.15503	0.85621	0.87013	17043258.5E 02	0.17817	0
-0.16424	0.85235	0.86804	17889229.7E 02	0.18923	0
-0.17339	0.84829	0.86582	18700651.0E 02	0.20027	0
-0.18242	0.84398	0.86347	19477471.5E 02	0.21127	0
-0.19133	0.83944	0.86097	20221672.0E 02	0.22223	0
-0.20012	0.83466	0.85831	20932876.5E 02	0.23315	0
-0.20879	0.82962	0.85548	21610356.7E 02	0.24402	0
-0.21723	0.82432	0.85247	22256335.5E 02	0.25483	0
-0.22553	0.81874	0.84924	22871502.5E 02	0.26557	0
-0.23361	0.81288	0.84579	23456021.7E 02	0.27623	0
-0.24150	0.80670	0.84207	24010952.5E 02	0.28679	0
-0.24910	0.80020	0.83808	24537277.7E 02	0.29723	0
-0.25639	0.79336	0.83377	25036125.7E 02	0.30751	0
-0.26333	0.78616	0.82910	25500025.2E 02	0.31762	0
-0.26986	0.77859	0.82403	25956959.5E 02	0.32749	0
-0.27589	0.77061	0.81851	26382433.5E 02	0.33707	0
-0.28136	0.76224	0.81251	26787570.5E 02	0.34628	0
-0.28619	0.75346	0.80597	27178216.7E 02	0.35504	0
-0.29019	0.74431	0.79887	27540019.5E 02	0.36323	0
-0.29333	0.73482	0.79120	27912516.0E 02	0.37074	0
-0.29552	0.72506	0.78297	28271110.0E 02	0.37742	0
-0.29669	0.71513	0.77423	28630011.7E 02	0.38321	0
-0.29684	0.70513	0.76506	28994965.7E 02	0.38799	0
-0.29599	0.69517	0.75556	29371052.5E 02	0.39175	0
-0.29421	0.68533	0.74581	29766431.2E 02	0.39448	0
-0.29159	0.67560	0.73591	30184180.5E 02	0.39623	0
-0.28823	0.66626	0.72593	30630250.7E 02	0.39705	0
-0.28424	0.65709	0.71593	31109490.2E 02	0.39702	0
-0.27969	0.64818	0.70595	31626533.2E 02	0.39619	0
-0.27469	0.63953	0.69602	32185897.2E 02	0.39464	0
-0.26929	0.63113	0.68616	32795295.0E 02	0.39240	0
-0.26360	0.62296	0.67639	33449734.7E 02	0.38954	0
-0.25761	0.61502	0.66671	34163669.5E 02	0.38608	0
-0.25167	0.60728	0.65714	34938709.0E 02	0.38207	0
-0.24490	0.59974	0.64767	35780690.5E 02	0.37751	0
-0.23811	0.59238	0.63831	36698178.5E 02	0.37244	0
-0.23078	0.58519	0.62905	37688632.0E 02	0.36687	0
-0.22264	0.57816	0.61992	38768041.0E 02	0.36081	0

-0.21642	0.27127	0.6 089	1094[illegible]08.5E 02	0.38427	0
-0.20664	0.26432	0.61198	41216392.9E 02	0.34736	0
-0.20184	0.25790	0.61319	42603[illegible]2.5E 02	0.33978	0
-0.19784	0.25140	0.61462	44119321.9E 02	0.33182	0
-0.18826	0.24591	0.5 596	45755402.0E 02	0.32340	0
-0.17849	0.23837	0.61787	47945740.0E 02	0.31491	0
-0.17064	0.23292	0.61920	49488875.9E 02	0.30815	0
-0.16279	0.22642	0.62099	51629911.0E 02	0.29831	0
-0.15471	0.22040	0.62298	53909836.8E 02	0.28800	0
-0.14669	0.21446	0.62496	56590941.6E 02	0.27421	0
-0.13845	0.20858	0.62713	59305277.0E 02	0.26293	0
-0.13044	0.20277	0.62 942	62374689.8E 02	0.25116	0
-0.12228	0.19702	0.63 184	65791494.0E 02	0.23885	0
-0.11406	0.19133	0.63439	69474449.0E 02	0.22613	0
-0.10580	0.18568	0.63707	73388842.0E 02	0.21285	0
-0.09753	0.18008	0.63988	77547934.0E 02	0.19907	0
-0.08921	0.17451	0.64283	81916940.0E 02	0.18477	0
-0.08088	0.16899	0.64591	86486412.0E 02	0.16995	0
-0.07253	0.16348	0.64912	91238157.0E 02	0.15461	0
-0.06416	0.15800	0.65248	10220630.1E 03	0.13874	0
-0.05578	0.15254	0.65597	11033018.8E 03	0.12234	0
-0.04740	0.14710	0.65961	11942064.9E 03	0.10542	0
-0.03900	0.14167	0.66339	12983257.4E 03	0.08796	0
-0.03060	0.13624	0.66732	14179436.5E 03	0.06997	0
-0.02220	0.13083	0.67139	15569743.9E 03	0.05146	0
-0.01380	0.12539	0.67562	17187136.2E 03	0.03242	0
-0.00540	0.11996	0.68000	19103821.2E 03	0.01288	0
0.	0.11646	0.68646	20831972.0E 03	0.00000	0
0.00830	0.11191	0.69109	23120108.7E 03	0.03034	0
0.01675	0.10753	0.69588	26319482.7E 03	0.04168	0
0.02511	0.10329	0.70083	30326679.0E 03	0.06269	0
0.03349	0.09932	0.70594	35491301.0E 03	0.08448	0
0.04177	0.09598	0.71121	42379681.5E 03	0.10677	0
0.05007	0.09340	0.71669	51997093.0E 03	0.12944	0
0.05834	0.09178	0.72225	66321497.6E 03	0.15766	0
0.06650	0.09212	0.72803	89040480.0E 03	0.17813	0
0.07490	0.09641	0.73397	13864233.7E 04	0.20061	0
0.08290	0.10066	0.73008	26078410.2E 04	0.22421	0
0.09230	0.10400	0.74684	0.	0.24230	0

BRANCH NUMBER 9

STEP SIZE= 0.0100

LOCUS REAL	LOCUS IMAG	DISTANCE TO ORIGIN	SENSITIVITY	DAMPING FACTOR	CODE
-0.00545	-0.00000	0.01005	0.	0.01063	0
-0.01841	-0.00906	0.01027	13967591.2E 01	0.02102	0
-0.02934	-0.00794	0.01042	27554324.2E 01	0.03301	0
-0.03926	-0.00664	0.01050	40775133.0E 01	0.04423	0
-0.04815	-0.00515	0.01051	53618202.9E 01	0.05444	0
-0.05601	-0.00348	0.01049	66080269.0E 01	0.06364	0
-0.06283	-0.00163	0.01042	78171002.0E 01	0.07184	0
-0.07862	-0.00000	0.01030	89888622.0E 01	0.08903	0
-0.08277	-0.00735	0.01179	10123450.4E 02	0.10022	0
-0.09467	-0.00493	0.01041	11221069.0E 02	0.11139	0
-0.10732	-0.00231	0.01004	12281978.4E 02	0.12256	0
-0.11732	-0.00000	0.01737	13306137.9E 02	0.13372	0
-0.12665	-0.00648	0.01777	14294101.3E 02	0.14486	0
-0.13632	-0.00326	0.01796	15246058.4E 02	0.15598	0

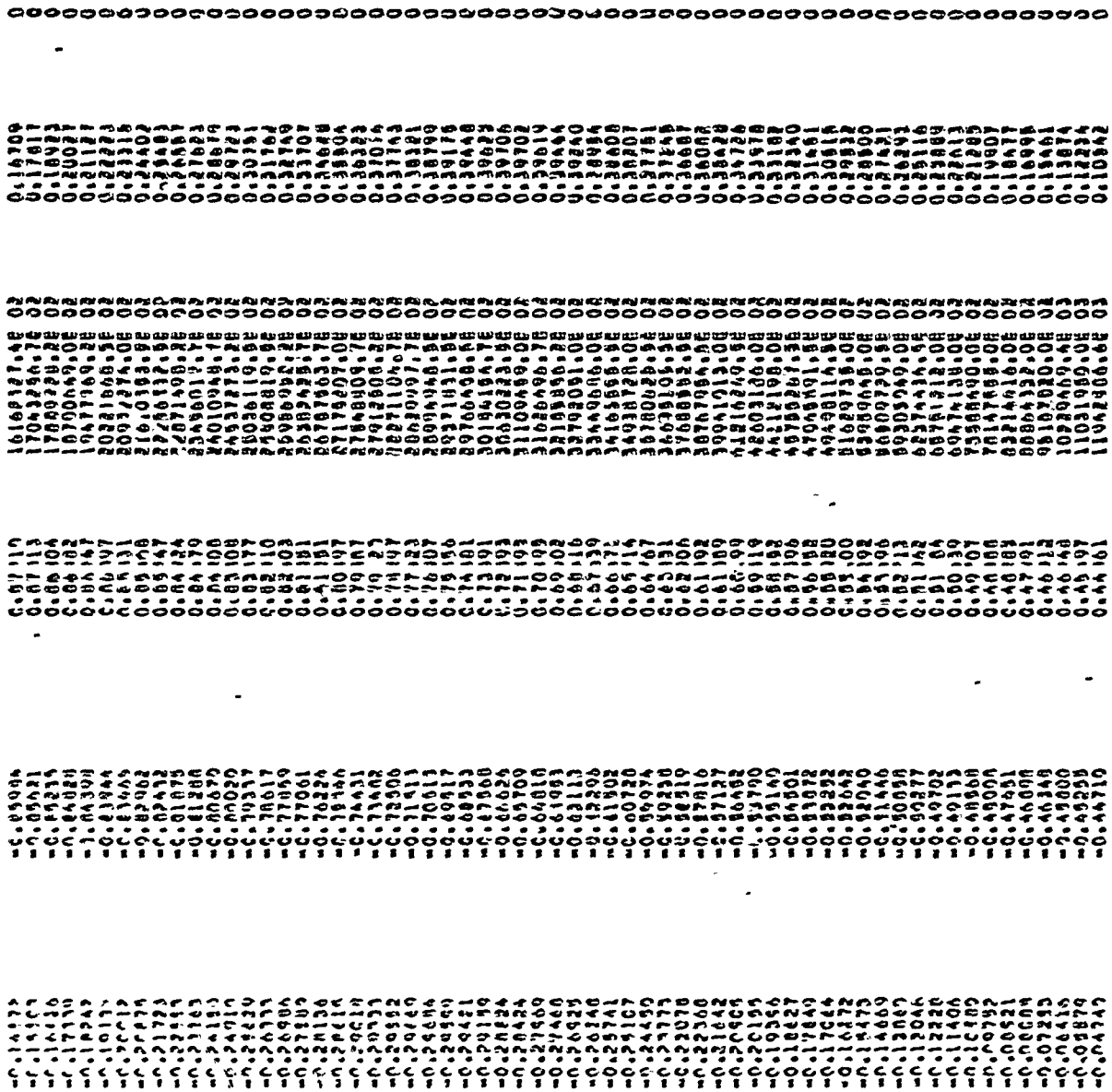

-0.03000	-0.44137	0.44339	12983167.6E 03	0.00796	0
-0.02000	-0.43624	0.43732	14179332.7E 03	0.00997	0
-0.02220	-0.43002	0.43139	15566623.9E 03	0.00146	0
-0.01200	-0.42539	0.42562	17186998.0E 03	0.00242	0
-0.00940	-0.41996	0.42000	19103653.7E 03	0.01207	0
0.	-0.41646	0.41646	20531969.0E 03	0.00000	0
0.00828	-0.41101	0.41109	23120106.2E 03	0.02039	0
0.01615	-0.40533	0.40588	26319878.9E 03	0.04128	0
0.02511	-0.40004	0.40083	30326670.2E 03	0.06265	0
0.03345	-0.39492	0.39594	35491393.9E 03	0.08448	0
0.04177	-0.38998	0.39121	42379673.0E 03	0.10677	0
0.05007	-0.38540	0.38668	51997639.0E 03	0.12959	0
0.05834	-0.37778	0.38229	63321477.9E 03	0.15262	0
0.06650	-0.37212	0.37803	77840419.0E 03	0.17613	0
0.07480	-0.36641	0.37397	93841227.4E 04	0.20001	0
0.08298	-0.36066	0.37008	26078206.9E 04	0.22421	0
0.09230	-0.35400	0.36684	0.	0.25230	2

BRANCH NUMBER 10

STEP SIZE= 2.0000

LOCUS REAL	LOCUS IMAG	DISTANCE TO ORIGIN	SENSITIVITY	DAMPING FACTOR	CODE
THE POLE AT X =	-02.30000 AND Y =	00.90000 IS OUTSIDE THE BOUNDARY.			

BRANCH NUMBER 11

STEP SIZE= 2.0000

LOCUS REAL	LOCUS IMAG	DISTANCE TO ORIGIN	SENSITIVITY	DAMPING FACTOR	CODE
THE POLE AT X =	-02.30000 AND Y =	-00.90000 IS OUTSIDE THE BOUNDARY.			

VITA

Lynn L. Gamble was born on 7 September 1941 in Bluffton, Ohio. He was graduated from Tiffin Columbian High School, Tiffin, Ohio, in 1959 and attended Kent State University, Kent, Ohio, from September 1959 to March 1960 and from March 1961 to June 1961. He was enlisted in the United States Air Force in December 1961 and was subsequently accepted to the Airman Education and Commissioning Program in 1964. Under the AECP, he attended the University of Wyoming, Laramie, Wyoming, from June 1964 to June 1966 from which he received the degree of Bachelor of Science in Electrical Engineering. He was commissioned in the Air Force following Officer Training School, Lackland AFB, Texas, in September 1966. Before entering the Air Force Institute of Technology, Captain Gamble served as a flight test engineer in the Directorate of Flight Test, Aeronautical Systems Division, Wright-Patterson AFB, Ohio. He is a member of the Eta Kappa Nu Electrical Engineering Honorary Fraternity.

Permanent address: 30 Parkview Drive
Tiffin, Ohio 44883

VITA

William L. Smith was born on 13 June 1940 in Bayboro, North Carolina. He was graduated from Havelock High School, Havelock, North Carolina in 1958 and attended North Carolina State College of Agriculture and Engineering from September 1958 to October 1960. He was enlisted in the United States Air Force in March 1961 and was subsequently accepted to the Airman Education and Commissioning Program in 1964. Under the AECP, he attended the University of Missouri, Columbia, Missouri, from August 1964 to August 1966 from which he received the degree of Bachelor of Science in Electrical Engineering. He was commissioned in the Air Force following Officer Training School, Lackland AFB, Texas, in October 1966. Before entering the Air Force Institute of Technology, Captain Smith served as a project officer in the Directorate of Materiel Management, Air Force Logistics Command, Kelly AFB, Texas. He is a member of the Eta Kappa Nu Electrical Engineering Honorary Fraternity.

Permanent address: 1722 Spencer Ave
New Bern, North Carolina 28560

This thesis was typed by the authors.

Security Classification

DOCUMENT CONTROL DATA - R & D

(Security classification of title, body of abstract and indexing annotation must be entered when the overall report is classified)

1. ORIGINATING ACTIVITY (Corporate author)
Air Force Institute of Technology (AFIT-SE)
Department of Electrical Engineering
Wright-Patterson AFB, Ohio 45433

2a. REPORT SECURITY CLASSIFICATION
Unclassified

2b. GROUP

3. REPORT TITLE
IMPROVED DUTCH ROLL STABILITY AUGMENTATION SYSTEM FOR A MODIFIED C-135B AIRCRAFT

4. DESCRIPTIVE NOTES (Type of report and inclusive dates)
Masters Thesis, Guidance and Control

5. AUTHOR(S) (First name, middle initial, last name)
Lynn L. Gamble, Captain, USAF
William L. Smith, Captain, USAF

6. REPORT DATE	7a. TOTAL NO. OF PAGES	7b. NO. OF REFS
May 1970	161	10

8a. CONTRACT OR GRANT NO.	9a. ORIGINATOR'S REPORT NUMBER(S)
b. PROJECT NO.	GGC/EE/70-8
c. N/A	9b. OTHER REPORT NO(S) (Any other numbers that may be assigned this report)
d.	

10. DISTRIBUTION STATEMENT
This document is subject to special export controls and each transmittal to foreign governments or foreign nationals may be made only with prior approval of the Dean of Engineering, Air Force Institute of Technology (AFIT-SE), Wright-Patterson AFB, Ohio 45433

11. SUPPLEMENTARY NOTES	12. SPONSORING MILITARY ACTIVITY
	Aeronautical Systems Division, Deputy of Engineering (ASN) Wright-Patterson AFB, Ohio

13. ABSTRACT

A stability augmentation system was designed for a C-135B aircraft which is modified by the installation of a large external fairing. Aerodynamic data for the modified C-135B were obtained from wind tunnel testing of the aircraft model.

The SAS consists of the basic Boeing series yaw damper augmented with lateral acceleration feedback. Analysis and design were done using root locus techniques.

The aircraft was then simulated on the analog computer to verify the design and make final system adjustments. Three flight conditions were simulated - two cruise conditions and power approach. In all the cases, the lateral-directional flying qualities were noticeably improved when the SAS was used. The biggest advantage of this particular SAS, namely, the acceleration feedback, is that both the damping ratio and the frequency of the Dutch roll were significantly increased without degrading flying qualities in some other area.

As required, the SAS is simple and inexpensive, and requires a minimum of subsystem redesign. In addition to the requirement that the standard series yaw damper be installed, the SAS consists of only one accelerometer and one additional flap switch.

DD FORM 1 NOV 65 1473

Unclassified
Security Classification

14. KEY WORDS	LINK A		LINK B		LINK C	
	ROLE	WT	ROLE	WT	ROLE	WT
Stability Augmentation System						
Acceleration Feedback						
Lateral-Directional Stability						
Large Transport						